`

Review of radar system performance and estimation of slope deformation threshold values for the Leveäniemi open pit

Janusz Niekrasz

School of Engineering

Master's thesis
Espoo 15.10.2018

Supervisor

Prof. Mikael Rinne

Advisor

Dr. Sraj Banda
Umar

`

Aalto University
School of Engineering

Aalto University, P.O. BOX 11000, 00076
AALTO
www.aalto.fi

Abstract of the master's thesis

Author Janusz Niekrasz

Title Review of Radar system performance and estimation of slope deformation threshold values for the Leveäniemi open pit

Degree programme EMMEP European Mining Course

Major Mining engineering **Code of major** ENG3077

Supervisor Prof. Mikael Rinne

Advisor Dr. Sraj Banda Umar

Date 24.4.2018 **Number of pages** **Language** English

Abstract

Slope stability is crucial for safety in operations during open pit mining. A slope failure could influence the environment, lead to human injuries and economic losses. To ensure proper management and mitigation of the stability problems it is necessary to provide accurate slope designs and constant and accurate slope monitoring procedures.

There are many techniques that are used for the slope monitoring. One of the most effective methods is the slope stability radar (SSR) technology. It allows for 24 h per day, real-time monitoring of slopes in all-weather condition. The SSR covers a large expanse of the wall slope and can detect deformations within the slopes well before slope failure occurs. This makes the SSR as an effective tool for an early warning signal for an impending slope failure. One of the requirements is the availability of the line of sight between the SSR and the monitored wall.

This study aims at reviewing the threshold values for input into a slope stability radar which is being installed at the one of Svappavaara open pit's- Leveäniemi open pit, for monitoring slope stability. The Leveäniemi open pit is located near Svappavaara in Swedish Lapland and is a part of LKAB. Threshold values are difficult to set as they depend on so many rock mass properties and pit geometry, which in turn also change from place to place (site-specific). Around the world, many mines use radar systems for the protection of slopes and avoidance of slope failure. Therefore, the threshold value for the Leveäniemi open pit will be estimated using other case studies. An expected outcome of the research is a range of deformation at which the SSR will give an early warning signal against a likely failure in the pit slopes. Moreover, the study will determine operating procedures for the radar system to be installed and establish a smooth reporting system for the data gathered through the radar.

Keywords Slope stability radar; Slope monitoring, Threshold value, Leveäniemi open pit

`

Table of Contents

`

`

List of Figures

`

`

List of Tables

`

Acknowledgments

At first, I would like to express my deepest gratitude to my advisor, Dr. Sraj Banda Umar, for continuous support on my thesis research. His guidance, patience, and motivation helped me during the project. He made perfect atmosphere during the research. I couldn't imagine a better advisor and mentor for this study. Thank you for your support, valuable advise and being my best friend through all time when I was writing this thesis.

I am also grateful to Prof. Mikael Rinne for the supervision provided for this research. Your valuable feedbacks, recommendations, and experience made this thesis professional.

I would like to express appreciation to LKAB, especially for Matti Sormunen to make this thesis possible. I received professional support during whole my stay at the Svappavaara mine. Thank you, that I could gain an experience and visit beautiful Lapland.

I would like to express my gratitude for company IDS GeoRadar. Special thanks for Augusto Merlo for training and continuous support during the radar installation and calibration process.

I am grateful for Dr. Gabriela Paszkowska, without her help, I could not finish my studies. She helped me every time when I have some doubts and encouraged me to study abroad. Without her, I could not be at the point where I am right now.

Special thanks for my Polish professors, Dr. Wojciech Milczarek and Prof. Anna Chrzanowska for support and comments on my thesis.

I would like to express my gratitude for all those, who helped me during whole studies and thesis writing. I appreciate everyone who encourages and support me along the way. Especially I would like to say thank you for all my professors and study colleagues.

Last but not least, I would like to thank my friends and my family. For their unconditional love, motivation, and encouragement through all my studies.

I would like to dedicate this thesis to my parents. To my mother, Jolanta Mularczyk -Niekrasz and my father Andrzej Niekrasz. Their love and support made my journey possible. Without their effort in my education, I could not finish my studies and made this thesis.

`

List of symbols and abbreviations

φ-angle of friction

c-cohesion

σ_n-normal stress

τ-shear strength

φ_r-residual angle of friction

i-angle of friction connected to roughness of surface

JRC-Joint Roughness Coefficient

JSC-joint wall compressive strength

L_0-length related to 100mm laboratory scale samples

L_n-length of the in-situ sliding surface

u-uplifting weight of rock by the water pressure

τ_{ff}-maximum shear stress at which the rock mass can maintain the value of normal stress

R-movement rate

t-time

V_{mp}-velocity at the midpoint in the progressive stage

V_o-velocity at the onset-of-failure point

V-velocity

S-slope of the line

V_{col}-velocity at the failure point

A-slope of the line in the plot of inverse velocity against time

α-constant which define curve of the line in the plot of inverse velocity against time

t_0- time when the plot of inverse velocity against time starts

V_0- velocity when the plot of inverse velocity against time starts

t_f-time of failure

X-displacement

ε-strain

t_e-life expectancy

u-displacement rate

t_y-time in the pre-failure range

u_y-displacement rate in the pre-failure rage

`

T_{fp}-predicted failure time

T_f-actual failure time

t_m-time at each instant of predicting failure time

R_0-distance between radar and an object

c-speed of light

T_0-time between sending signal and receiving an echo

ΔR-range resolution

τ-pulse duration

B-bandwidth

$\Delta\phi$-cross range resolution

L-length of a radar antenna

λ-wavelength

d-displacement

t_w-flight time of wave

f-frequency

n-specific refractive index

$\Delta\phi_{def}$-change in phase related with displacement

$\Delta\phi_{atm}$- change in phase related with atmosphere

φ-phase

Acc-radar accuracy

N-number of accusations per hour

V_{min}- minimum measured velocity

$\Delta\phi_{snow}$- change in phase related with snow

Δh_{snow}-thickness of snow layer

v_{snow}- speed of light in snow

λ_{air}- wavelength in the air

Δd_{snow}-displacement recorded by radar related to snow

SSR – Slope Stability Radar

LKAB-Luossavaara Kirunavaara Aktiebolag

FS-Factor of Safety

GPS-Global Positioning System

`

LIDAR-Light Detection and Ranging

InSAR-Interferometry of Synthetic Aperture Radar

TDR-Time Domain Refractometry

3-D-three dimensional

CUSUMs-Cumulative Sum control charts

RMR-Rock Mass Rating

TARP-Trigger Action Response Plan

OOA-Onset Of Acceleration

TOF-Time Of Failure

LoS-Line of Sight

RS-Radar Sensor

LS-Linear Scanner

PSU-Power Supply Unit

FL-Field Laptop

DTM-Digital Terrain Model

`

1 Introduction

1.1 Background

To get to the ore, an open pit mine must be excavated to a depth, thereby creating man-made slopes that may be at a risk of slope instability. For this reason, it is necessary to properly design the slopes in the mine. But even the best construction can lead to instability due to unexpected conditions. Unstable slopes are dangerous for the people who are working in the open pit mine as slope failures may have potentially tragic consequences. Therefore, it is important to detect and alert movements of pit walls (McHugh, et al., 2018). Since the 1960's, various devices have been developed and implemented in open pit mines as slope stability monitoring tools. These devices allow determination of slope movements prior to a failure, therefore it is possible to apply suitable measures to mitigate the risk. The most efficient and effective devices are those ones which allow for a remote slope monitoring. Within this group of tools, the most outstanding is a slope stability radar (SSR), which has many advantages. The slope stability radar can provide real-time 24-hrs monitoring, has a high resolution and precision and doesn't require extensive labor. This thesis, therefore, presents data reviews and investigation done on the SSR installed at LKAB's Svappavaara mine at the Leveäniemi open pit.

1.2 Problem statement

Using SSR technology comes with its challenges. As this is intended to be an early warning system there is a necessity to define threshold values that will inherently affect the radar monitoring system to alarm or signal for action. Setting the threshold value range is a difficult task as it depends on many varied factors such as rock mass properties, geologic conditions as well as the geometry of the slope to mention but a few. This thesis, therefore, is intended to analyze and attempt to provide solutions to the above challenges through the following aims and objectives.

1.3 Aims and objectives

The aim of this study is to define the threshold value range that the SSR can be operated on at the Svappavaara Mine, Leveäniemi open pit. This task will be achieved through the achievement of the following sub-objectives:

- Increase an understanding of the operation of the SSR system by looking at several case studies from other areas in which threshold values for slope stability radar have been estimated.
- Establish operating procedures after completing reviews of the rock mass properties of the Leveäniemi open pit, and the slope parameters used to determine the slope responses to stress changes and its deformation patterns for the SSR at the Leveäniemi pit.

1.4 Scope of the study

The Leveäniemi open pit presents a unique opportunity to study the operation of the SSR. In this pit, the western wall has a potential for slope instability due to the existing geologic structures. This study is limited to the monitoring of the southern and western walls of the Leveäniemi pit.

In addition to estimating threshold values at which the SSR will operate effectively, this study is also scoped to review rock mass parameters that may directly or indirectly influence the deformations in the pit slopes.

`

1.5 Overview of the study area and field investigation

The Leveäniemi Open Pit is located in Norrbotten County, in the Swedish Lapland (Figure 1), near the village Svappavaara. Leveäniemi is one of three projects owned by Luossavaara-Kirunavaara AB (LKAB) in the Svappavaara area. The mine had been closed in 1984 due to economic reasons, but in 2010 LKAB decided to reopen and start production again. The iron content within the orebody is 44%. The yearly production of the ore is 12M tonnes. The mineral resources are estimated at 113 million tonnes in total proven and probable resources. Planned life of mine is 20 years, until 2035.

Figure 1 Location of the Leveäniemi Open Pit

The Leveäniemi deposit is a magnetite, iron ore deposit. The orebody is classified as magnetite-apatite ore and belongs to the iron-oxide-copper-gold (IOCG) deposits. The deposit is hosted by highly-deformed schistose metasediments and metavolcanics rocks of the Svecokarelian orogen. The ore appears as massive and as veins or breccia of magnetite. Host rocks show varying degrees of an alteration, potassium feldspar alteration and tremolite, magnetite alteration are common. The deposit is strongly affected by foliation. There are two main fold

`

occurrences: shear zone-related folds and gentle folding, creating large-scale undulating structures in some areas of banding in Trachyandesites (SRK Consulting, 2014).

The ore is exploited by open pit method, using drill and blast excavation. Using shovel excavators and wheel loader, the ore is loaded on trucks. After an extraction, the ore is subject to the comminution process, where ore is comminuted by a crusher and then mills. Ore is process using magnetic separators and flotation , later pelletized and sent to customers.

`

2 Literature study

2.1 Open pit slopes and their stability

Surface mining is a type of mining method used when the orebody is located near the surface, covered by a layer of the soil and the rock, which must be removed (called stripping) before extraction of the ore. One of the most common methods of the surface mining is an open-pit mining. For this type of ore excavation, it is necessary to form slopes. Slopes are optimized to be steep enough to gain access to the ore at a reduced cost of stripping, but flat enough to prevent slope failure. The slopes are planned to guarantee a low-risk level of injury and equipment damage caused by falling rocks and slope failures. A proper design must include an influence of geologic structures, rock mass properties, and hydrogeologic conditions. The main components of the slope design are (Figure 2) (Sullivan, 2006): a bench and a berm geometry, the inter-ramp slope angle and height and the main slope angle and height.

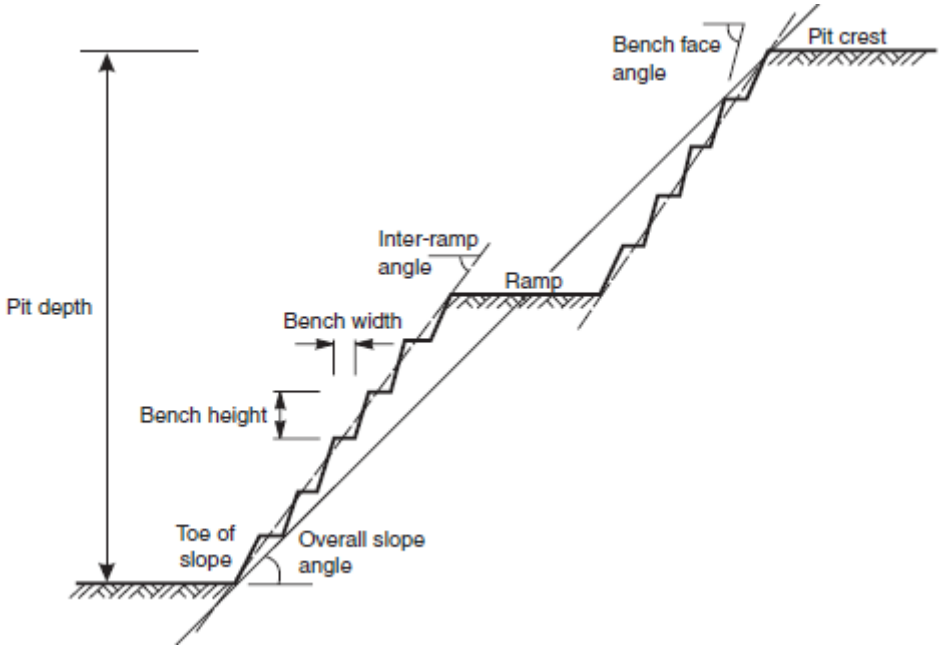

Figure 2 Main elements of the slope (Sjöberg,1999)

Movements of the ground in open-pit mines is mostly caused by blasting and stress response to an excavation. The movement is tolerable if it is not unexpected or disastrous. In big open pits, slope failures can have a catastrophic effect (Harries, et al., 2009). From the economical point of view, as pointed out above, pit walls should be as steep as possible to ensure a minimal waste removal and maximum ore extraction. Nevertheless, steeper slopes cause the higher potential of the slope instability (McHugh, et al., 2018).

The state of the slope stability depends on two forces: driving forces and resisting forces. Driving forces push the slope downwards, whereas resisting forces stop the movement. When driving forces exceed resisting forces the slope is unstable. Driving forces are mainly caused by gravity. Opposite to the gravity force is the shear strength, which produces a resistance (Watkins & Hughes, 2018). There are a few factors that influence driving and resisting forces and therefore the slope stability: slope geometry, especially a slope angle and a slope height; presence of geological structures for example: joints, faults or a foliation; a lithology, a water

`

level; type of a mining method, dynamic forces due to vibrations, blasting or seismic events; a cohesion; an internal angle of friction; a rock mass strength properties.

2.1.1 Shear strength of discontinuities

A possible sliding surface will be identified by the definition of its most important discontinuity characteristics, this includes cohesion and frictional angle. Other characteristics include surface roughness, length and thickness, and properties of an infilling. Moreover, it is necessary to check how water will affect an infilling.

In many cases rock slope designs are based on the Coulomb theory (Figure 3), where a slope shear strength of the sliding surface can be defined using an angle of friction (ϕ) and a cohesion (c).

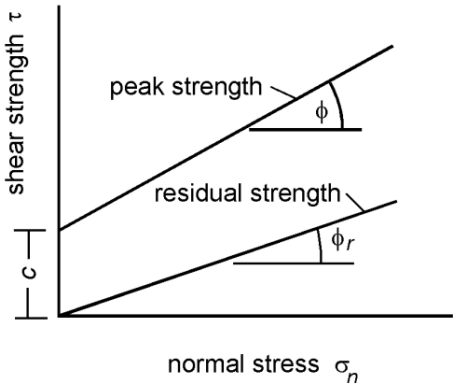

Figure 3 Mohr plot of peak and residual strength (Hoek, 2006)

For planar sliding surfaces, a plot will usually fall along approximately linearly. The peak shear strength line is equal to a friction angle of the rock surface and intercepts with a shear strength axis. The point of interception represents cohesion of the infilling material and is independent of the normal stresses. The peak strength can be described as the Coulomb-Mohr equation:

$$\tau = c + \sigma_n tan\phi \quad (1)$$

Where c is a cohesion, σ_n is a normal stress and ϕ is an angle of friction.

For the residual strength, cohesion is vanished due to a broken cementation of infilling material. Moreover, the friction angle is smaller than this in the peak shear strength, because a shear displacement causes shearing of irregularities and makes a sliding surface smoother and lower. The residual strength can be described by the following equation:

$$\tau = \sigma_n tan\phi_r \quad (2)$$

Where ϕ_r is the residual friction angle (Hoek, 2006).

The friction angle of a rock material is an important characteristic for the shear strength along discontinuity surfaces. For a planar, without infilling discontinuity, there is no cohesion and the shear strength is only defined by the friction angle. It is connected to the size and shape of grains at a fracture surface. Rocks with fine-grained material or with a high mica content are going to have a low friction angle, whereas rocks with the coarse-grained material, such as granite, has a high friction angle (Wyllie & Mah, 2005).

Every natural discontinuity surface has some level of roughness. As shown on the Patton's equation (3) asperities and irregularities have a big influence on the shear strength, which it effects a stability of the rock mass (Hoek, 2006). Depending on the scale it is possible to

`

distinguish two types of asperities (Figure 4): first-order (major irregularities) and second-order (small bumps and ripples), which has usually higher i values.

$$\tau = \sigma_n \tan(\phi + i) \tag{3}$$

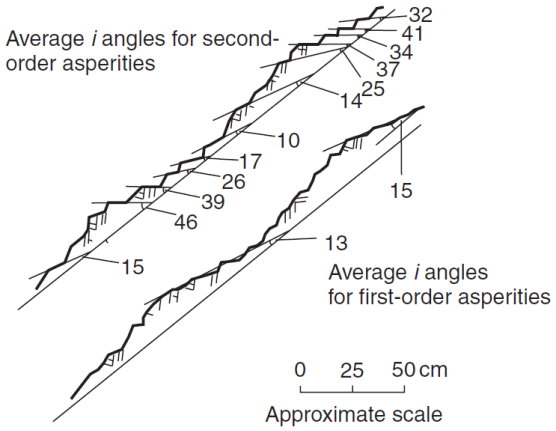

Figure 4 Classes of asperities (Wyllie & Mah, 2005)

A rough surface, which is originally undisturbed has the peak friction angle of (ϕ+i). When the normal stresses and displacement growth, the asperities will be sheared off. The initial friction angle will slowly decrease to the residual value of a rock friction angle (Wyllie & Mah, 2005).

Barton studied the behavior of the shear strength. Based on the Patton's equation, Barton defined equation, where includes joints characteristics:

$$\tau = \sigma_n \tan\left(\phi + JRC \log_{10}\left(\frac{JSC}{\sigma_n}\right)\right) \tag{4}$$

Where σ_n is the effective normal stress, JRC is the joint roughness coefficient, JSC is the joint wall compressive strength.

Values JRC and JSC are affected by a scale effect. When a size of discontinuity increase, both values are less correlated. It is because small-scale roughness has a slight influence on large discontinuities and large ripples have a bigger influence than roughness, which is related to first- and second-order asperities. Barton and Bandis proposed two equations, that decreases the effect of scale:

$$JRC_n = JRC_0 \left(\frac{L_n}{L_0}\right)^{-0.02JRC_0} \tag{5}$$

and

$$JRC_n = JRC_0 \left(\frac{L_n}{L_0}\right)^{-0.03JRC_0} \tag{6}$$

Where JRC_0, L_0 (length) are related to 100mm laboratory scale samples and L_n is a dimension of the in-situ sliding surface. (Wyllie & Mah, 2005)

The big influence on the shear strength is the infilling of a discontinuity, which can influence the cohesion and friction angle of a discontinuity surface. The shear strength of an infilled discontinuity is mostly modified by thickness and characteristics of the infilling material. Infilling materials can be divided into two groups: clays (whose friction angle is between the

`

range of 8 and 20 degrees, and cohesion values from 0 up to 200 kPa, some clays can have a high cohesion even up to 380 kPa) and faults, shears and breccias materials such as granite, diorite, basalt (which friction angle varies from 25 to 45 degrees and cohesion values from 0 up to 100 kPa).

Another important parameter, which affects the shear strength is water. The water pressure does not change the cohesion and friction angle, but it decreases the normal stress by uplifting the weight of rock by the water pressure u. Reduced normal stress is called the effective normal stress. The shear strength with the water pressure effect can be presented as follow (Wyllie & Mah, 2005):

$$\tau = c + (\sigma - u)\, tan\phi_p - peak\ strength \tag{7}$$

or

$$\tau = (\sigma - u)\, tan\phi_r - residual\ strength \tag{8}$$

2.1.2 Limit equilibrium method

The ratio between driving forces and resisting forces (9) is a factor of safety (FS) and it is related to the Coulomb-Mohr theory of limit equilibrium (Figure 5). It is used to define if the slope is stable or not.

$$FS = \frac{Resisting\ Forces}{Driving\ Forces} = \frac{\tau_{ff}}{\tau} \tag{9}$$

Where:

τ_{ff} – the maximum shear stress, at which the rock mass can maintain the value of normal stress of σ_n,

τ-actual the shear stress loaded on the rock mass

This equation can be written in another form:

$$\tau = \frac{c}{FS} + \frac{\sigma_n tan\phi}{FS} \tag{10}$$

Where:

c-cohesion

ϕ-friction angle (people.eng.unimelb.edu.au, 2018).

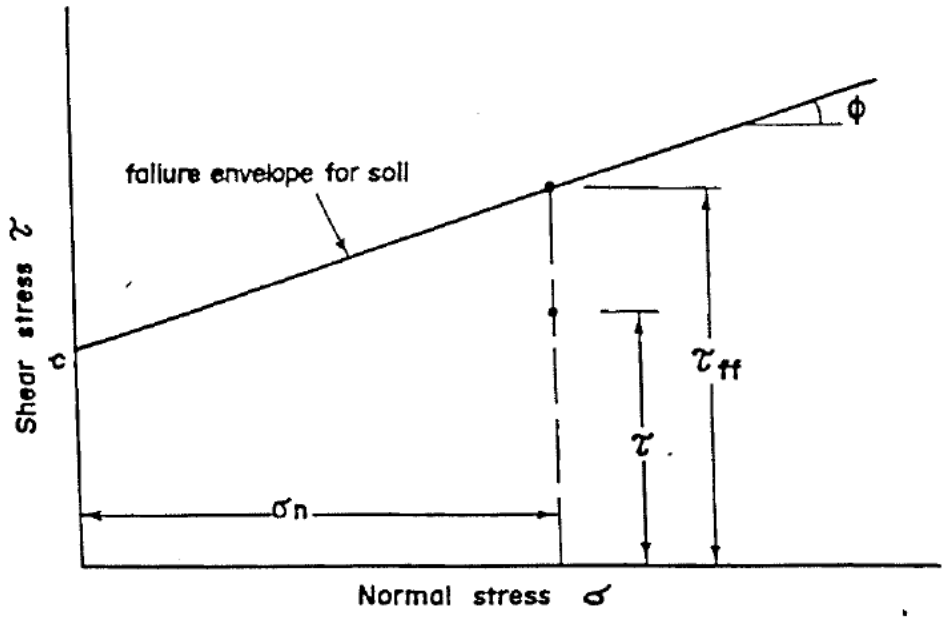

Figure 5 Coulomb Mohr diagram

To estimate the FS it is required to take into consideration many aspects, such as the life of the slope (long-term vs. short-term), a permissible outcome of the slope failure, a geometry and a state of a foundation, a type and a structure of the slope material, a knowledge about the shear strength parameters within the slope and type of analysis method used for calculation. All those parameters are specific to the site and based on the engineer experience. Therefore, it is difficult to do establish one, universal technique for all cases (Chaulya & Prasad, 2016).

Theoretically, FS bigger than one is adequate for stable slopes, but from a practical point, the input data must be a base of FS. The usage of FS depends on the life of the slope, for short-term slopes stabilities analysis FS must vary between 1,2 to 1,3, whereas for long-term slope stability analysis between 1,4-1,5. For calculation, it is better to use lower realistic values, which are the fundaments of the design procedure and average values of mechanical parameters (Fleurisson, 2012).

2.1.3 Requirements for slope stability

Slope failures are a common problem in many open pit mines. The instability of slopes can cause a quarantine of the ore reserves exposed to a risk, while it causes big financial and production losses. The unexpected failure of the slope could lead to death or serious injury of employees, damage to mining equipment and disturb the mine plan (Harries, et al., 2009). It is important to protect miners against slope movement. There are three main types of protection: a proper geotechnical design; rockfall catchment, support and stabilization systems; monitoring systems (J. M. Girard, 2002).

Slopes are designed in the way that geometry will guarantee a safety of the structure and minimal financial cost of excavation- minimizing the rock mass volume, which must be excavated. This leads to choosing a proper factor of safety which determines an optimum design of the slope (Kumar & Villuri, 2015). Support methods improve the rock mass strength and catch benches will decrease the number of rock falls. Despite that, even in the most carefully designed and supported slope may occur the failure, due to unknown geologic structures, unexpected weather patterns, or a seismic shock (J. M. Girard, 2002). Therefore, it is essential

`

to provide a continuous monitoring and examination of the slope, to ensure a quick slope failure detection and connected with it hazard risk (Kumar & Villuri, 2015).

2.2 Slope failure

Mercer (Mercer, 2006) describe the definition of "collapse", "functional failure" and "instability":

> *"Collapse" is defined as the complete overall loss of rock mass integrity and*
>
> *structure.*
>
> *"Functional failure" is defined as the situation where a slope cannot perform the function for which it was intended. This implies that it does not necessarily involve overall collapse although localized sections of the structure may have collapsed. Examples would include haul roads and ramps.*
>
> *"Instability" is defined as any other deformational movement or behavior that does not involve collapse and/or functional failure.*

Even the best design can fail due to unexpected conditions in the slope, such as intensive rainfalls or undefined geological structures. Geotechnical engineers have many indications that the slope is unstable and soon can collapse. Prior signs of the possible slope failure are openings of cracks on the wall surface and crest, audible cracking, fracturing, rolling of loose material and increased trickling of spoil from the rock face. It is problematic to forecast the development of those signs, especially with high walls and in-pit, because the slope movement may increase the speed with small or without warning. Therefore, mines must use more reliable methods to allow to work close to a potentially unstable slope, employees, and equipment. The careless decision could influence on the mine productivity and security (B. Reeves, 2001).

Based on basic structural geology it is possible to understand slope behavior. There exists four-time dependent strain reactions on rocks (Figure 6):

1. Instantaneous elastic and\or plastic creep,
2. Transient creep at a decelerating rate (primary),
3. Steady-state creep (secondary),
4. Accelerated creep prior to failure (tertiary) (Ramamurthy, 2010).

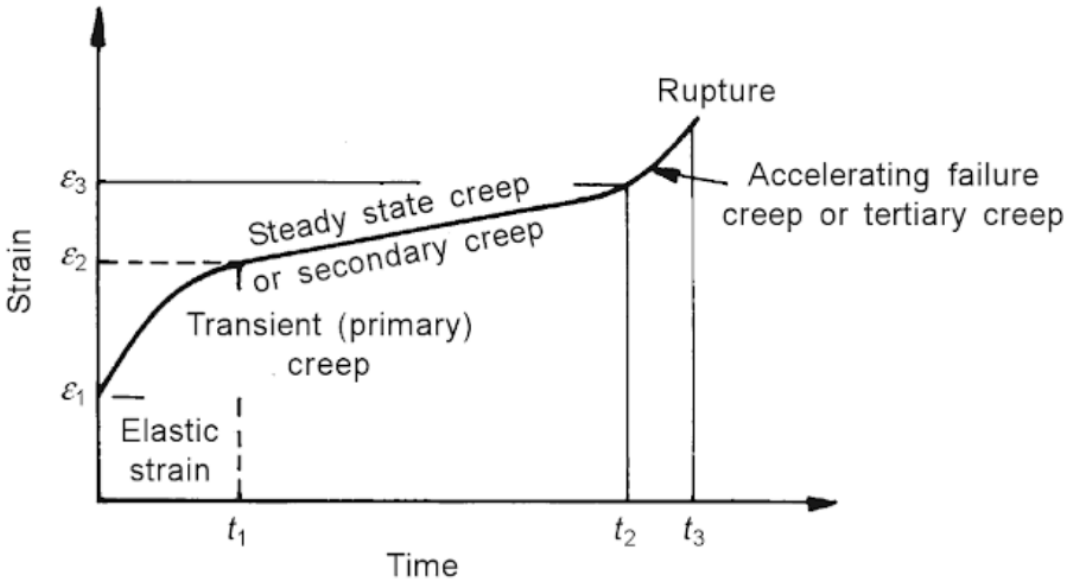

Figure 6 Creep curve (Sullivan, 1993)

Based on that, Sullivan (Sullivan, 1993) divided horizontal slope movements into four types: elastic movements (depended on the rock type displacement for hard rocks or shallow is in scale of mm and mm to m scale in deep and/or soil/soft rock), creep movements (10s to 100s mm), cracking and dislocation (0,2 m to few meters) and collapse (greater than 0,5 m).

Using those classes Sullivan made ground reaction curves, where he plotted movements against a pit depth (Figure 7). Curve 1 shows failure (wedge or plane) where the failure is prone as the pit depth is increasing. Curve 2 represents situation when with increasing a pit depth a risk of failure also grows, where the final stage is the slope collapse. Curve 3 represents conditions when, deepening a slope can react as a creep movement, which is not leading to a failure. Curve 4 presents plastic movement. Displacements of elastic and creep movement are small and do not disturb a mining operation. During the cracking and dislocation phase, a movement could not affect a mining activity until effects will be dangerous and lead to failure.

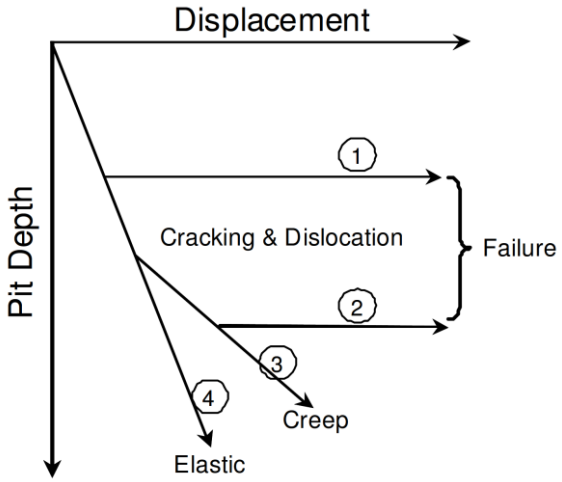

Figure 7 Ground Reaction Curves (Sullivan,2007)

`

In the past, post movements and a post-slope behavior after a slope failure were receiving smaller attention. Usually, after a failure material falls down to the pit, is cleaned up and a mining activity comes back to the pit. However, there exists a type of failure that not simply accelerate until the point of collapse and then after a failure stops to develop. “Liquefaction type failures” which occurs in the post-failure period are very dangerous. In this failure, type deformations are very large with high velocities. The mechanisms of the movement change from rock mechanics into fluid mechanics. This example causes that Sullivan adds the fifth stage to his model – a post failure deformation (Figure 8).

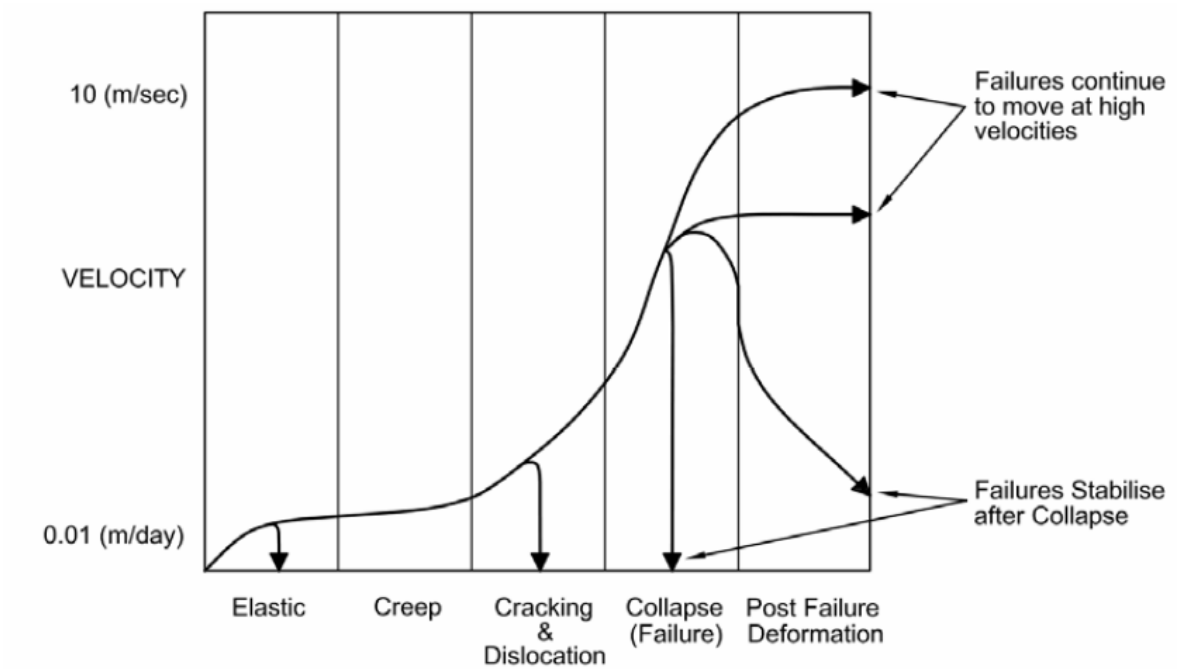

Figure 8 Slope movement stages (Sullivan, 2007)

Martin (Martin, 1993) developed models in which he describes a time behavior of slopes. He distinguished three stages of deformation (Figure 9):

1. Initial response
2. Strain hardening
3. Progressive failure

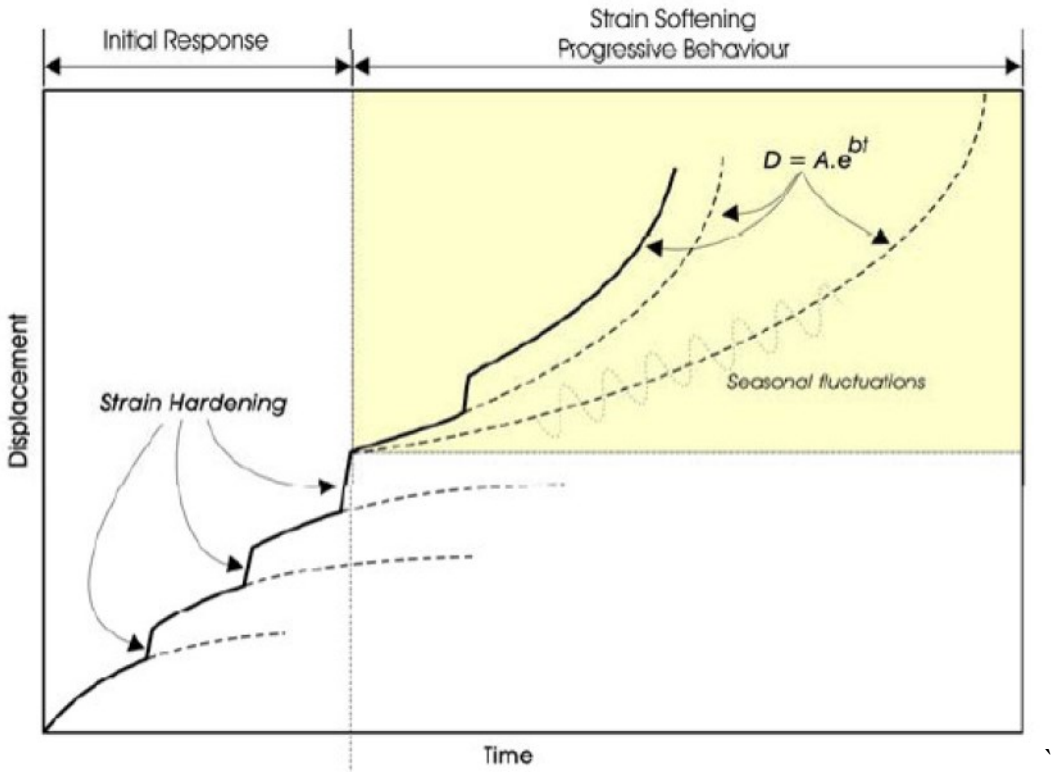

Figure 9 Typical time-dependent behavior (Mercer, 2006)

The excavation of rock mass creates stress changes, which appear as slope initial response period - a consequence of the elastic rebound, relaxation, and/or dilation of the rock mass. The initial deformation or rebound takes place usually without any extension signs of a specified surface failure or the failure mechanism. Development of the slope rebound and an extension is made along joints in the rock mass or along weak discontinuities (Kliche, 2011). The initial response movement has a spread between 0.10 to 4 mm/d, but even higher rates could occur at the precise time of excavation. At the time of the initial response period, the rate of movement decelerates with time and finally drops to zero. This deceleration of movement can be described by a followed formula:

$$R = A * e^{-bt} \tag{11}$$

Where:

R –is the movement rate and t-time (days).

A and b- are fixed indicators - functions of the rock mass characterization, slope properties: the slope height and the slope angle, mining rate, external forces, and failure mechanism. Values of A are distributed between 0.113 and 2.449 when values for b vary from 0.0004 to 0.00294 (Zavodni, 2000).

If the slope failure is going to take place after the initial response, one or more tension crack(s) occur(s) close to or in the slope crest. The progress of those cracks is an indicator that the slope is at the balance limit - driving stress (forces) are the same as or higher than the resisting stress (forces). During limiting equilibrium, a growth of the driving stresses (forces), a reduction of the resisting stresses (forces), or by changing both the driving and resisting forces (stresses) lead to a lower slope stability.

`

Strain hardening can be described as “locking up the rock mass through dilation” during all available shear strength of the rock mass or the sliding surface is mobilized. In this stage after a short period of an increased movement rate the movement decreases. Mobilization of shear strength increases the slope stability. There can be few stages of a strain hardening, as a reaction for a mining operation.

In the progressive failure stage (strain softening) the shear strength of a rock mass or sliding surfaces decreases, where a displacement or a strain grow. This effect can be increased by external factors such as rainfall or blasting and results as an acceleration of movement until a slope failure (Martin, 1993).

As is stated by Broadbent and Zavodni (Broadbent & Zavodni, 1982) the final decision of the monitoring system, if failure will occur or not, depends on the rate of deformation and relaxation. The graph of time versus displacement may be used for the classification of mine slope failures. Broadbent and Zavodni (Broadbent & Zavodni, 1982) described three types of deformation: progressive deformation, regressive deformation, and transactional deformation. Sullivan (Sullivan, 1993) add a fourth type – a stick-slip (Figure 10).

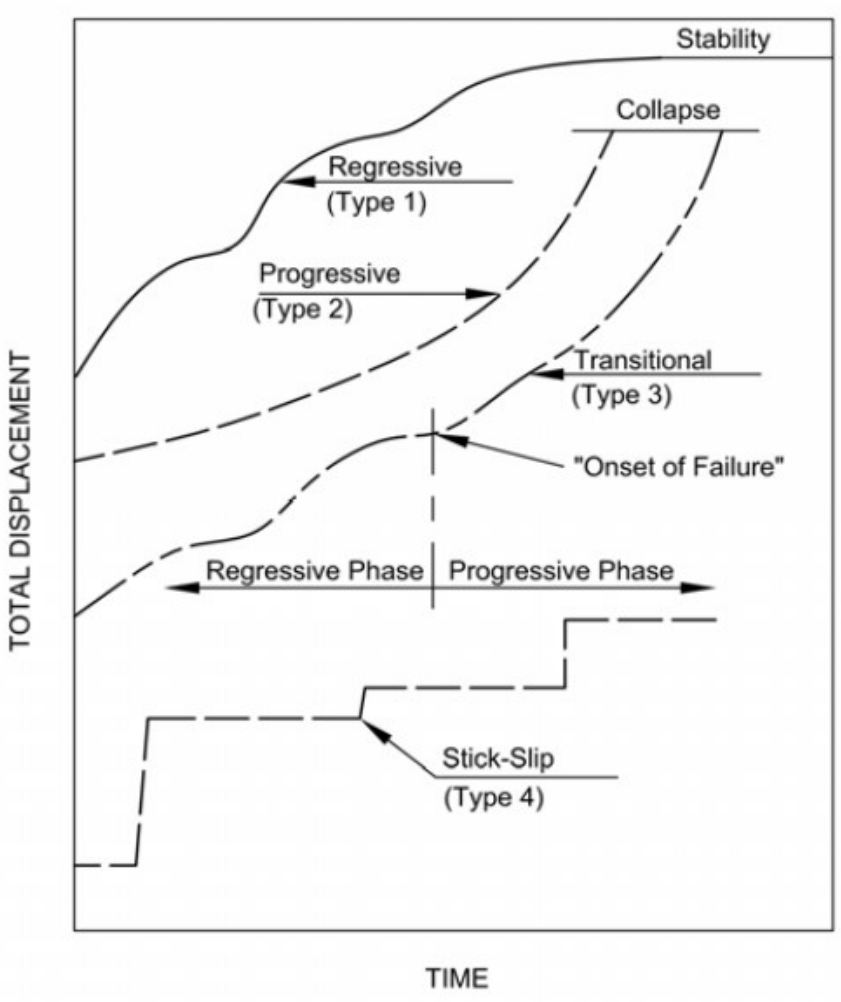

Figure 10 Typical displacement vs time graph curves (Sullivan, 2007)

The state of slope stability depends on the type of deformation. If in the slope the regressive type occurs, it means that the slope failure decelerates. The progressive deformation is the opposite, the slope failure has an accelerating rate, which can be algebraically predicted, to the

`

point where the slope will collapse if any control measures are not taken. The third type of deformation is the transactional deformation (regressive/progressive) (Zavodni, 2000).

The curve type 1 located on the top of the plot presents the regressive displacement. It is a series of accelerating or decelerating movements trends. The deceleration of each trend between external impulse distinguishes this curve as a regressive. When the driving force influences (stress) for a short time more than resisting force(stress) the slope is considered as a start point for those cycles. During this situation, the slope stability drops a bit below the safety factor of 1. If the external disturbance would be removed, the velocity of displacement will stop. The external event such as a mine blast, earthquake, precipitation event, temperature change, groundwater pressure change, or excavation of buttressing rock is usually the reason, that the driving force is superior to resisting force. Typical for this type of system is that the slope with time is going to be more stable and movement is slowing down or the slope has stick-slip behavior. Another characteristic of the regressive system is that the ratio of driving stress to resisting stress is smaller with the displacement (Kliche, 2011).

The second type of deformation is the progressive deformation (type 2). The nature of this movement is a continuous acceleration until the point, where the slope collapse. It is possible that cycles of deaccelerating would occur, but they are almost indistinguishable in long-terms. Zavodni states that the progressive displacement of extensive failures occurs in a short period of time, usually 4-45 days (Zavodni, 2000).

The third type of deformation is the transactional deformation (regressive/progressive deformation). It takes place when the regressive form of deformation transforms into a progressive form and lead fast to collapse as shown in Curve type 3. This transformation takes place when is for example excavation of rock at the toe of a slope, mining of sliding surface, breakup, or an increase in water pressure (Kliche, 2011).

The stick-slip deformation (type 4) is defined by sudden movements, followed by time without or with a small movement. The slip part can be caused by an event such as rainfall or blasting, whereas the stick stage is a strain hardening (Sullivan, 1993).

This classification has some limitations. It cannot be a representative tool for longer time range displacements where the movement is accelerating. Moreover, it shows that prior to a failure there is always a long period of time with movement and an extensive displacement. In this categorization is the lack of other types of movement patterns. For all those reasons Sullivan ((Sullivan, 2007) established a new classification system. He divided pit slope movements into three phases: pre-failure movements, failure movements, and post-failure movements as presented in Figure 11. This classification has few advantages: presents a wide range of movements types that can lead to the onset point of failure, allows to distinguish different type of accelerations at the failure stage and categorize post-failure behaviors.

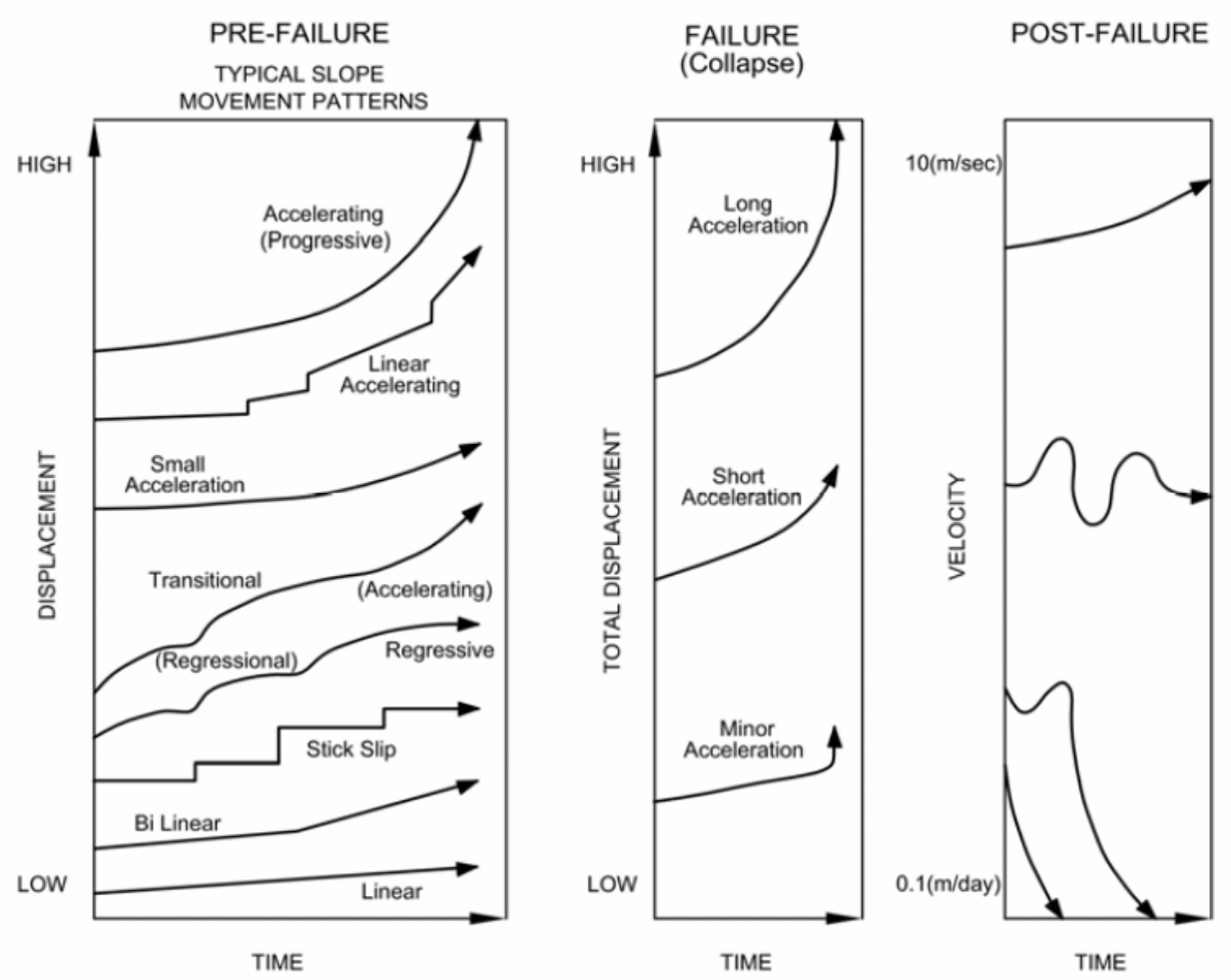

Figure 11 Modified failure classification system (Sullivan, 2007)

Mercer (Mercer, 2006) during his detailed research noticed that each rock slope is different and there are not existing two slopes that behave in the same way. He found out that there are two categories of a pre-onset-of-failure behavior. To the first category, he classified those failures which are related to a macro event (a mining operation), where on-set-failure depends on the rate at which a mining remove a material which acts as a buttress and control stability. The second category includes those failures which are not related to a macro event and occurs without a prior warning in the deformation pattern. Often those failures are related with the micro event (blasting, excessive rainfalls), joint stiffness, crack propagation and/or related with time a decrement of the static coefficient of friction. Usually, second category failures take place as small, fast rock failures which develop in “hot spots” in the slope and can occur on a slope above the pit floor.

Mercer develops a deformation behavior model using numerous rock mass deformation case studies spread across the World and correlate them with each other. He suggests to divide that time and event deformations can be classified into five stages (Appendix 3):

- Stage 1: pre-collapse, primary rock mass creep modes,
- Stage 2: pre-collapse, secondary rock mass creep modes,
- Stage 3: post-onset-of-failure to collapse behavior modes,
- Stage 4: post-collapse behavior modes,

`

- Stage 5: post-mining/recovery behavior modes.

Stage 1 and Stage 2 are characterized by sudden acceleration, after which comes a deformation reduction, which finally goes back to zero. In Stage 1, the recovery period is short and ends up with a steady creep phase. In Stage 2 the recovery period is longer and does not come to a steady creep phase. Both Stages can be defined as a regressive behavior and it is difficult to distinguish the exact point of transition between a stages change.

During Stage 3 the deformation has a progressive behavior. An acceleration of deformation is constant until the point where is a slope failure.

Stage 4 takes place after the failure, but before recovery of failure or mining starts. The recovery can be a complex process. Mercer in his research defined six principal modes.

Stage 5 represents a deformation behavior when slope does not collapse and recover to stabilization.

2.3 Failure classification

The worst scenario is when the deformation leads to the slope failure. There are four main types of failures which occur in the open pit mining and road slopes, which differ by the acceleration of movement and the point of failure. These are plane, wedge, toppling and rotational (B. Reeves, 2001). Additionally, it is possible to distinguish rockfalls as a type of failures

2.3.1 Rotational failure

The rotational failure occurs when the rock material slide along a curved surface as a circular arc or non-circular curve (Figure 12 a and b). Those types of failure depend on the homogeneity of the soil, the circular type develops in the homogenous soil, whereas the non-circular in non-homogenous soil (Priya, 2016). It occurs mainly in regions with interbedded strong and weaker rocks or between permeable and impermeable rocks. The main cause is strong rainfalls which can lead to undercutting the layers (Queen University Belfast , 2018).

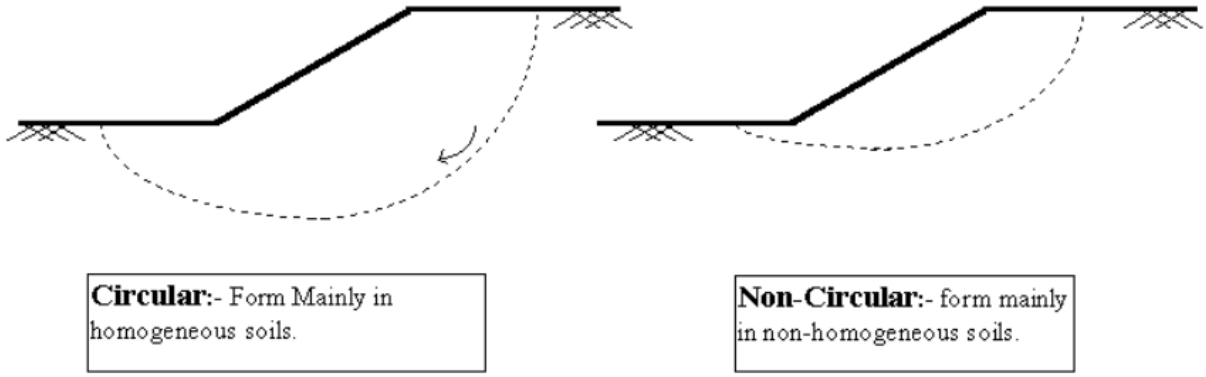

Figure 12 a and b Types of the rotational failure (Priya, 2016)

2.3.2 Plane failure

The plane failure (Figure 13) slides along the failure surface. It is a reaction to a single discontinuity. As Fleurisson described, plane failure is a result of one of the following geological formations: bedding joints in sedimentary formations, foliation or schistosity planes in metamorphic formations or a crack or a lithological contact between clayey weathered rocks

`

and bedrock (Fleurisson, 2012). Plane failure needs to meet some requirements for it to occur: the strike of the sliding plane and the strike of the slope face must be situated parallel (with an angle of ±20°) to each other, the dip angle of the slope face should be greater than the dip angle of the failure plane and the angle of friction φ is smaller than the dip of the sliding plane (Priya, 2016).

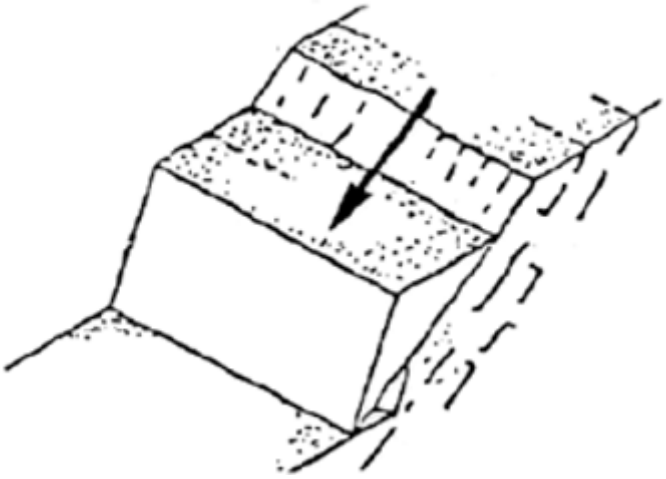

Figure 13 The Plane Failure (Reeves, 2001)

2.3.3 Wedge failure

This type of a failure occurs when the failure slide across at least two intersecting sets of discontinuities (Figure 14). The lines of intersections nearly perpendicular to the strike of the slope and decline in the direction of the plane of the slope. Preferable lithologies where the wedge failure takes place is inclined bedding, foliation, and well-defined cleavages. The most favorable rocks are shale, limestones, and slate. The requirements which need to fulfill that the wedge failure occurs are: the angle of friction of the joint slope surface must be smaller than at least one of dip angles of intersections; the dip angle of the slope surface should greater than the dip angle of the intersection-daylight on the slope and the friction angle of the slope should be smaller than the plunge line of intersection (Prajapati, 2017).

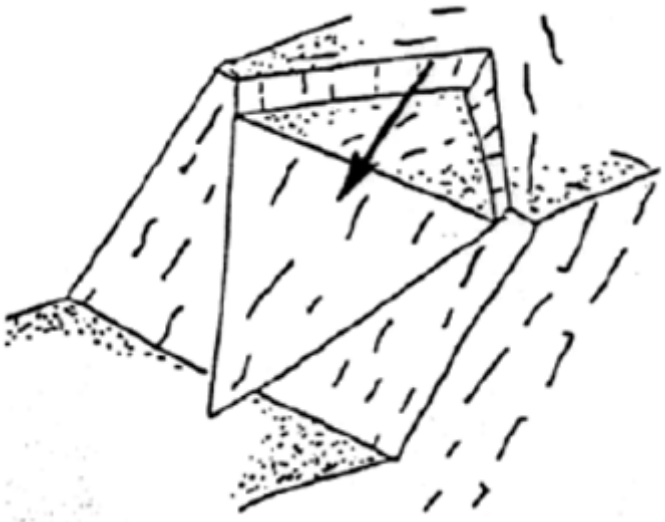

Figure 14 The wedge failure (Reeves, 2001)

`

2.3.4 Toppling failure

Toppling failure (Figure 15) takes place in the steep dipping discontinuities, where rock columns rotate around a point in the base of the slope and layers between discontinuities slip down. The toppling is due to the center of gravity of columns is outside of a point in the base of a slope. One of a reason for the toppling failure development is an overburden removal or a confining rock, which can lead to a constraining stress decrease. The main condition for the toppling failure is a rock mass nearly located to each other with a steeply dipping discontinuity series. There are three types of the toppling failures: flexural toppling, block toppling and block flexural toppling (Prajapati, 2017).

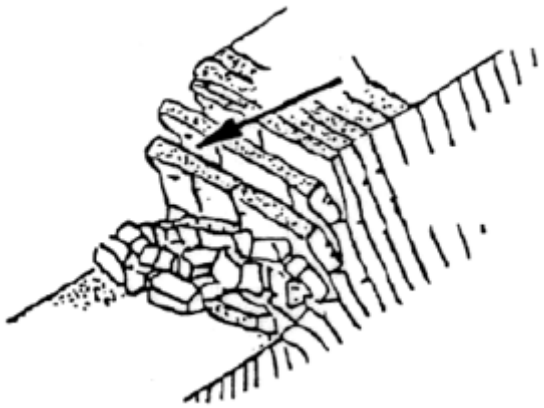

Figure 15 The toppling failure (Reeves, 2001)

2.3.5 Rockfalls

Rockfall is a block a serious of blocks which is detached from the rock face (where is small shear resistance) and freely falling down causing damages. It can force out loose rocks or slam into other falling rocks causing more falls or landslides. It is caused by changes in forces on a slope. The main reason is weathering, an erosion or an increment of water pressure (www.civildigital.com, 2018).

2.4 Slope monitoring

All excavations (natural or artificially made), change shape and deform with time as a reaction due to stress reorientations (Kliche, 2011). The most suitable determinant of an unstable slope is the quantitative measurement of outward movement and acceleration of material as a mechanism of the instability builds up. There are clear proofs that earlier movements of a rock wall appear for a long time (weeks, months) before a slope collapse (N. Harries, 2009). A dangerous slope instability condition is mostly related to a progressive development of one or more tension cracks behind the slope crest. This move of the slope allows for the time-displacement slope monitoring (Zavodni, 2000). Practically, all slope monitoring methods use the slope acceleration to identify a possible failure (Wyllie, 1979).

Main purposes of the slope monitoring are: avoid human loss of life or injury, prevent against damage to equipment , provide better maintenance for slope regions which are examined, determine deformation (to analyze if a monitored part of a slope behaves as planned), provide preventive support (if an observed area doesn't behave as planned, slope monitoring provides controls for measures to be undertaken, which can mitigate a problem), allow to meet law requirements (in places, where is a strict safety law, it is obligatory to have a slope monitoring

`

system in open-pit mines) and collection a data which is used in deformation models or other researches (Toit, 2015).

To achieve that, a monitoring system should meet some requirements. A slope monitoring system should protect a whole mine against all possible dangerous movements of soil and rocks and provide early warning before the failure occur. To ensure that, it is required to determine a slope movement with sub-millimeter precision. This accuracy is required to carry out exact measurements of a slope deformations and raise an alarm about wall movements. If a measurement is unprecise, this can lead to a failure development on a slope or a pit wall. The level of an accuracy should be at least 10mm, but the accuracy of 0,1 mm is more favorable. An equipment should be easy in use and doesn't cause any problems as like as delays or obstacles in a mine operation to allow to keep a production on a schedule (Kumar & Rathee, 2017).

A monitoring system must cover effectively an area part, or all of the open-pit and detect all types of failures, no matter if it is circular, plane, wedge, toppling or rock mass failure. This condition is important to give suitable preventive measurements. Furthermore, only a continuous, 24 h per day measurement, which can withstand all weather conditions, provide a full slope stability protection. Moreover, geological engineers need to understand a structural geology of an area, climate, groundwater, in situ stress conditions, rock mass strengths and seismicity to assess a rock failure mechanism (Kothari & Momayez, 2018). Those factors allow for better awareness about the geomechanics of a slope deformation and implement an early warning for a people and equipment evacuation from a mine, which minimizes a risk for a mining stuff, maximize a production and give a higher profit due to a lower number of downtimes (Kumar & Villuri, 2015).

It is important that the data is collected, analyzed and interpreted correctly. A wrong interpretation could lead to poor decision making. Relaying of false information must be avoided, because it may cause wrong or unnecessary alarms in the mine, or even lead to quarantining dangerous areas. In addition, data analysis should be relatively easy and fast for the operators, that they can make a suitable and exact risk assessment (Kumar & Rathee, 2017).

Monitoring methods can be divided into four categories as shown in Figure 16. Some of those methods can be classified into two different groups.

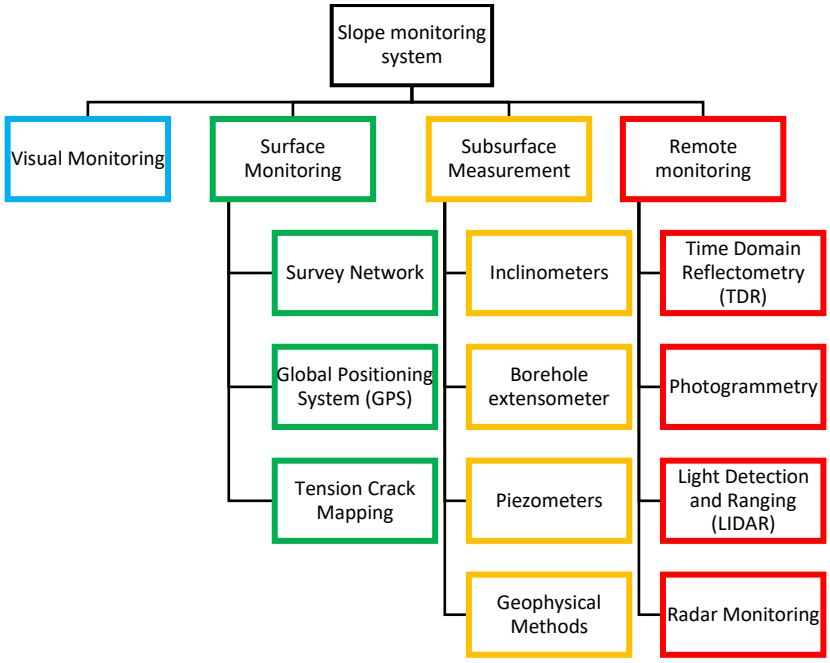

Figure 16 Slope monitoring system (Osasan, 2012)

A visual inspection is a primary method of slope monitoring. As a daily routine, the geotechnical engineer inspects the areas where is a possible slope failure danger by comparing prior inspections with the last one to find visual slope changes and possible areas of an instability. Mainly the geotechnical engineer checks the stability of the slope by inspecting the pit, access ways, high wall, low-walls. Not only the geotechnical engineer must do the inspection. For safe production, any other workers involved in the mine operations have to report about changes in the slope face.

Surface monitoring includes all methods which can define surface changes of the monitor area for example position changes of reference points, cracks propagation and movement of Global Positioning system (GPS) antennas. The main techniques are a surveying, a GPS and cracks monitoring.

Using subsurface measurement techniques is possible to observe changes in rocks conditions and parameters below the ground. It is possible to measure the type, size, and rate of the slope deformation, determine shear zones, monitor groundwater conditions, rock electric characteristics or seismicity of the area. The main methods are inclinometers, borehole extensometers, piezometers, and geophysical methods.

All remote monitoring methods observe slope movements from a certain distance. It does not require physical contact to track changes on a slope. It collects data by using advanced technology such as lasers, an interferometry or a photogrammetry. The most popular methods are Light Detection and Ranging (LIDAR), Interferometry of Synthetic Aperture Radar (InSAR), Time Domain Reflectometry or Slope Stability Radar (SSR). All those methods are described in following subchapters.

2.4.1 Time Domain Reflectometry (TDR)

A Time Domain Reflectometry (TDR) is an electrical method of measurement slope instability similar to a radar. It consists of two elements: a combined transmitter/receiver (TDR cable tester) and a coaxial cable (Figure 17). An electrical pulse is sent by a cable tester along a coaxial cable located in a borehole. When a pulse finds a discontinuity in a cable, it is reflected.

`

A system can detect a discontinuity location, a magnitude and a rate of deformation (Kane, et al., 2001).

The main advantages are a cheap installation, a possibility of continuous monitoring, a remote data collection, a longer lifetime than inclinometers, whereas main disadvantages include a necessity of using surface devices for proper measurements, no information about a direction or a discontinuity orientation, this method requires proper grouting, it can be used only to localize shear deformations and it cannot be used for significant measurements (>2cm/a) (Work Package 6, 2008)

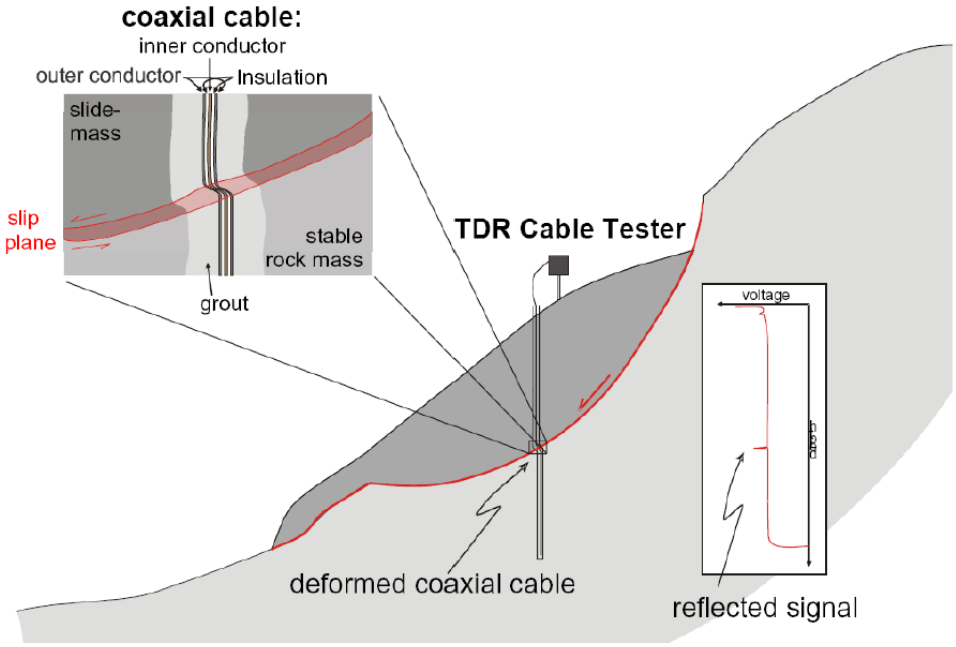

Figure 17 Basic setup of TDR (Work Package 6, 2008)

2.4.2 Photogrammetry

In a photogrammetry, a mine is photographed from two different locations to acquire various lines of sight from each place. Photos can be taken by satellites, cameras, drones, aircraft, helicopters. There are used to produce three-dimensions (3-D) images of a mine. It allows to marked joints, faults, dikes, potential failure faces and other discontinuities on an image. This procedure is repeated in the same intervals. Comparison of 3-D images of a mine gives a possibility to discover a discontinuities developments or new discontinuities. It is a cost-effective, a labor-saving method of slope monitoring, but it's not precise compared to other methods (Kumar & Villuri, 2015) (Work Package 6, 2008).

2.4.3 Light Detection and Ranging (LIDAR)

LIDAR is a 3-D laser scanning technology which includes a terrestrial laser scanning and an airborne scanning. This method measure distance and a location of an object (Hu, 2013). The LIDAR uses a laser beam, which sends a pulse in an object direction and then a backscattered laser radiation is registered by optical lenses. A device measures time between send a pulse to the ground and receive back a signal and using the speed of light is possible to determine a distance from a device to a slope. A result of the scanning is a cloud of points, which represents a slope surface in three-dimensions. There are many advantages of this equipment such as a wide range of materials which can be measured, a high resolution and a high quality of a

`

measurement, a scanning can measure inaccessible places (Ampatzi, et al., 2016), a leveling is not required, it is fast and battery charged. Whereas a system has a lot of advantages it has one big disadvantage it cannot provide an early failure warning (Kumar & Villuri, 2015).

2.4.4 Interferometry of Synthetic Aperture Radar (InSAR)

InSAR measures slope displacements using satellites. Satellites located in the space send electromagnetic waves as signals. A device collects signals and creates an image. In the second phase device compared images collected at different times. Then by a phase subtraction between two images an interferogram which represents ground movements is created. A measurement is between two images taken. Main advantages are a high accuracy on a big surface, but there are many disadvantages such as atmospheric influence on a measurement

cannot be eliminated, a long slope monitoring is impossible due to possible decorrelation (images must be all the time in correlation), time between images is relatively long (days) (Work Package 6, 2008).

2.4.5 Slope Stability Radar (SSR)

Ground-based radar is a remote sensing technology that uses the phase-change interferometry to measure a surface deformation of a slope over time. Ground-based SSR systems remotely measure a surface deformation of a slope from a stationary platform without a need for reflectors or prisms (Reeves et al. 2001). A system scans a region of a slope and divides an area into pixels. An amount of movement is measured for each pixel and compared with an amount of movement from the previous scan. Remote monitoring using ground-based radar allows for active monitoring of a slope with deformation alerts of a sub-millimeter precision, making the data available for interpretation usually within minutes. Weather conditions such as rain, fog, dust or smoke don’t affect a measurement (Dick, et al., 2014).

2.5 Failure prediction

The monitoring system is used to predict time to a failure. A data collected from the slope monitoring can be presented as a displacement or velocity versus time curves. After analyzing those plots it is possible to determine if there exists a trend or a trend change which can lead to the slope failure.

For progressive movements, the simplest method is to extrapolate the time- displacement curve for the point(s) which is moving fastest to the point where the curve will be vertical or almost vertical (Figure 18). With this method there are associated problems: the shape of the curve is scale-dependent (using different scale is possible to obtain different results) and numerous monitoring locations are required (Kliche, 2011).

`

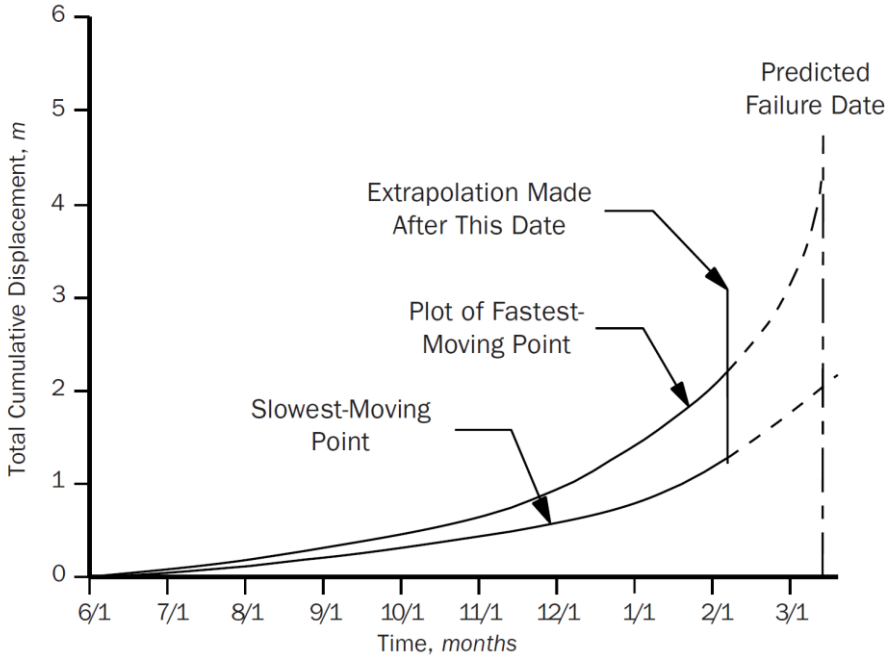

Figure 18 Plot of cumulative displacement against time for the fastest and slowest moving points (Kliche, 2011)

Broadbent and Zavodni (Broadbent & Zavodni, 1982) established a similar method to estimate the number of days prior to a failure using the predicted velocity at the point of a collapse (Figure 19). They noticed that:

$$\frac{V_{mp}}{V_o} = K \tag{12}$$

Where:

V_{mp} - velocity at the mid-point in the progressive stage, V_o – velocity at the onset-of-failure point, K- a constant (mean value is estimated to 7.21, and range from 4.6 to 10.4)

Equation for the straight-line fit log-normal chart has a form:

$$V = Ce^{St} \tag{13}$$

Where:

V-velocity, e-base of the natural logarithm, C- constant, S- the slope of the line (in days^{-1}), t-time (in days)

Assuming that V_o=C at the onset-of-failure equation (13) takes the following form:

$$V = V_o e^{St} \tag{14}$$

Using this formula 12 and formula 14 it is possible to determine the velocity at failure point:

$$V_{col} = K^2 V_o \tag{15}$$

The difficulty with this method is to determine the onset-of-failure point. They concluded that this point occurs between 4 to 45 days prior to the slope failure.

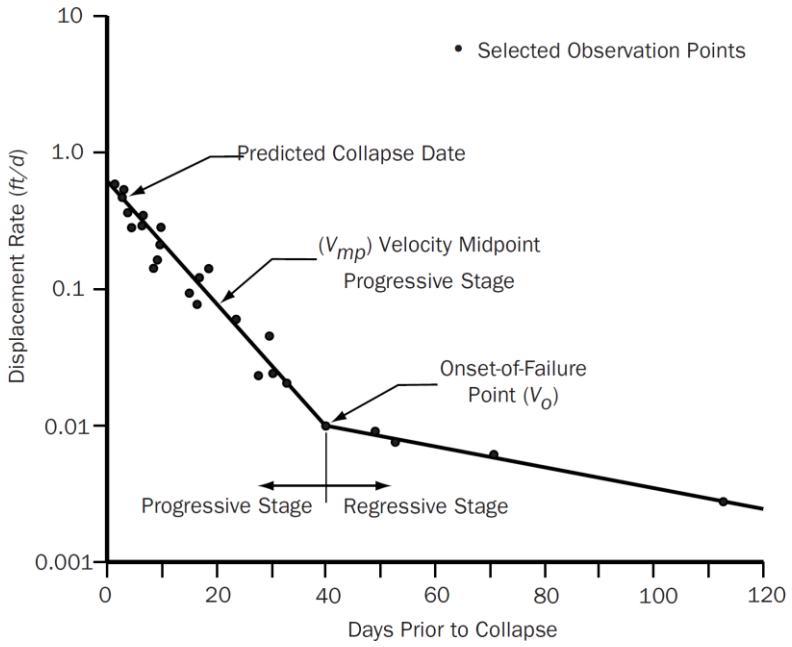

Figure 19 Broadbent and Zavodni failure prediction method

Another method is to use average velocity versus time graphs (Figure 20). Velocities in the point of collapse points towards the infinity. Velocities, as is presented on the graph, appears as surges, after which peaks settled down for a certain period of time. It is possible to misunderstand those surges as a point of collapse. However, it is possible to plotted velocity trend (dashed line), which can determine a point of collapse (Kliche, 2011).

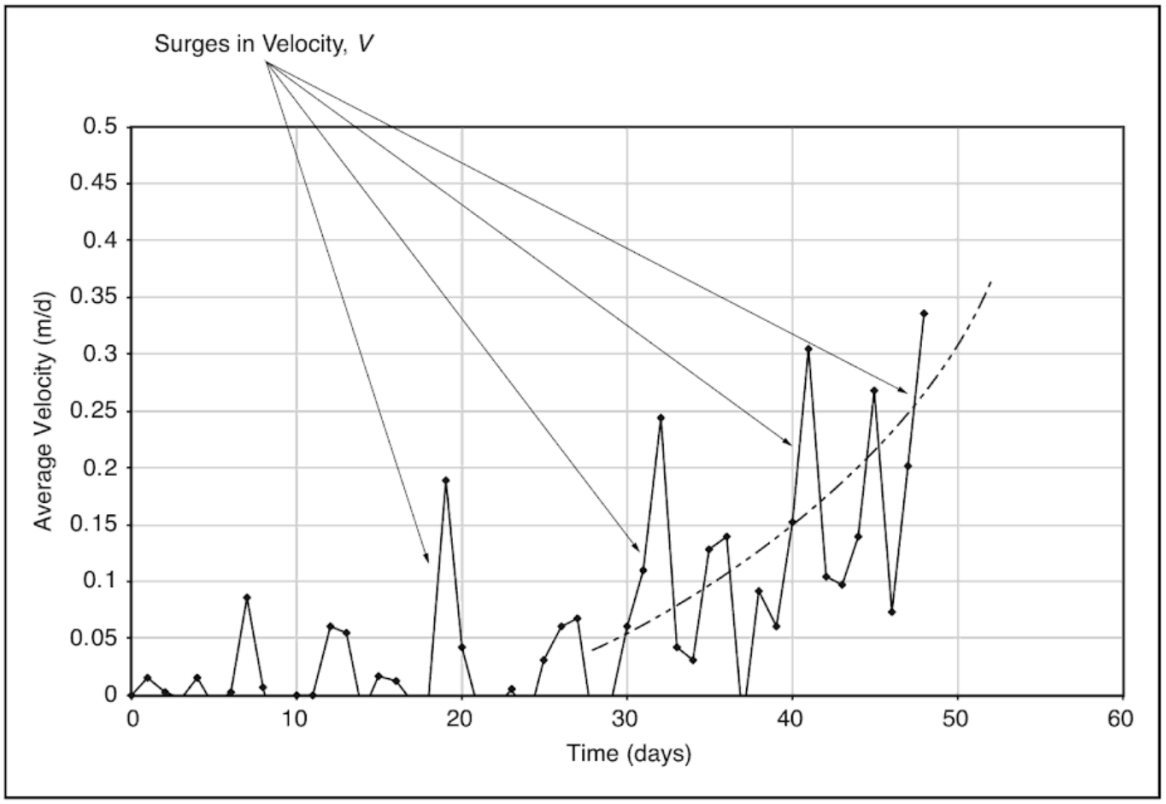

Figure 20 Average velocity against time graph

`

The better method developed Fukuzono (Fukuzono, 1985) which is commonly used in the mining industry. An inverse velocity is plotted against time. As a velocity will increase towards the infinity, inverse velocity values will point towards 0. It is possible to extrapolate the inverse velocities values as a straight line. Interception with horizontal axis will give an expected time when the slope can collapse. Using formula (16) Fukuzono obtain three curves (concave, convex and linear) which can be used for a collapse prediction.

$$\frac{1}{V} = [A(\alpha - 1)]^{\frac{1}{\alpha-1}} * [t_f - t]^{\frac{1}{\alpha-1}} \quad (16)$$

Where: A and α are constant, t_f is a time of failure.

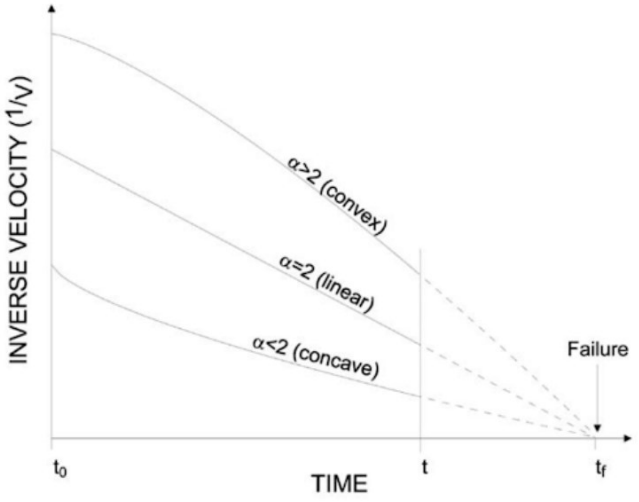

Figure 21 Inverse velocity against time relationships preceding slope failure

As presented in Figure 21 curve appearance depends on a value of α. Rose and Hungr (Rose & Hungr, 2007) simplify equation (16) by substituting this value of α as 2 (linear curve):

$$\frac{1}{V} = \frac{1}{V_0} - A(t - t_0) \quad (17)$$

Where: t_0 is a daytime in days when the plot is starting and V_0 is the velocity at this point.

Setting the inverse velocity as 0 a time of collapse can be obtained:

$$t_f = \frac{1}{AV_0} + t_0 \quad (18)$$

When the slope of the line (A) and the point of interception of y-axis are known it is possible to calculate predicated velocities and predictive relative displacements (X) at the time t.

$$V_{predicted} = \left[\frac{1}{V_0} - A(t - t_0)\right]^{-1} \quad (19)$$

$$X_{predicted} = \frac{1}{A}\left\{ln\left(\frac{1}{V_0}\right) - ln\left[\frac{1}{V_0} - A(t - t_0)\right]\right\} \quad (20)$$

Predicated can be compared to actual slope monitoring data to check if predicted values fit reality or if potential slope behavior changes can occur.

It is a simple method but requires to pay attention to the accuracy of the monitoring system and a data filtering which can influence the trend prediction. It is necessary to take into

`

account potential changes in the slope behavior. Therefore it is necessary that a specialist with experience should interpret the data to obtain the time of possible failure (Rose & Hungr, 2007).

The CUSUMs (cumulative sum control charts) method, which describes Sarunic and Lilly (Sarunic & Lilly, 2006) can be used as well to help rock mechanics engineer to identify the point where the slope deformation trend change behavior. The technique uses plots, where the cumulative sum of differences between a constant value K and each data point in the sequence. Authors explain the method as following steps:

1. *Let x_1, x_2, x_3... x_n be the series of values measured in sequence.*
2. *Select a constant, K. The mean of the data set for which the analysis is being undertaken is often chosen as the value of K so that trends can be tracked relative to the mean (rather than some arbitrary) value.*
3. *Subtract K from each value in the sequence and then add the differences in a series of partial sums; that is:*
   $S1 = x1 - K$;
   $S2 = (x1 - K) + (x2 - K) = S1 + (x2 - K)$; and
   $Sn = Sn\text{-}1 + (xn - K) = x1 + x2 + x3 + \ldots + xn - nK$

The S values represent a cumulative sum series (or cusum) and S is plotted versus position in the sequence.

When is no trend in values CUSUMs will be more or less constant, the plot will be more or less horizontal. If the local mean values will be greater than K, then the CUSUMs curve will slope upwards. The steeper line means the bigger differences between the constant K and the local mean. Figure 22 presents a typical CUSUMs graph.

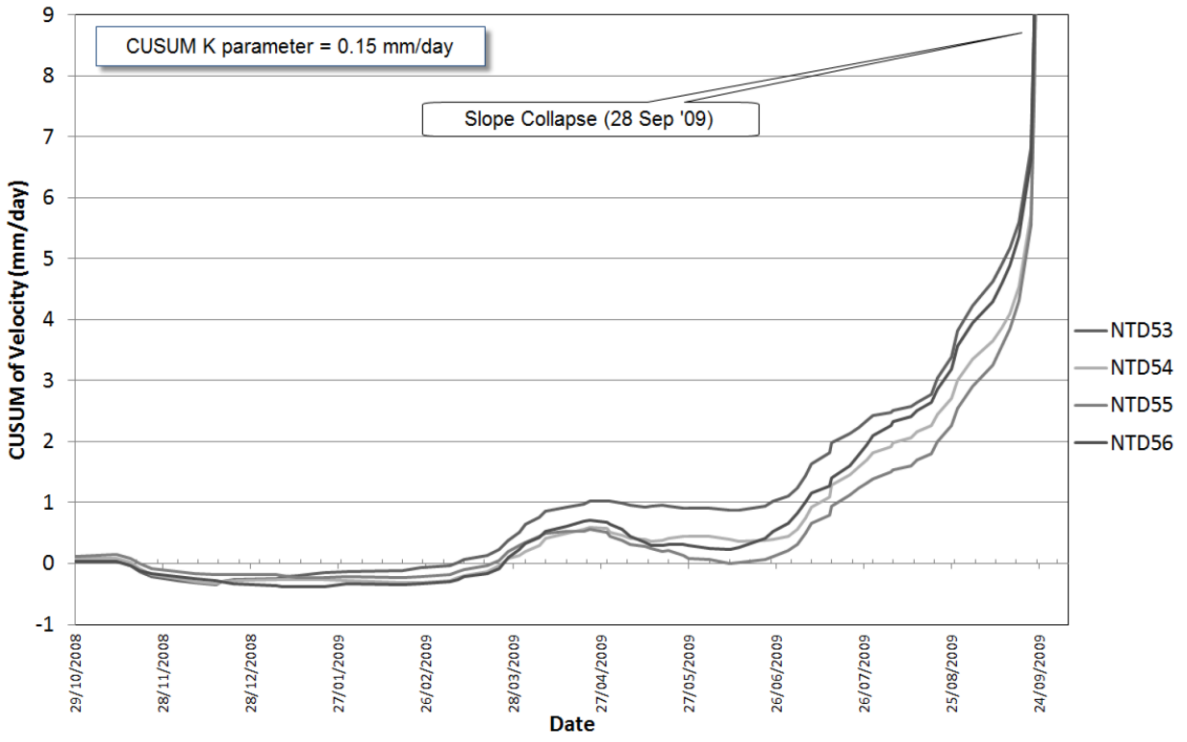

Figure 22 Cusum of velocity graph (Sarunic & Lilly, 2006).

`

To use the CUSUMs method it is necessary to use appreciate value for rock mechanics engineer because the average of total displacement or movement rates have not practical significant meaning. Authors recommend to use a threshold value of displacement or velocity at 'change of state' occurs- for example, the point where progressive behavior occurs (Sarunic & Lilly, 2006).

Other methods involve a high wall strain as a method of failure prediction. Brox and Newcomen (Brox & Newcomen, 2003) developed a technique that is correlating Rock Mass Rating (RMR) defined by Bieniawski and strain thresholds. They found out that the lower rock quality, the higher is potential stain at a slope collapse and that RMR (Rock Mass Rating), which can be a tool for estimation of deformability, defines the strain which a pit wall can accommodate prior to a collapse. For the research, they define strain as '*the total movement measured at the surface divided by the height of the slope below the prism*' and expressed as a percentage. This definition of strain does not represent actual strain at pit surface but is a simple technique to estimate close enough a real strain value. Authors divided failures into two group: planar and wedge failures and rock mass and toppling failures. For each group, they define a different threshold value Therefore, it is important to define in this method type of failure mechanism. For planar and wedge failures 3 % will be the reasonable value of threshold an for rock mass and toppling failures 4 %. This method can be good as a 'first check' to define the stability of the slope and determine if a closer monitoring is required (Brox & Newcomen, 2003).

Mufundirwa and Fujii (Mufundirwa & Fujii, 2008) proposed a method based on the equation for the tertiary creep of rock developed by Okubo and Fukui.

$$\varepsilon = -Blog\left(t_f - t_e\right) + C \tag{21}$$

Where: ε is a strain, B and C are constant, t is time, t_f is failure time, t_e – t is a life expectancy.

Instead of the strain they use u – displacement rate and by differencing both sides received the following formula:

$$\frac{du}{dt} = \frac{B}{T_f - t} \tag{22}$$

Where $\frac{d_u}{d_t}$ is a displacement rate , B and T_f – t values are obtain by approximating du/dt-t curve by using a nonlinear least squares method.

By re-arranging equation (22) it is possible to receive equations (23) and (24):

$$t\frac{du}{dt} = T_f\frac{du}{dt} - B, \tag{23}$$

$$\frac{du}{dt} = -\frac{t - T_f}{B} \tag{24}$$

t_f is obtained as a slope of t(du/dt)-du/dt curve for equation (23) and it is named as a new method-SLO. T_f can be also evaluated as an interception of the x-axis and of(dt/du-t) curve for Eq.(4). This method is named INV.

Mufundirwa and Fujii proposed also data filtering technique which uses *n*th observation to calculate rate as follow:

$$\left(\frac{du}{dt}\right)_i = \frac{u_i - u_{i-x}}{t_i - t_{i-x}} \ (i = x+1, x+2, \dots, y) \tag{25}$$

`

Where $\left(\frac{du}{dt}\right)_i$ are calculated displacement rate points, t_m and u_m are the time and last displacement in the pre-failure range.

They develop the concept of "safe" and "unsafe" predictions presented in Figure 23.

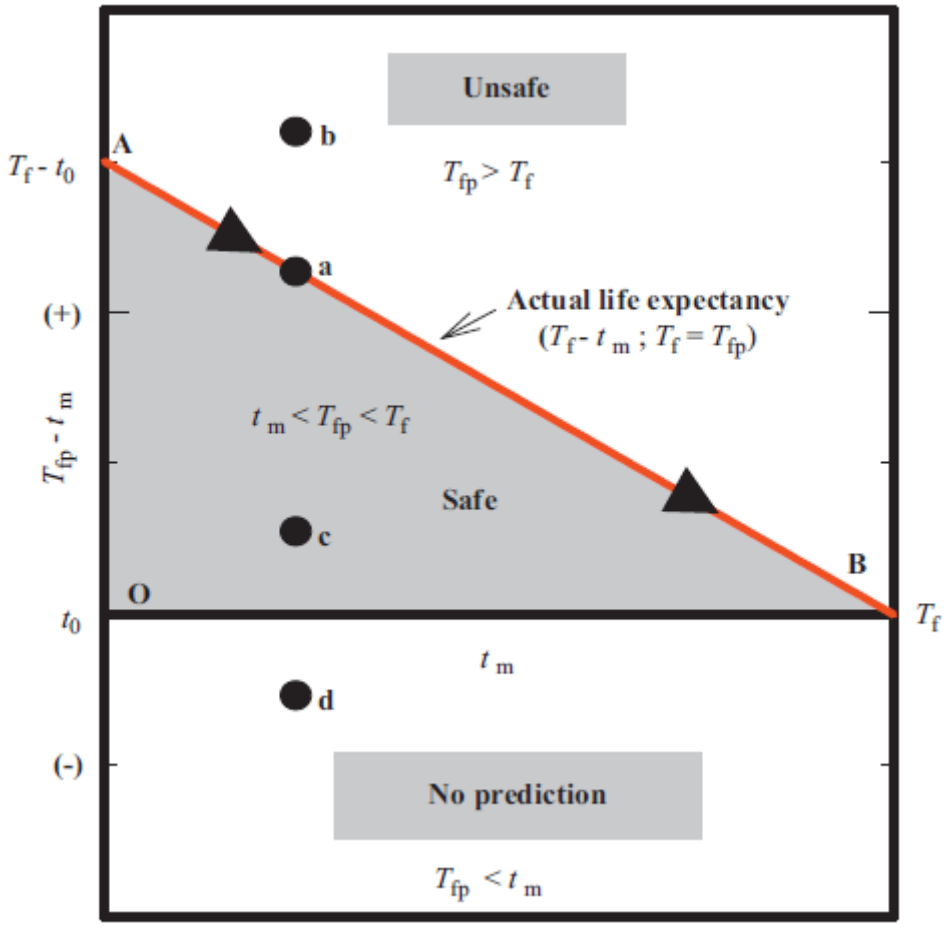

Figure 23 Concept of "safe" and "unsafe" predictions

T_f is actual failure time, T_{fp} is the predicted failure time, t_m is the time at each instant of predicting failure time. The y-axis represents the predicted time of expectancy at tm (T_{fp}–t_m). The line AB shows an actual life expectancy. T_{fp} is equal to T_f when t_m is located on the line AB (point a). When the point is above the line is unsafe $T_{fp} > T_f$ (point b). This means that failure will start before prediction T_{fp}. Therefore, if $T_{fp} < T_f$ (point c) and is situated in the OAB region then the prediction is safe. If $T_{fp} < t_m$ (point d) then failure occur before time t_m which make prediction meaningless (Mufundirwa & Fujii, 2010).

There exists a method which uses velocity-acceleration graphs described by Federico and others (Frederico, et al., 2012), but this method requires further research to confirm the proposed technique.

Mines need to define slope movement rates that are necessary for safe operation and in the worst case decide about the closure of mining areas. Those movement rates are named as threshold values. There are many factors that influence threshold values such as a monitoring system accuracy, a knowledge about slope failure behavior and mechanics, possibility to implement remedial measures such as buttressing, offloading, drainage holes etc. and time

`

required to install those measures, time required for evacuation of people and equipment from dangerous area, availability to access other mining faces.

When threshold values should low enough to allow to for flexibility for a remedial measures implementation in right time, as well as to start monitoring dangerous areas as soon as possible changes in the slope behavior. Threshold value should also include a safety margin, in response to the slope behavior uncertainty (Rose & Hungr, 2007).

Many authors propose movements thresholds as an indicator of the slope behavior. Appendix 1 presents displacement rates and description of threshold values in different case studies.

A threshold value is site-specific, or even slope specific because each slope has different rock mass parameters, unique geology, and geometry. Values presented in Appendix 1 can be used as a guide for threshold value estimation. Threshold values can be used as a tool which will make aware rock mechanics engineer about changes in the slope behavior. Those value should be verified and adjust using a back analysis of the site. Specific incidents in the slope behavior can provide additional data which can be used for a threshold value optimization.

Carla (Carla, et al., 2017) proposed thresholds sequence which can be used at the mine site:

1. Threshold Level 1: it is a value slightly above the radar noise level which can be generated on the line of sight. It is used as an initial emergency to identify a possible hazard.
2. Threshold Level 2: it uses a higher velocity value for the area which has exceeded the value of threshold level 1. This value might be increased when the mechanism and size of instability are known.
3. Threshold Level 3: combines velocity and acceleration and defines the border between failures and no-failures incidents. When this value exceeds the continuous monitoring is required.

2.6 Failure management

The monitoring process is site-specific and dynamic. It starts with daily visual inspections of slopes, checks of a ground-water level as well as a data from the monitoring system. Prakash (Prakash, et al., 2015) proposed time frames at which certain movement has to be a monitor, as presented in Table 1.

Table 1 Suggested monitoring frames

Points undergoing movement	Frequency of monitoring
0mm to 2mm per day	Once per month
2mm to 5mm per day 5mm	Once per week
5mm to 10mm per day	Once every 2 days
10mm to 50mm per day	Once per day
> 50mm per day	Require continuous observation

`

Rose and Hungr (Rose & Hungr, 2007) suggest that all remedial methods should start to implement at least one month in advance prior to a failure. This time zone gives a maximum flexibility and provides safety. Before all measures will be implemented, rock mechanics engineer should check if the slope is in a regressive stage or continues an accelerating. If velocity increases, slope monitoring should be performed at least daily. All factors which can influence slope stability should be included in the assessment, for example, blasting, ground-water recharge etc.. One week prior to failure, all mining activities should be stopped.

Dick and others (Dick, et al., 2014) developed a procedure on how to react when a slope monitoring alarm appears on the slope stability radar monitoring system. Figure 24 presents a chart for the real-time time-of-failure analysis methodology.

When alarm appears on the screen of rock mechanics engineer, it is necessary to define a benchmark pixel. There are two methods to define the pixel: use the pixel which initiates an alarm or chooses a pixel with the highest accumulated deformation, if a trend of an acceleration is noticed.

Geotechnical stuff needs to observe deformation trends. It is recommended to observe two trends: one for benchmark pixel and one for 50% deformation increment, where multiple pixels are selected, by deformation percentage of benchmark pixel based on “the percent deformation “ method. Failure does not collapse as a coherent mass. Therefore, a single pixel will provide the most valuable result, because it is located in the most critical area. It is necessary to compare both results to receive as an accurate prediction as possible and the understand a rock mass behavior during the early stage of the failure event.

Next step is to implement or remove the Trigger Action Response Plan (TARP), which explains what preventive action should be taken due to a raised alarm. A TARP is a list of prepared procedures and responses for trigger events, based on signals levels define by certain threshold values. Those levels are placed in order which leads to a collapse. Responses planned in a TARP must be applied at a site when a threshold value will be exceeded for a particular level (Saunders, et al., 2016). It also provides a procedure of an assessment of a slope stability and related with it risks. During this stage is necessary a continues deformation monitoring.

Later it is necessary to determine Onset-Of-Acceleration (OOA). It can be established using four different plots:

1. Cumulative deformation versus time
2. Deformation over a given time period versus time
3. Deformation rate (velocity) versus time
4. Inverse velocity versus time

For plots 2,3,4 it is necessary to use to different time periods, for example, 3 and 12 hours. This technique allows to better understand behavior. A long period of time, is less noisy and better visualize long-term data trends and therefore an earlier OOA point. A short period of time is noisier but shows short-term data trends. All plots should be monitor until end of acceleration for both benchmark pixel and 50 % deformation increment. If the OOA point cannot be defined an evaluation of TARP removal has to be carried out. If all collected data indicate a false alarm, the monitoring system can continue its work normally. When the point

of OOA can be determined it is necessary to do a more detail evaluation of the monitoring data.

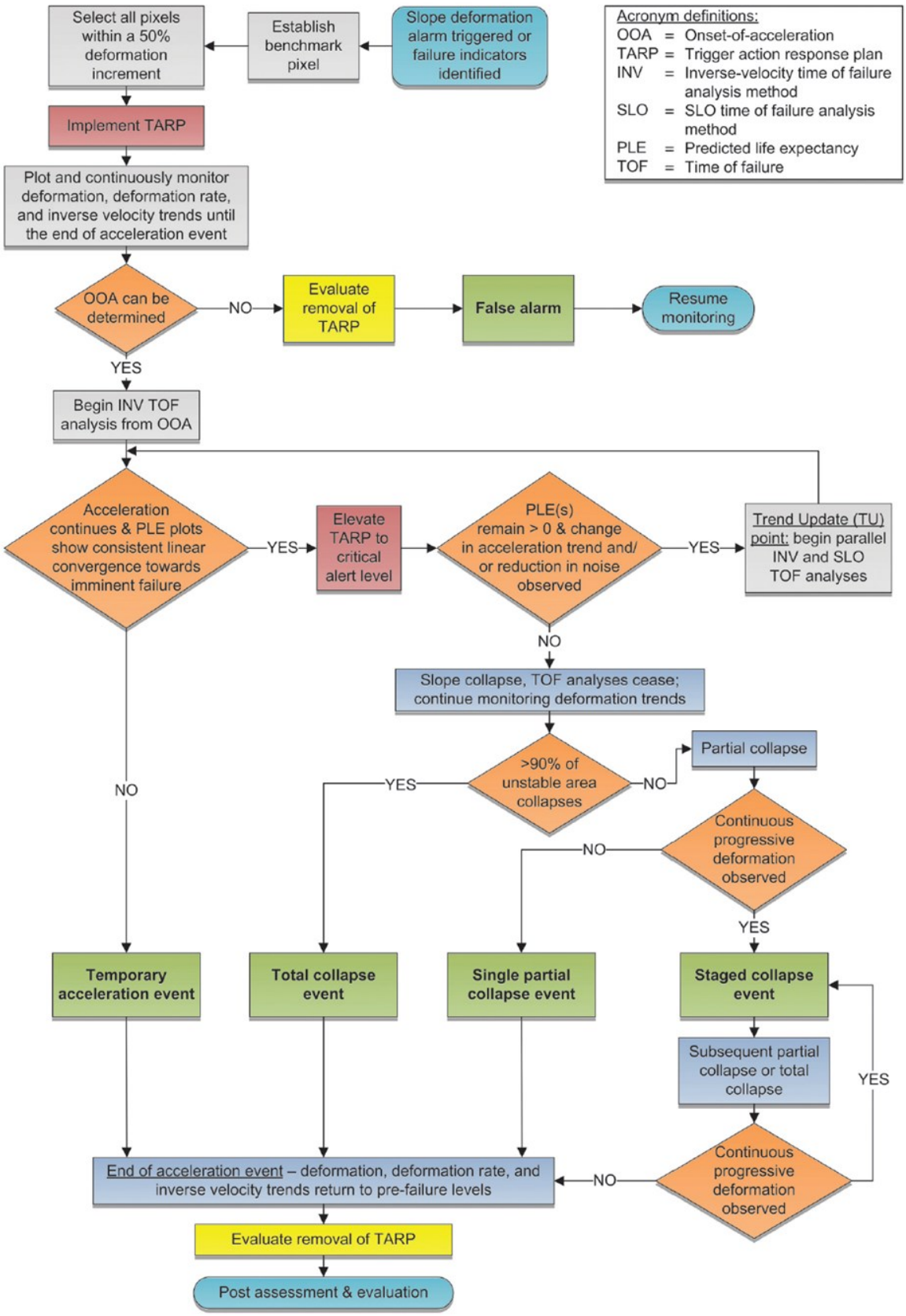

Figure 24 Real-time time-of-failure methodology (Dick, et al., 2014)

`

First, it is necessary to accurately define the OOA from inverse velocity plots for benchmark point and 50% increment points. After that, each sequential predicted life expectancy is a plot on the life-expectancy graph, up to current time. For each new radar deformation measurement, new predicted life expectancy point can be plotted on the graph. It allows analyzing historical Time of Failure (TOF) results. This method should be used to the point when there is not anymore an acceleration event.

If the acceleration trend behavior changes notably and/or data noise decreased in benchmark point or 50 % deformation increment datasets, Trade Update point (TU) analysis should be carried out, which must be provided simultaneously with an original OOA investigation. TU omitted historical data to receive new measurements, which can be used to find out more accurate TOF study results. Each measurement after TU point can be evaluated using inverse-velocity and SLO TOF methods. Each additional analysis after TU point has to plot separately. There can be many TU points selected as it is presented as a loop on the chart because the new analysis is necessary for the new trend changes or to provide additional data comparisons.

As a TOF procedure is settled the rock mechanics engineer must carry on monitoring of the deformation trend and life expectancies plots. There two possible results of the TOF analysis: instability accelerates and fails or decelerate and comes back to stability state (defined as a temporary acceleration event). When predicted life expectancies start to show negative linear trends in the direction of 0, it demonstrates that the slope is close to a failure.

There are four main acceleration events, which are distinguished by collapse characteristics and deformation-time trends. To define if the failure is a total collapse event or partial, it is necessary to identify an area of instability. If the failure comprises more than 90 % of instability it is a total collapse event, if not it is a partial collapse event. The partial event can consist of few events or occur as single when no additional failures have taken place. When few events occur it is named as a stage collapse event. The SLO TOF and the inverse-velocity analysis cannot predict subsequent collapse events. If this stage is reached it is necessary to provide continuous monitoring of the deformation, deformation rate, and inverse velocity to ensure that the mine is safe and the trend is regressive and comes back to the pre-failure stage. This is presented as a loop on the chart.

After the collapse, it is necessary to evaluate removal TARP or reduction of alarm level by risk assessment and inspection. It is also important to evaluate emergency procedures. It is crucial to find areas of success and places where is necessary to improve procedures. Dick and others (Dick, et al., 2014) proposed questions which a rock mechanics engineer should answer after slope acceleration event for a better post-failure assessment:

- *Did initiation of a critical alert level allow sufficient time for evacuation of the endangered area?*
- *Were the trigger thresholds suitable to provide sufficient response time or do they need to be reassessed?*
- *Did all personnel understand and follow the appropriate TARP or emergency response procedures?*
- *Did the event expose any flaws in the TARP or emergency response procedures that need to be addressed?*

`

- *Were any new indicators of future instabilities recorded during the post-failure visual inspection?*

2.7 Principles of SSR technology

2.7.1 Radar

Radar is an acronym for Radio Detection And Ranging. A radar sends electromagnetic waves in the space to find out aims. Aims reflect parts of the energy of the wave, called echoes or radar returns back to a radar. Echoes are collected by a receiver and process to acquire information about an aim. The information can consist of a size, a shape, a velocity, a direction of a movement, a range, an angular position and an identification of an aim. Figure 25 presents radar principles.

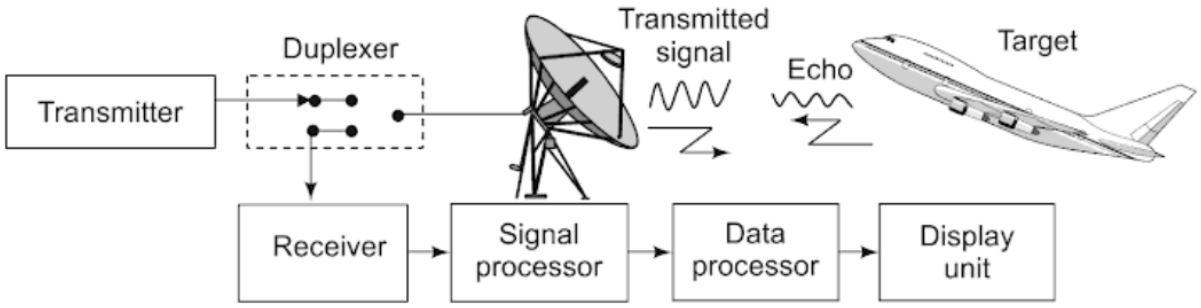

Figure 25 Scheme of a basic radar system (IDS, 2017)

The main elements of radar are a transmitter, a receiver, a duplexer, an antenna, a signal processor, a data processor, and a display unit.

A transmitter produces a short, strong signal (pulse of energy) at a defined frequency to a transmitting antenna.

A receiver gathers an echo signal from an antenna, separate noises, amplify a signal and send it to the signal processor.

In some of the radars, a receiving and a transmitting antenna are the same. Therefore it is necessary to separate signals. It is done by a duplexer, which alternatively switches an antenna to a receiving and transmitting mode. A high transmitter power could destroy a receiver.

An antenna transforms a transmitter signal into an electromagnetic wave and sends in the direction of an object. Another function of an antenna is collecting an echo signal and convert into an electric signal and send it to a receiver. An antenna can be used for both purposes by using a duplexer.

A signal processor is used to process a collected signal from a receiver. A processor decreases the noise-signal ratio and produces information about an aim.

Another type of a processor used in radars is a data processor. A data processor processed, store and convert all information about an object provided by a signal processor into simply comprehensible coordinates. Then a processed data is sent to a display unit.

A display unit presents understandable for operators and supervisors a data about a monitored object (Raju, 2008).

`

2.7.2 Measurement of displacement by SSR

Electromagnetic energy is moving at constant speed, nearly the speed of light c -300,000 kilometers per second. Due to a constant speed, it is possible to define a distance between a reflected object and a radar, by calculating the time between pulses. Moreover, electromagnetic energy moves in a straight line. It can be pointed in a defined direction using special antennas, therefore am azimuth and an elevation of a measured reflected object can be calculated.

The radar sends a signal towards an aim, and receive a reflected signal (echo) in the time T_0 (Figure 26). Knowing that the waves are traveling with the constant speed of light, it is possible to determine a distance (R_0) between a radar and an object.

$$R_0 = \frac{c * T_0}{2} \tag{26}$$

Where c is the speed of light, T_0 is time between sending a signal and receiving an echo.

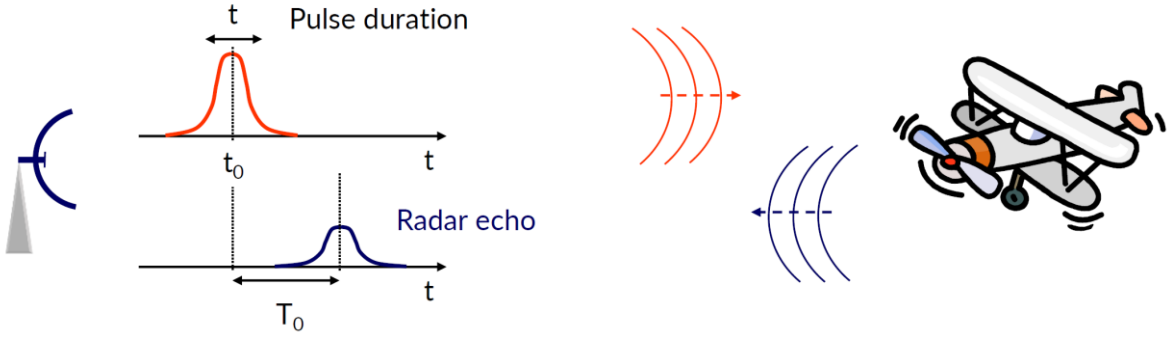

Figure 26 A radar signal and an echo (IDS, 2017)

In general, all waves can be seen in the two ways in a time domain, which demonstrates how waves behave in time and a frequency domain (Figure 27), which represents how much of a signal is in a given frequency rate.

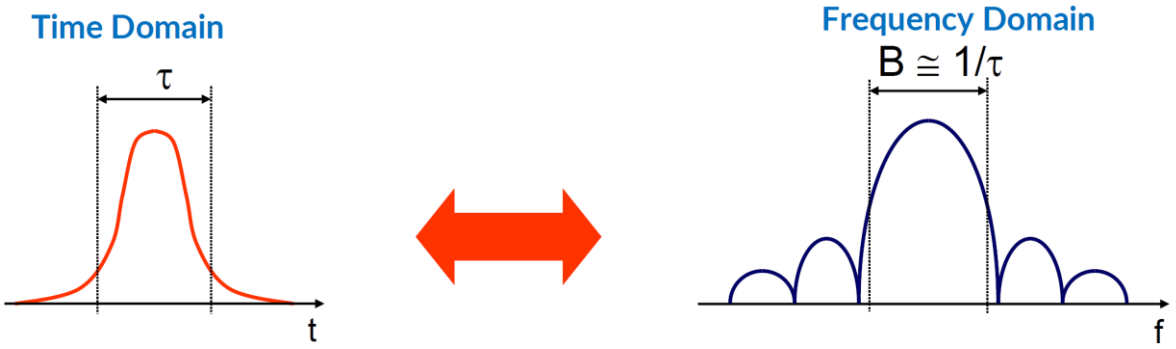

Figure 27 Graphical presentation of time and frequency domains (IDS, 2017)

A range resolution is a radar capability to recognize objects which are located in the same direction but at different radial distances. A radar range resolution can be express only by the function of a bandwidth.

$$\Delta R = \frac{c\tau}{2} = \frac{c}{2B} \tag{27}$$

Where is ΔR is a range resolution, τ is a pulse duration and B is a bandwidth (1/τ). (Wolff, 2018)

`

To define an angular resolution (Cross-Range Resolution), which allows defining objects at different azimuth angles the SSR uses the SAR (Synthetic Aperture Radar) technique. A radar is fixed to a moving platform. A movement of a radar creates artificially a linear array, which allows defining targets at an angle or an azimuth. To calculate a cross range resolution following formula is used:

$$\Delta\varphi = \frac{\lambda}{2 * L} \tag{28}$$

Where Δφ is a cross range resolution, λ is a wavelength of a radar and L is a length of a radar antenna- length at which radar is moving. (The University of Alabama in Huntsville, 2018)

Using a range resolution and a cross range resolution the SSR can define a two-dimension map of pixels- representation of an area. During each a data acquisition session, a radar collects an echo from each pixel. An echo consist of two different information: signal amplitude and phase φ

A signal amplitude defines a backscattered power, at which a pixel reflect a signal. A high amplitude means a good reflection. A phase is a relative shift between sent a sine wave and received one. A full sine wave cycle is equal to 360° or 2π (range from – π to π). A phase difference($\Delta\varphi$) between two data acquisitions allows to make a interferogram. An interferogram is a map, which can represents a deformation (d) of each pixel, which is:

$$d = -\frac{\lambda}{4\pi} * \Delta\varphi \tag{29}$$

Where d (Figure 28) is a displacement, λ is a radar wavelength and Δφ is a difference in phases.

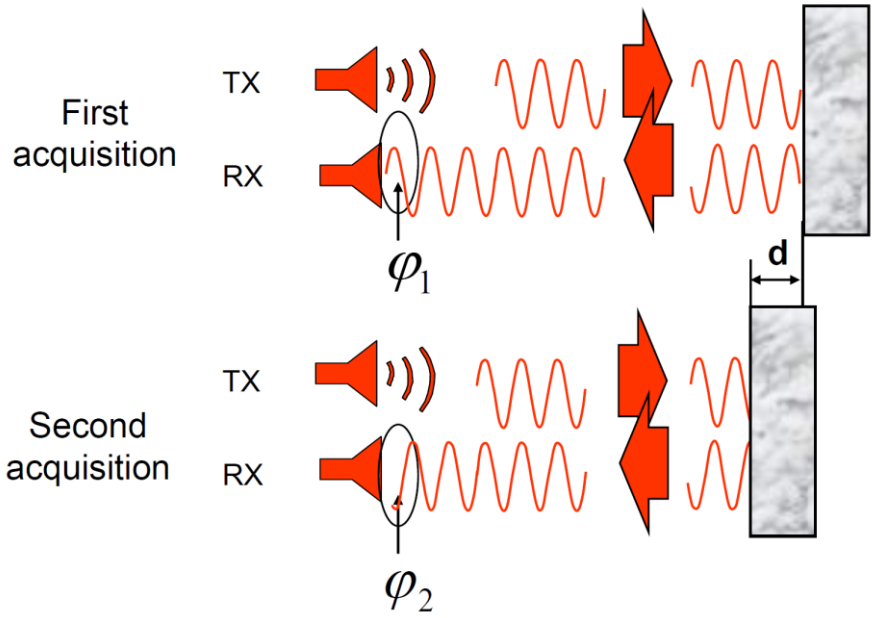

Figure 28 Measurement of a displacement by the SSR (IDS, 2017)

It is important to take into consideration during calculations a phase ambiguity. The SSR can only detect a phase difference equal to π. Another limitation of the SSR is a line of sight (LoS). If a movement of a monitored object is orthogonal, the SSR will not detect a movement- some failures cannot be detected (IDS GeoRadar, 2017).

`

2.8 Advantages of the SSR over other methods

One of the biggest advantages of the SSR is that it remotely and continuously scans open pit slopes and determines (detect and warn) all surface movements with a huge accuracy- a sub-millimeters precision. The radar can detect ground movements overbroad, large surface areas. Those factors give a better understanding of deformations within a slope. It is possible to estimate a magnitude of a possible failure and lead to an early warning time of an instability. A radar system doesn't require an intensive labor or a large number of a manpower. A measurement is taken fast. Moreover, a radar allows for working under all-weather conditions. The SSR give reliable measurements 24/7 during both a day and a night and can penetrate through fog, dust, rain, and smoke. A system has a big advantage over optical methods because it doesn't depend on the solar or other an illumination (for example from machines) (Harries, et al., 2007). Moreover, the SSR takes a picture of a whole area. It scans an entire wall not only points (prisms) like it is in robotic total stations. Furthermore, it is safer because a prisms mounting can be dangerous. Prisms are located in areas where a sliding could occur. Prisms are also exposed for a damage or a displacement, which lead to improper measurements. The SSR gathers a data without prisms or other reflecting surfaces.

The SSR is more accurate than other methods. As stated in the Bye research (Table 2), the slope stability radar has 93 % of a success rate in detecting slope failures, whereas other methods have the rate below 90%. Combining the radar with other methods allows receiving almost 100% success rate (Osasan, 2012).

Table 2 Bye's monitoring type analysis

Monitoring Type	Success Rate
Visual Monitoring only	32%
Prism/Crack Meters only	45%
Visual + Prism/Crack monitors	63%
Visual + Prism/Crack + Laser	86%
Radar Only	93%
Visual + Prism/Crack + Radar	97.50%
Visual + prism/crack + laser + radar	99%

2.9 Radar and risk management

The slope stability radar can be used as an early warning system. In general, an early warning system has few main aims such as monitoring, which consists of a data collection and it a transmission, as well as a maintenance of the equipment; a prediction and an analysis, it can be done by different methods such as thresholds, an expertise of a rock mechanics engineer, prediction methods and other; warning -rising an understandable alarm which informs about forthcoming threats and a response- regarding a reaction of people and their an understanding of a warning signal (Intrieri, et al., 2012).

Harris and others (Harries, et al., 2009) have developed a special framework for a slope stability risk management. The first step is a context selection - a placement and a function of the SSR, for example, a monitoring of a rapid, bench size failure. A next phase is an identification of a

`

hazard. A hazard is identified by a rock mechanics engineer, who can see on a computer screen a rocks deformation. A deformation is highlighted on a color image of a mine. A personnel in charge of the SSR system examine and determine this information by checking a size of an area which is possible to fail and a type and a rate of a deformation. Subsequently, a data about a slope damage can be evaluated using organization rules (for example a bench failure can be small enough that a catch bench will neutralize the threat). After a hazard evaluation, if it is necessary to treat a hazard. There are two main options for a risk reduction. A possibility of a failure can be decreased by for example de-pressurizing of water pressures or supporting an area where a failure will occur using a buttress. Another most common possibility is a reduction of failure effects. The most favorable option is an alarm evacuation of a personnel and machines from a mine (Harries, et al., 2009).

An evacuation alarm is one of the alarm types. The mines mostly are using four alarms:

- Green Alarm- a small system failure, during which the SSR is close down and the SSR program has to be restarted according to procedures.
- Yellow Alarm- a radar system failure, which causes that a pit superintendent receives an information about the unavailability of a radar and a geotechnical department is informed to determine a problem with a help of an equipment producer.
- Orange Alarm- in other words, “a geotech alarm”, an announcement of a ground movement development, which should make a geological department conscious of possible dangers.
- Red Alarm-serious situation at which a pit superintendent must evacuate an area of concern or a whole pit (Harries, et al., 2007).

Alarms can be announced by different methods, such as SMS send to personnel mobile phones; e-mail to responsible persons, an alarm on the computer software; sirens and flashing light signals and traffic lights, which will stop an equipment to move into the dangerous area (Harris & Holmstrom, 2007).

A data collected from a radar is sent to a computer room and presented in the real time on the screen, which allows monitoring a slope behavior by a rock-mechanics engineer. A deformation, a velocity rate and a size of a failure are most common in use to define a threshold value for a slope monitoring (Harries, et al., 2007). The most important in an alarm application is to define a linear deformation trend, which is a sign that a risk level has increased. After an identification of a linear deformation trend, a deformation velocity can be a remark and a new velocity can be set as an alarm, which determines when a deformation changes behavior to a progressive stage. A progressive deformation is a signal that the level of risk has increased. At this stage is possible to start predicting when a failure could occur and set alarms to inform a rock-mechanics engineer when a slope deform significantly (Saunders, et al., 2016).

`

3 Case study

3.1 Reasons behind radar system in Leveäniemi open pit

The Leveäniemi open pit is a complicated mine due to an existing geology and weather conditions. Rocks are weathered and strongly metamorphosed. Within the rock mass are located many faults and joints. Those conditions lead to a weak rock mass, therefore it is more likely that a slope failure will occur. Another problem is precipitation in an area of the Leveäniemi open pit.

The mine is placed 150 km above North Circle, where prevails a subarctic climate. This type of weather characterizes short, cool summers and long, cold winters. Snow covers the ground from late September until mid-May. During a freezing and a thawing process a rock mass breaks, cracks become wider due to the expansion of water volume, when it changes into ice. The mining area is surrounded by a high groundwater table, and such as relies on continuous water pumping from the pit. Moreover, a huge amount of water flows into the pit during spring due to the melting of snow and ice.

The life of mine is estimated to reach the year 2030. Current production in going at the level 250 m, while the pit rim is at 370 m. The planned pit bottom of the mine is at level 100 m. Therefore slopes will be steeper than they currently are and will need stricter monitoring as they may have a higher potential for failure.

Due to all these factors, LKAB decided to purchase the SSR to protect people and equipment located in the mine against possible slope failures.

3.2 Radar system review

The SSR unit installed at the Leveäniemi Open-Pit is a device made by an Italian company IDS Georadar- IBIS FM. The radar can detect small movements due to a high spatial resolution (0.5 m x 4.4 m resolution of a cell at a 1 km distance). The maximum range that the radar can work is 4,5 km. IBIS FM can cover a broad monitoring area - up to 5 km^2. A single data acquisition takes around 2min at 1km range. It could operate remotely using a Wi-Fi antenna and solar panels or a diesel generator to charge batteries. The radar works in almost all kinds of weather condition and temperatures from -25 °C or -50°C if the radar is placed indoor up to +50 °C. The IBIS FM can raise different alarms at various deformation levels defined by a user (www.idsgeoradar.com, 2018). The radar has been mounted on the trailer.

The radar basic configuration is made up of a hardware and a software.

3.2.1 Hardware

The basic hardware (Figure 29) consists of Radar Sensor (RS), Linear Scanner (LS), Power Supply Unit (PSU) and Field Laptop (FL).

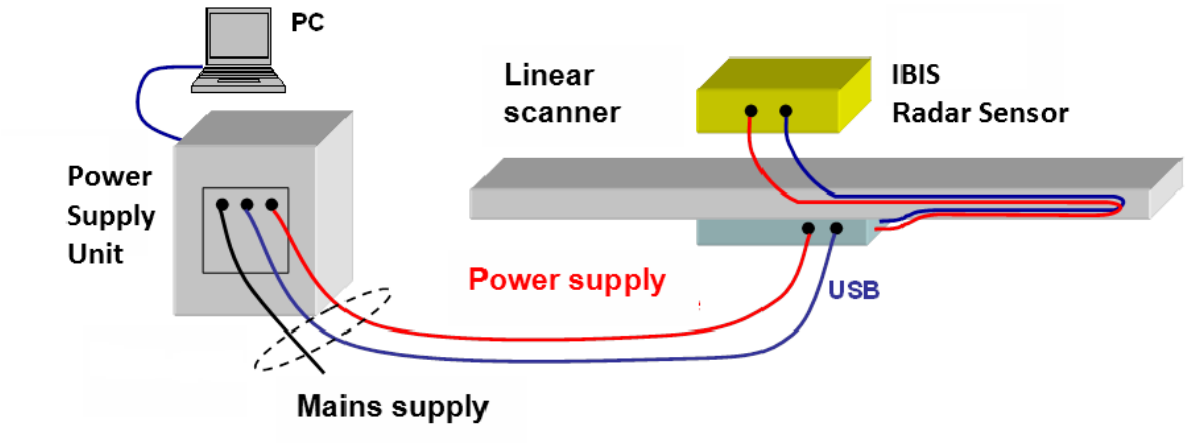

Figure 29 Hardware connection (IDS, 2017)

Additionally, the system can be equipped with: an eagle-vision camera, a weather station, a power generator, solar panels, a Wi-Fi radio or a watchdog.

A Radar Sensor (RS) (Figure 30 and Figure 31) it is a yellow box, which generates, transmit, receive and acquire a radar signal. The main task of a radar sensor is to acquire data and send it to IBIS Controller.

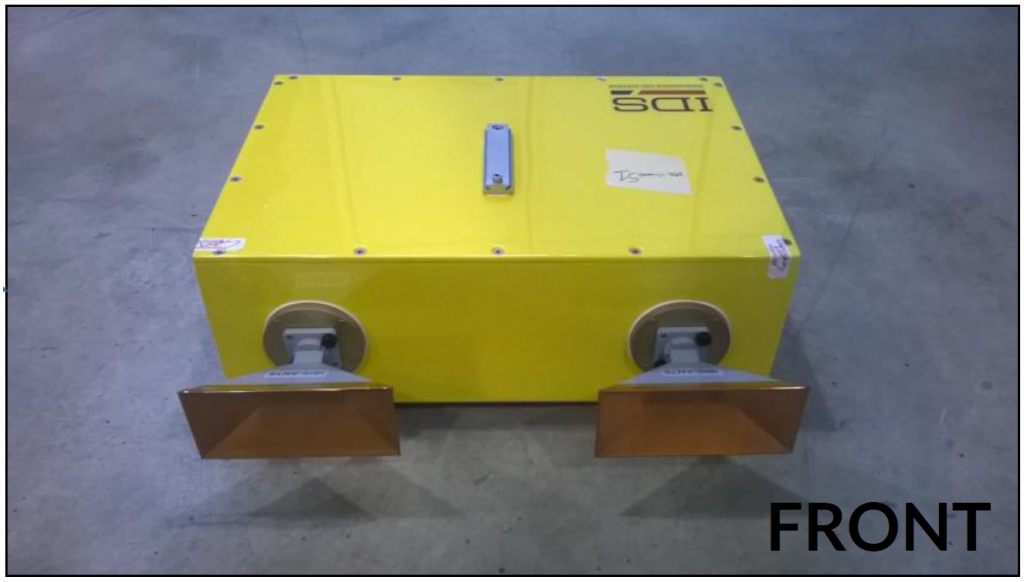

Figure 30 Front of the Radar Sensor (IDS, 2017)

`

tt 

Figure 31 Rear of the Radar Sensor (IDS, 2017)

To a box are attached in front two IBIS-ANT7 antennas (Figure 32), where one is sending an electromagnetic pulse and second is receiving an echo. Antennas are operating in the vertical polarization and can gain maximum 14dBi. Main lobes (-3dB and -10 dB) are presented in Table 3. Lobes define the spatial limits of the measured area.

Table 3 Main lobes width of IBIS-ANT7 antennas

IBIS-ANT7	Beam Width	
Power gain	Horizontal Plane	Vertical Plane
-3 dB	50°	31°
10 dB	83°	66°

In the back of the RS (Figure 31) are located plugs for USB and power supply connections with a Linear Scanner (LS).

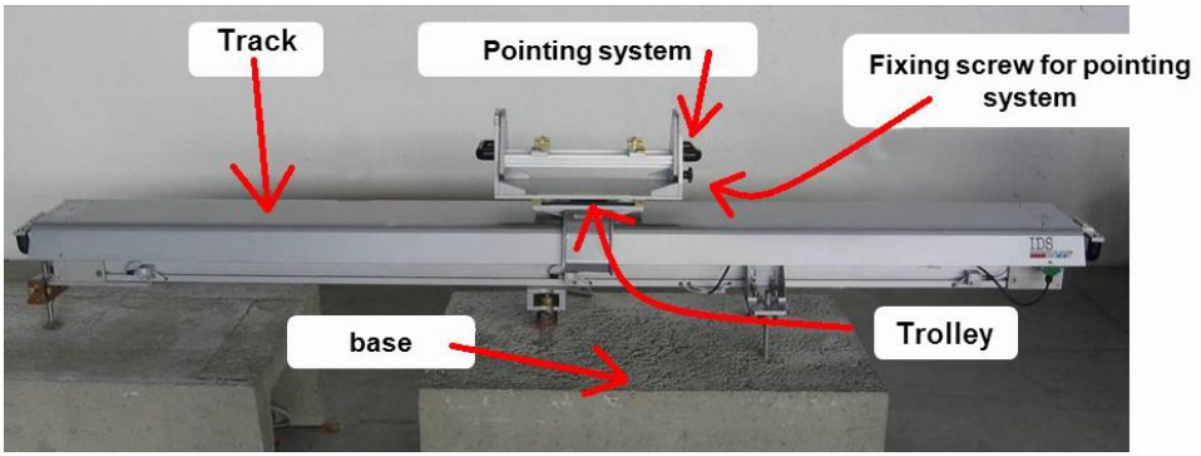

Figure 32 The Linear Scanner (IDS, 2017)

`

An LS (Figure 32) allows an RS to move along the track orthogonally to the direction of measurement. It is necessary to obtain a SAR technique, which is used for the cross-range resolution. The instrument consists of a track, 2,5 m long on which the RS is moving; a trolley, which is a connection between a sensor and a track; an elevation pointing system installed on a trolley, which allows tilting an RS to an appropriate position. It is necessary that an RS has a right line of a sight.

During a data acquisition trolley with mounted on it, an RS moves from the left end side to the right end side of an LS. The maximum movement of a trolley is 2m. An LS has to be fixed to a platform (base) which must have right dimensions for a robustness and an appropriate inclination of an LS. The LS is connected by a USB cable and a power cable to s Power Supply Unit (PSU).

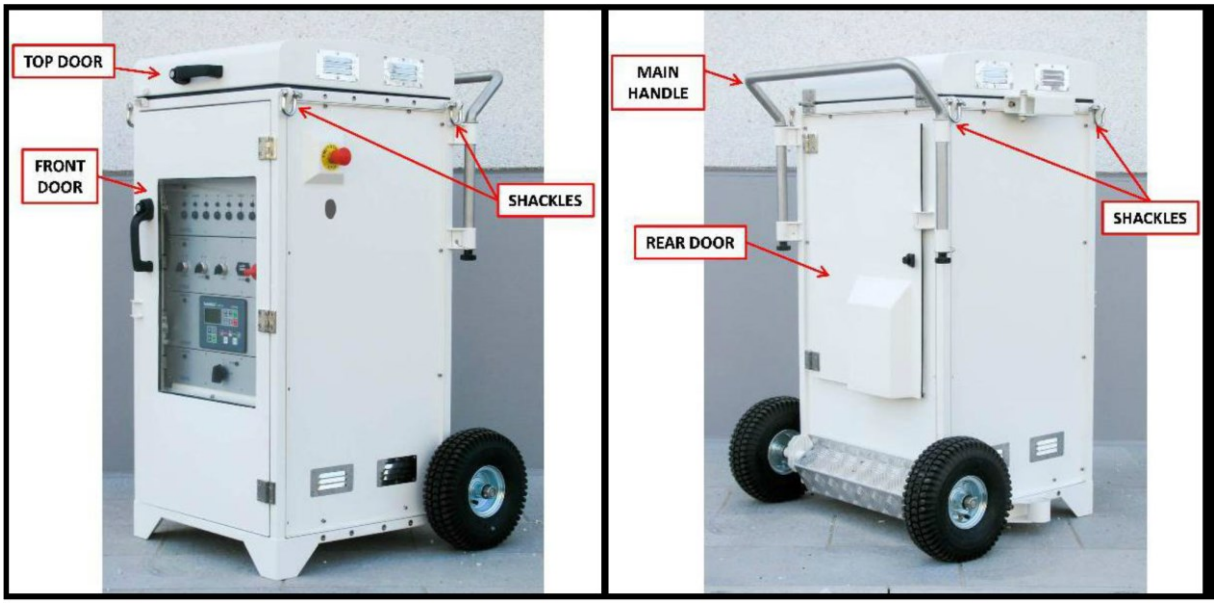

Figure 33 The power supply unit (IDS, 2017)

A PSU (Figure 33) provides and controls the electricity supplying for all IBIS-FM system devices. The main aim is to: supply power to the RS, LS and other peripheral devices connected to a system; receive electricity power from a power generator, solar panels, batteries or the main supply; charge batteries, which in case of the main power supply cut provide electrical power to devices.

A PSU is a box mounted on two wheels with three doors. Each door allows access to different modules. The front door gives access to batteries, control and power module panels. The rear door gives access to a sockets board and an interfaces panel. The top door gives access to a Field Laptop (FL) (Figure 34).

An FL allows communication between all devices in the system by software IBIS Controller.

`

Figure 34 The field laptop workplace (IDS, 2017)

The Leveäniemi Open Pit Radar System is equipped additionally with an Eagle-Vision Camera (EVC) (Figure 35) and a Watchdog (Figure 36).

Figure 35 Eagle-Vision Camera (IDS, 2017)

An EVC collects HD pictures of the area of an interest, stitch them together into one panoramic view. A view is linked to a digital terrain model of a mine to recognize visually moving areas. Furthermore, an EVC allows displaying a real-time video stream of monitoring areas.

A watchdog is a device, which raises alarms about problems related to a radar system. It can alert about problems related with a power supply, hardware devices, an acquisition of data and raise an alarm about exceeding threshold values in a monitoring system. A watchdog also

`

informs about an internal status. A device can also initiate external instruments with an alarm activation.

Figure 36 Watch Dog

3.2.2 Software

A software of the radar system consisting of two connected between each other programs: IBIS Controller and Guardian.

The IBIS Controller (Figure 37) manages entire hardware devices and sends a data to the Guardian. In the IBIS Controller is available to turn on and off, check an actual status, change export settings of all instruments in a radar system. Furthermore, within the program is possible to manage a data- it is possible to change the setting of a data transfer and an archiving, as well as disk management. A data acquisition session is also started in this software.

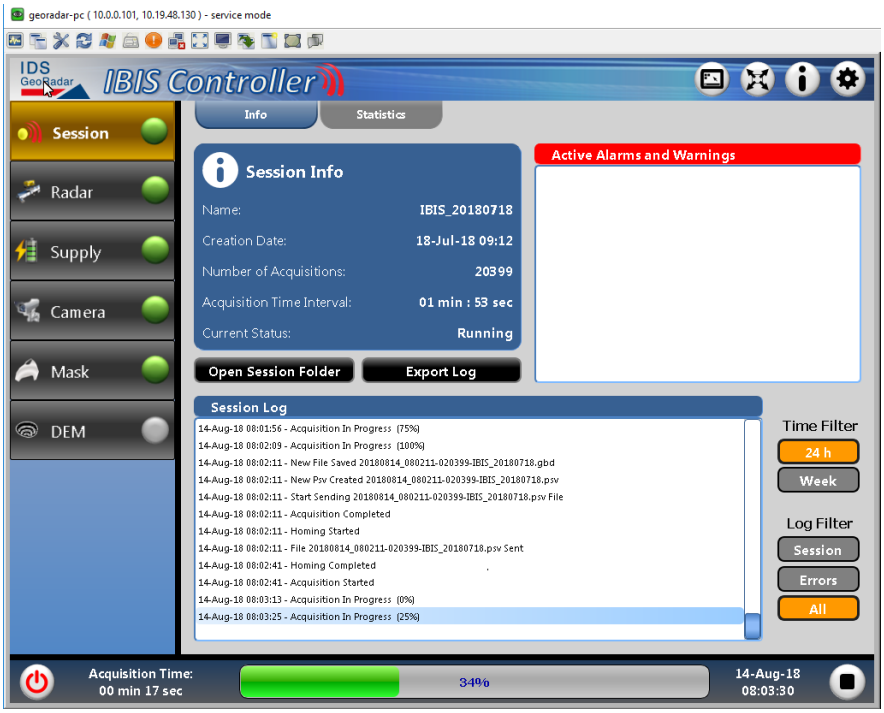

Figure 37 IBIS Controller

The Guardian (Figure 38) software process, manage, display and store results of a data acquisition from the IBIS Controller. The program is an early warning software which provides a real-time movement monitoring. Within the software is possible to produce different maps, such as displacement, velocity or hazard maps in which can be defined as different threshold values. When a movement exceeds a certain threshold value it possible to define alarms (visual alarms, e-mails or text messages), which the Guardian can send to supervisors or a geotechnical team.

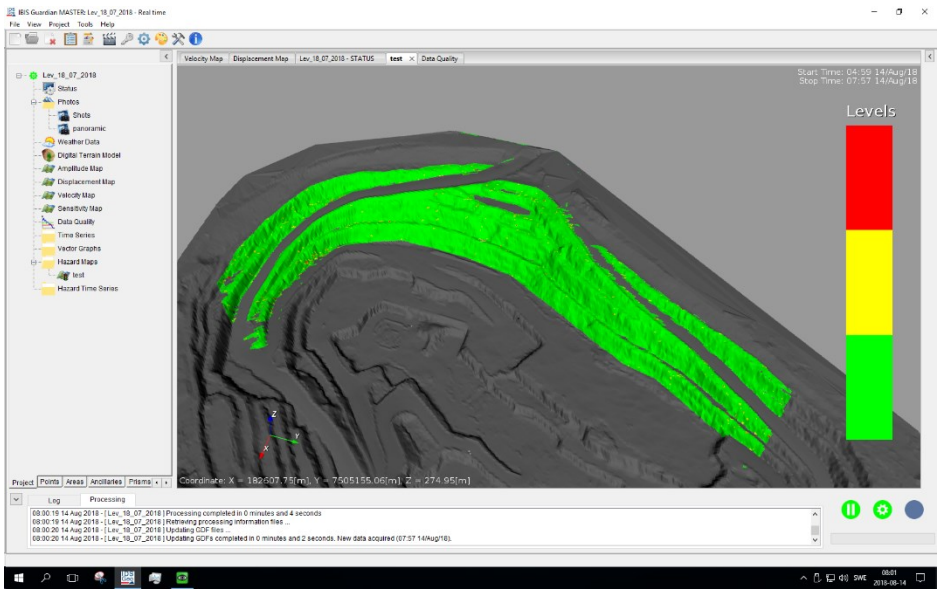

Figure 38 The Guardian

`

Both programs are combined - for a real-time monitoring two together must be turn on. They are connected through IBIS Wi-Fi Network or a mining network to allow data flow between computer programs (Figure 39).

The IBIS Controller creates 3 types of files, during each scan: GBD (raw data), MSK (selection mask) and PSV (pre-processed).

GBD files are raw data files. Each file corresponds to one acquisition of a data. It contains information about an amplitude and a phase, as well as a pixels matrix. A pixels matrix is depended on a maximum distance, a range, and a cross-range resolution. A size of the GBD file varies from 10-20 MB.

An MSK file is created when a new data acquisition session is generated. It is a spatial mask, which defined pixels spatial selection of a measured area and quality thresholds on a raw data. A mask is linked to GDB files and reduces a points number which will be implicated in a monitoring. Furthermore, it allows for a better connection between the IBIS Controller and the Guardian. A mask file has to be updated periodically. An update is necessary because a mine is constantly developing, therefore an area of interest required changes. An update is done with an incremental logic. Pixels can be added, but never removed. Mask changes can be only provided when a data acquisition session is not running.

PSV files are pre-processed files. They are results of imposed MSK files on GDB files. It is a pixel matrix of selected points from a mask. PSV files contain information about an amplitude and a phase after focusing. Typical size of a PSV file vary from 0,1 to 0,4 MB.

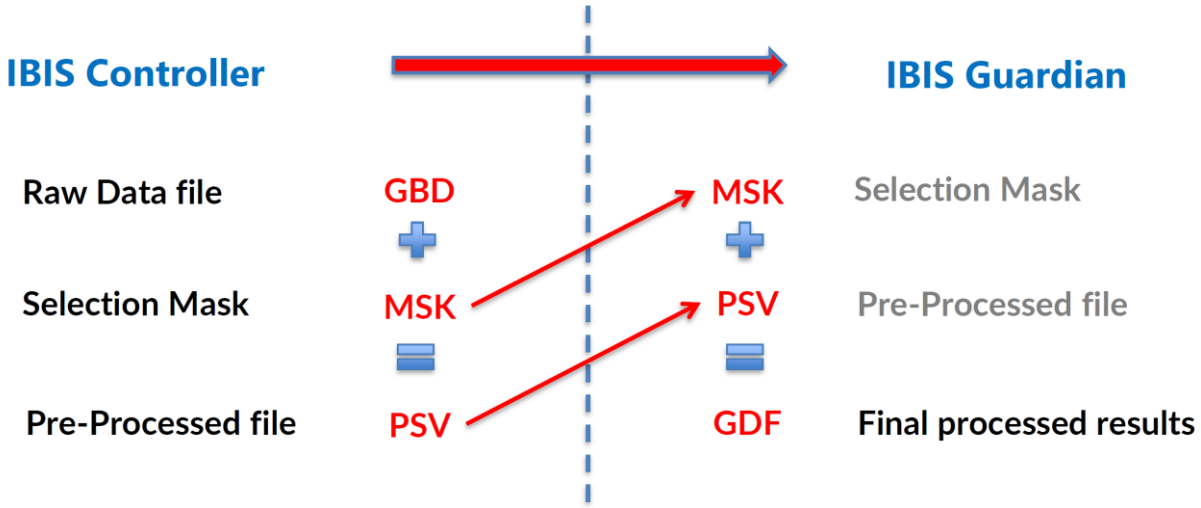

Figure 39 Data flow between programs (IDS, 2017)

The IBIS controller sends to the Guardian MSK and PSV files (Figure 40). The Guardian receives automatically both types of files from the IBIS Controller. A mask is necessary for a geocoding (a calculation of compatibility between a digital terrain model and radar pixels) and for pre-processed data (PSV files) to receive a final process data. Both types of files are a process to get a GDF file.

GDF files contain an final information about a amplitude and a phase, after an atmospheric correction of PSV files. A GDF file is related with many PSV files and consist of the permanent amount of data (133 MB). After a processing of each PSV file, GDB file is continuously updated.

`

There is also additional software- IBIS Planning Tool, where is possible to find the best radar LoS. The IBIS FM detects movements and calculates displacements towards it (Figure 42). Therefore, movements which are orthogonal to the radar will be no detected and the displacement value will be zero.

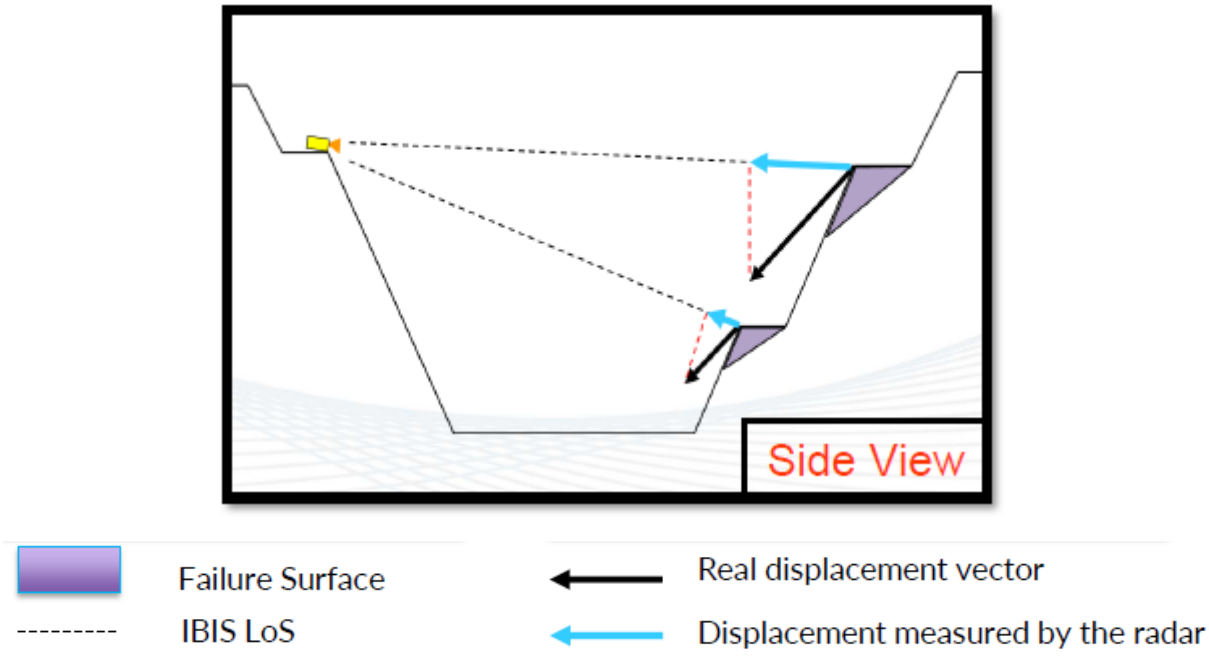

Figure 40 Line of Sight (IDS, 2017)

There are two types of maps which represents the LoS: a coverage map and a sensitivity map.

The coverage map (Figure 41) represents a 3-D geocoded map -an area, which the radar can cover with a range. The map is based on the local topography and a power of the back-scattered signal and represents a rough estimation of the return signal quality for each pixel. Areas which are orthogonal to the radar LoS have a high coverage (high quality of return signal), whereas areas parallel to the radar LoS a have low coverage (low quality of return signal). Coverage in the reality can vary depending on factors not related to topography: roads, vegetation, machinery etc..

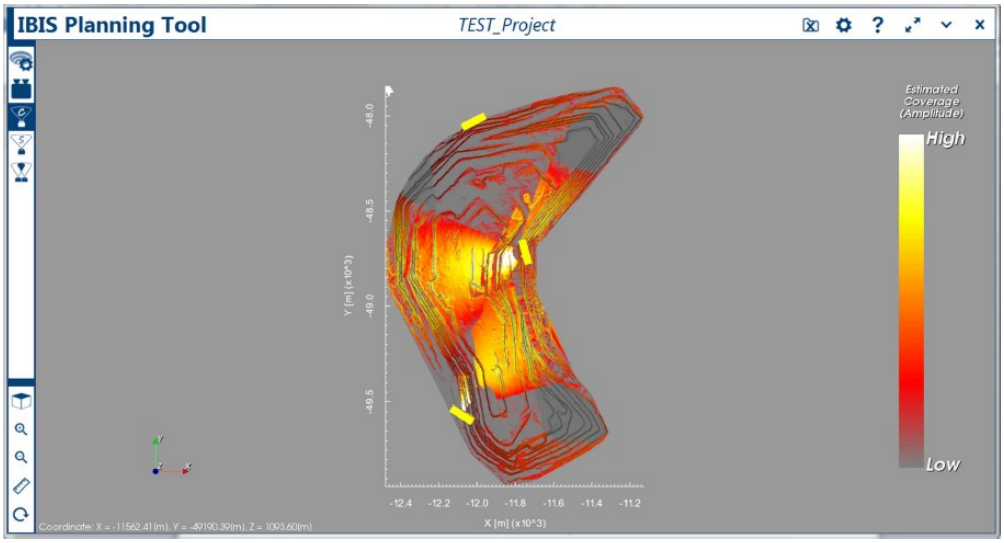

Figure 41 Coverage Map (IDS, 2017)

`

The sensitivity map (Figure 42) shows how good is the radar LoS depending on the expected movement direction. The radar sensitivity is calculating by using the value of the cosine of the radar LoS and the movement direction of the slope. There are three possible directions: steepest (along with the steepest direction of the slope), horizontal- along with the horizontal plane (a horizontal component of the steepest sensitivity map) and vertical-along vertical plane (a vertical component of the steepest sensitivity map).

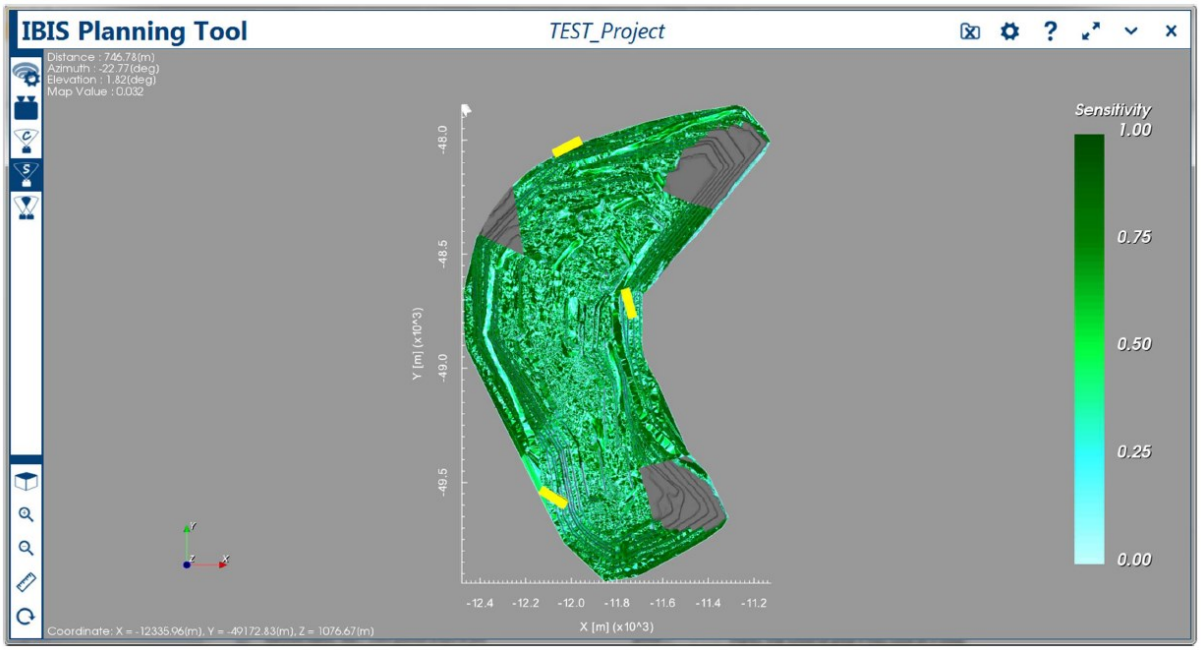

Figure 42 Sensitivity Map (IDS, 2017)

The value range of the sensitivity map varied from 0 up to 1, where 0 is the lowest sensitivity and 1 is the highest sensitivity.

3.2.3 Data processing

Data is firstly processed in the IBIS Controller, where PSV files are made by a filtering data of GDB files by the mask. PSV files have information about an amplitude and a phase of each measured point. To obtain an interferogram, a map of a displacement it is necessary to calculate a phase difference between two PSV files (Figure 43).

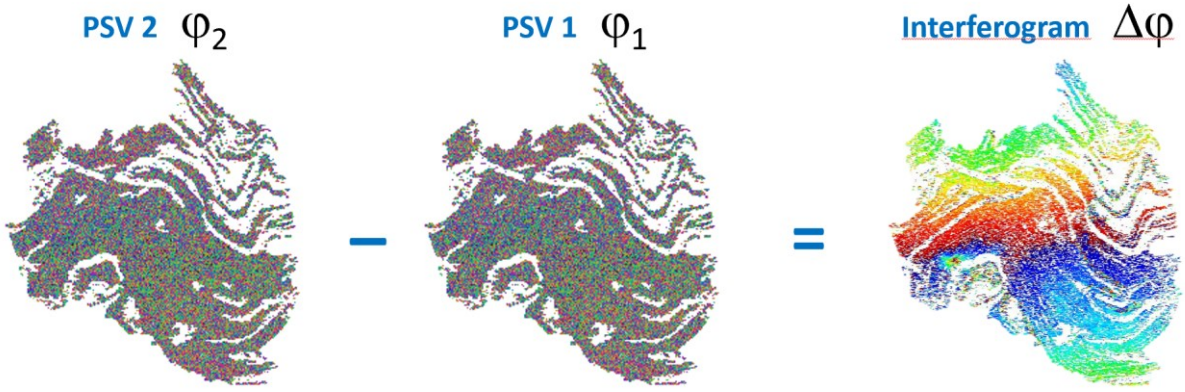

Figure 43 Interferogram obtainment (IDS, 2017)

`

The radar has two limitations in slope movement monitoring related to a measurable range Due to the phase ambiguity (the maximum phase difference recorded by the IBIS radar is π), the maximum displacement detectable is equal to

$$\pm\frac{\lambda}{4} = \pm 4{,}38\ mm \tag{30}$$

Therefore, assuming a data acquisition time of 2 minutes the maximum recorded velocity is equal to:

$$V_{max} = PA * N = 4{,}38\ mm * \frac{60}{2} = 131{,}4\ mm/h \tag{31}$$

Where:

PA it is the phase ambiguity and

N is a number of acquisitions per hour.

When a deformation exceeds the maximum measurable velocity, the Guardian cannot appropriately follow a displacement trend, but it can be easily evidenced. It can have resulted in a flattering of a displacement trend (Figure 44) and/ or an unusual color in the fast-moving area, mostly because a movement approach negative value (Figure 45).

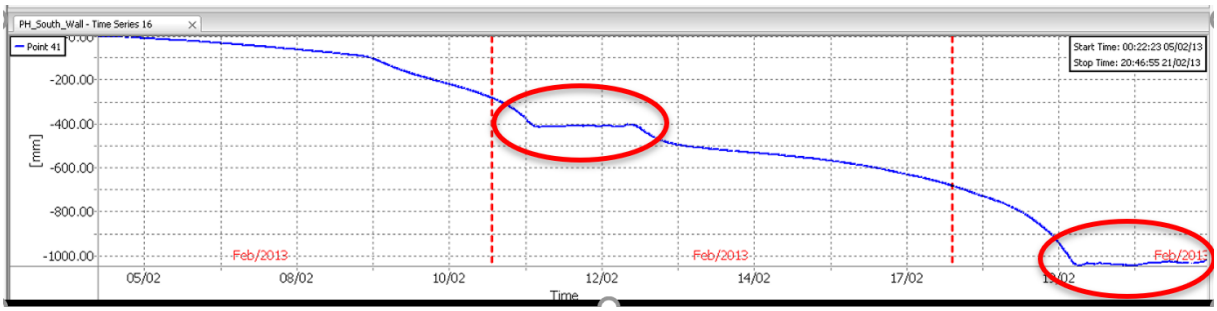

Figure 44 Flattering of a displacement trend

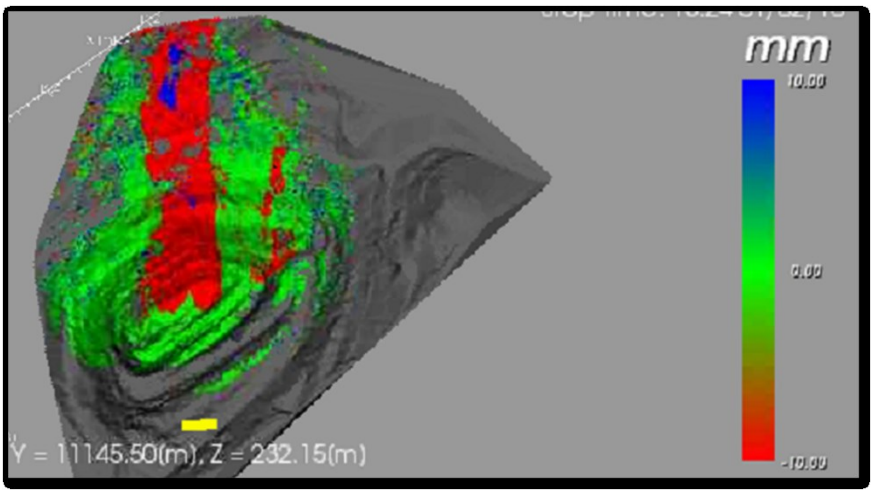

Figure 45 Color change due to approach negative value

The minimum measured velocity (V_{min}) is related to a device accuracy. The radar can detect a movement with 0,1 mm accuracy(Acc). Then the minimum detected velocity is:

`

$$V_{min} = Acc * N = 0{,}1\ mm * \frac{60}{2} = 2\ mm/h \quad (32)$$

The Guardian detects movements, which are less than 0,1 mm at any interval as a noise and remove them from results. To make the program possible to follow low rate movements instead of a real-time monitoring, it's possible to increase an interval of a data processing. Therefore slow movements are visible for the software. This process is named a subsampling (Figure 46).

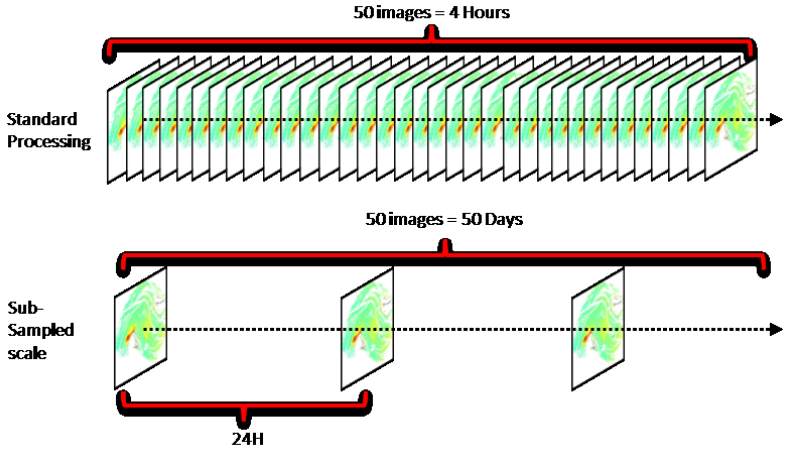

Figure 46 Subsampling (IDS, 2017)

Due to the Leveäniemi open pit location snow and ice can affect a data monitoring interpretation. Radar waves can penetrate through snow and reflect a signal from the slope wall. A signal travels through snow at a lower speed, therefore a wave has a shorter length (Figure 47). When the snow layer is stable, the radar system will produce reliable results, but every modification in the snow thickness affects outcomes.

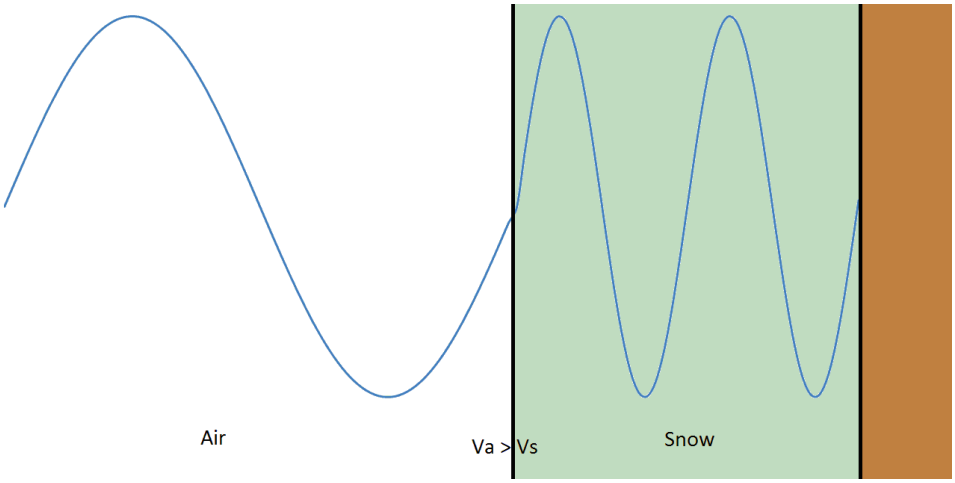

Figure 47 Change of wavelength due to a snow layer

When the layer of snow will change, a signal phase as well will change as presented in equation 41.

$$\Delta\phi = \Delta\phi_{def} + \Delta\phi_{atm} + \Delta\phi_{snow} \quad (33)$$

A change in phase related to a snow layer can be calculated from the following formula:

$$\Delta\varphi_{snow} = \frac{4\pi c \Delta h_{snow}}{\lambda_{air}} \left(\frac{1}{v_{snow}} - \frac{1}{c} \right) \quad (34)$$

Where Δh_{snow}-thickness of snow layer, v_{snow}-speed of light in snow, λ-wavelength in the air

A displacement which is a consequence of a change in the thickness of snow layer determined as:

$$\Delta d_{snow} = \Delta h_{snow} \left(1 - \frac{c}{v_{snow}} \right) \quad (35)$$

Substituting the speed of light (3.00 *10^8 m/s) and the speed of light in ice (2.29 *10^8 m/s), the displacement measured by the radar is equal to:

$$\Delta d_{snow} = -0.31 \Delta h_{snow} \quad (36)$$

Snow accumulates and melt spatially and produce a pattern, therefore, the displacement related to snow events differ from the real slope movement and can be easy to interpret (Figures 48-51) (Freeport-McMoRan, n.d.).

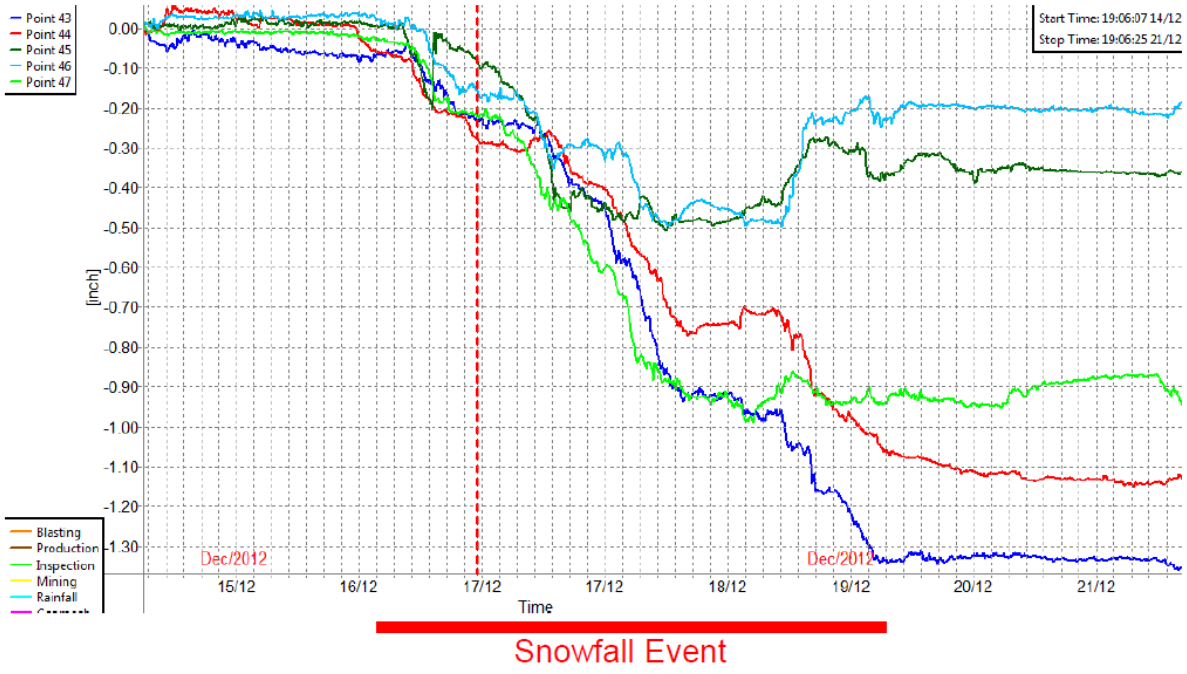

Figure 48 Time series for stable points during a snowfall event (Freeport-McMoRan, n.d.)

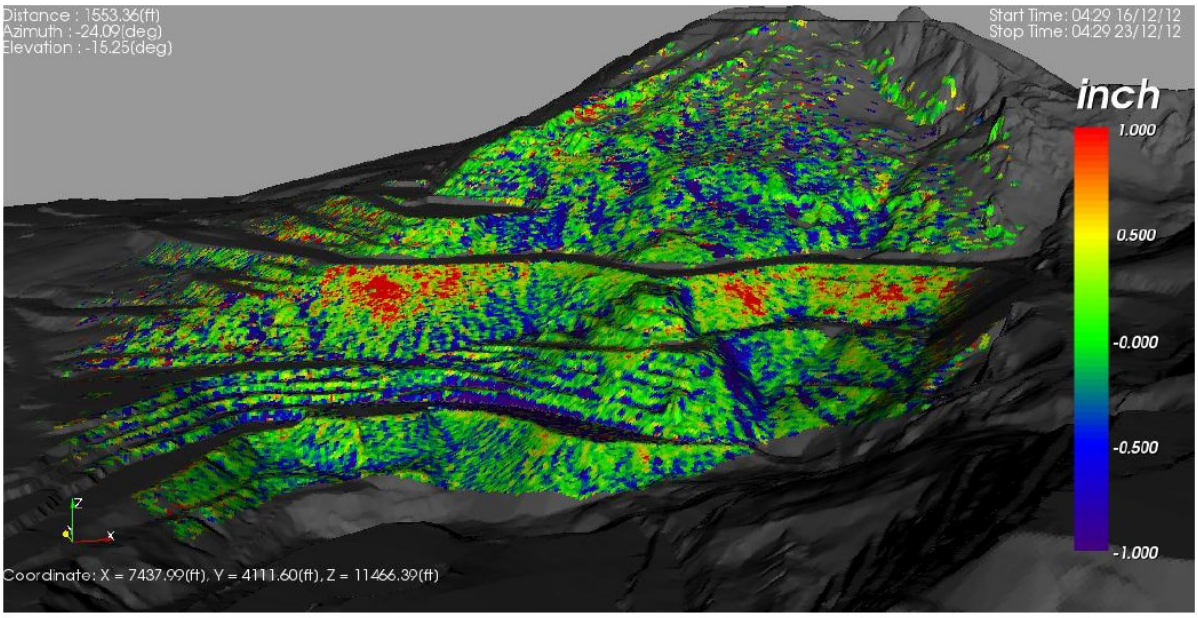

Figure 49 Displacement map during a snowfall event (Freeport-McMoRan, n.d.)

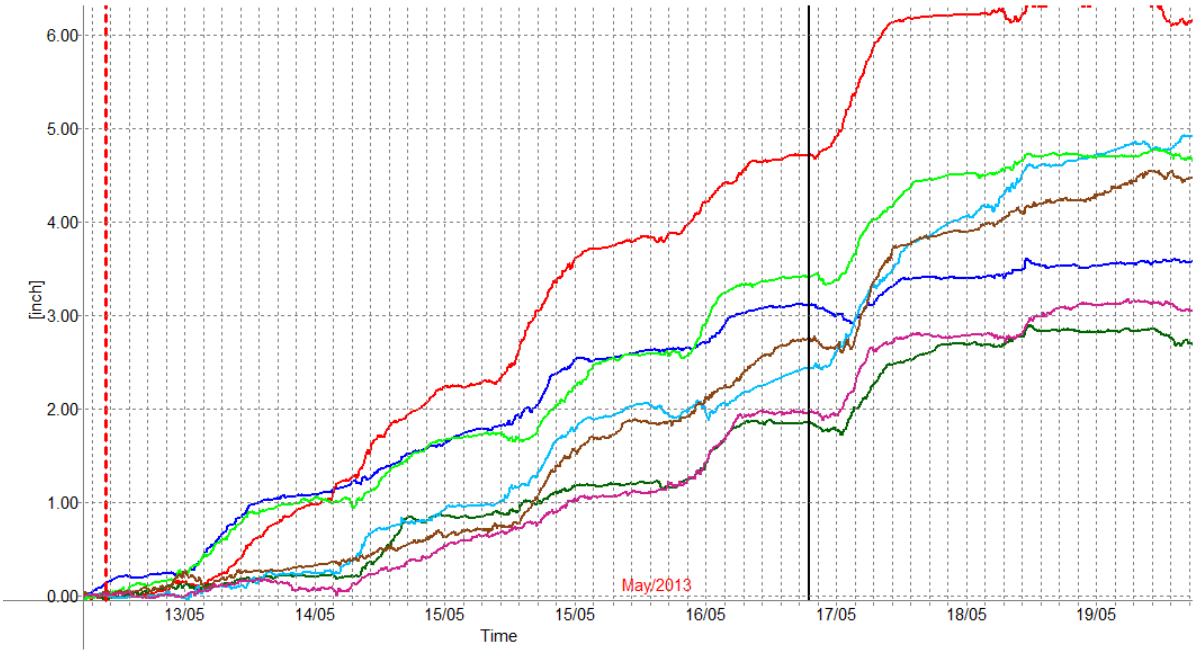

Figure 50 Time series for stable points during snow melting (Freeport-McMoRan, n.d.)

`

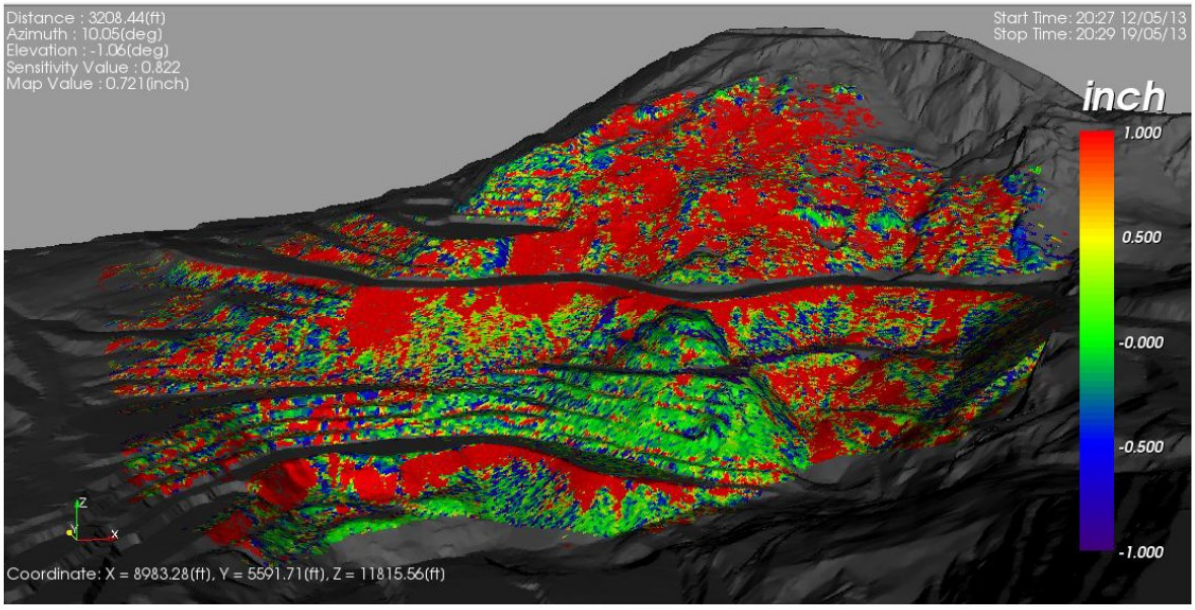

Figure 51 Displacement map for stable points during snow melting (Freeport-McMoRan, n.d.)

3.3 Radar placement

The most problematic wall in the Leveäniemi open pit is the southwestern wall. The water level in this wall is high and it is possible to see leakages on the wall surface (Figure 52). There has been installed drainage pipes, which are used to decrease a water pressure within the rock mass.

Figure 52 Moisture at the Southwestern Wall surface

The wall is placed in a strongly metamorphosed rock mass. There occurs a strong foliation-rocks at which the rock mass can slide. Foliation is dipping towards the pit, which increases a possibility of a failure (Figure 53). The competent part of the rock mass has a well-developed

`

spaced cleavage- biotite-rich layers are interlayered with the competent rock. Biotite appears as weak flakes, which are easy to break. This mineral reduces a resistance to shear stresses.

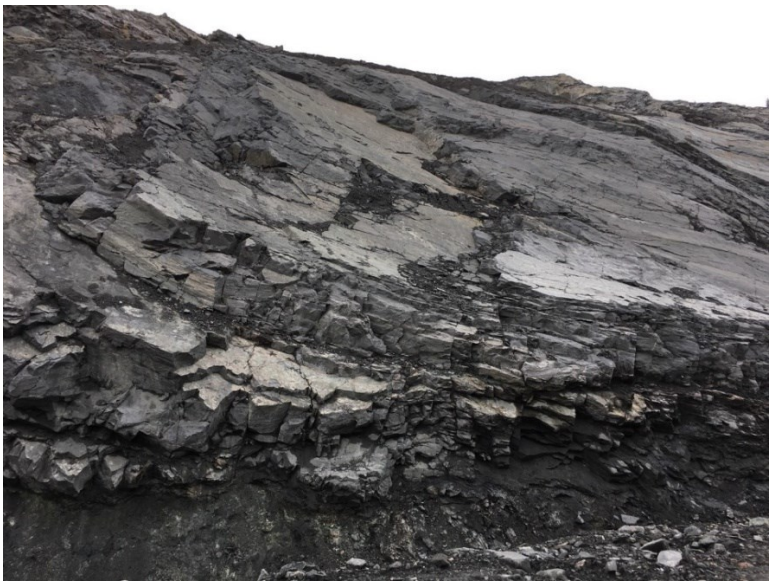

Figure 53 Foliation at the Southern Wall

This wall has been chosen as the main aim of a radar monitoring. It was necessary to find an appropriate place for a radar location for a proper monitoring of this place. Few locations were considered as a possible placement. The main factors which influence a place for radar installation are: safety (the radar must be located in an area were flying rocks from blasting will not destroy the device), an easy access to media (to an electricity and the Internet mine network), the device should not disturb a mine operation and a line of sight has to be efficient.

In the software, the IBIS Planning Tool (Figure 54) using a digital terrain model of a main is possible to check a line of sight of the radar.

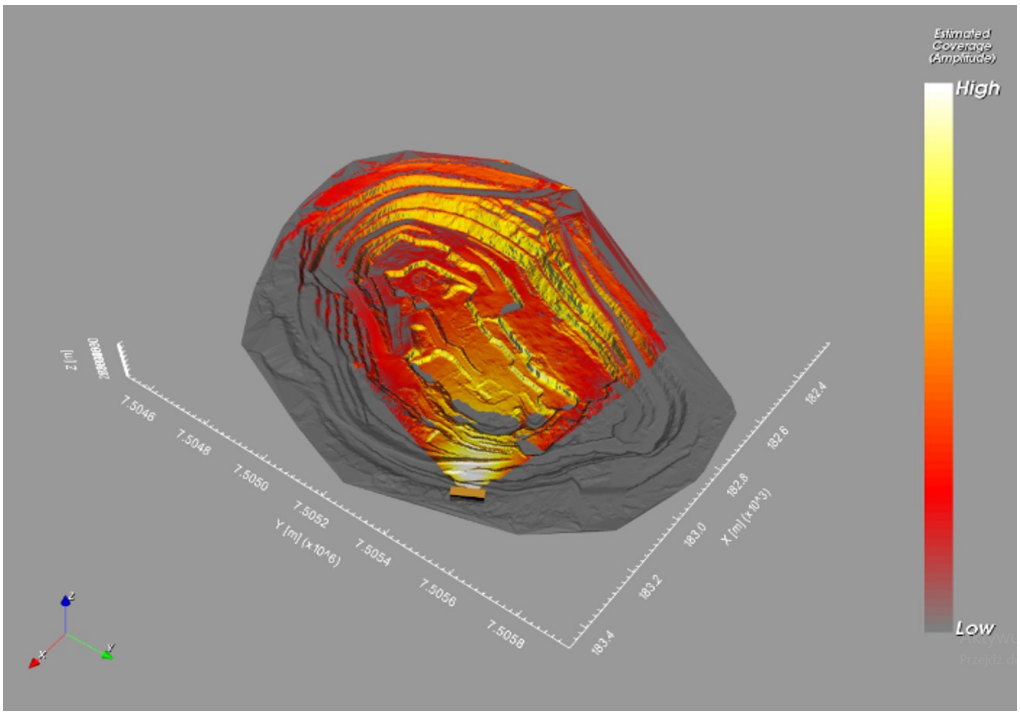

Figure 54 The line of sight at IBIS Planning Tool

`

The bench on the north is the best for the radar location. The place which has been chosen is located far enough that blasting will have no influence on the radar. Next to the place is located a media mast with an accessibility to all required media. The mine will not expand in this direction, therefore the radar will not disturb a mine operation. The radar in this location has a good line of sight for the most crucial part for the pit – the southern wall. The SSR system covers with it range almost half of the pit.

3.4 Radar settings

During a new acquisition session, it is necessary to set up various parameters on the radar settings. The default value for each acquisition time interval is set for 2 minutes. In the mine, the maximum distance from the radar towards slopes is approximately 1km. It is not required to change a basic setting. The quality of measurements will be sufficient.

Another important setting is a selection mask. The radar is catching unnecessary areas such as buildings, waste dumps etc. which are not required to monitor. Therefore those areas must be excluded from measurements. Moreover, almost every week a blasting has a place in the pit. The mine is not changing fast, but the selection mask requires a frequent update. The automatic update has been set for 21 days- three blasting. The update is set at midnight when mine is closed to have not any disturbances.

Data acquisition time has been left as in the basic settings – 2 min. It is not required to put a higher value- measurements are sufficient for this size of the pit.

The camera picture of the mine has been also set for an automatic update. Every Sunday at 3 p.m. camera will take a picture of an entire monitor area. This setting must be set off during winter due to lack of Sun.

Another important setting is the radar data management. The hard disk has a limited space. The threshold has been set at the default value- 30 GB. When the disk will exceed the threshold value, the IBIS Controller will automatically start deleting the data starting from the oldest files in the current session.

The Digital Terrain Model (DTM) has to be updated as frequently as possible. The DTM of the mine will be updated manually at least every month by a geotechnical engineer.

For the right measurements, the radar and the camera position has to be implemented to the Guardian in the local coordinates system.

The Leveäniemi open pit is divided into four rock mechanics domains as presented in Figure 55. Radar with it ranges measures displacement within two domains. Due to different rock mass conditions in each domain, it is necessary to implement this information into the radar system.

`

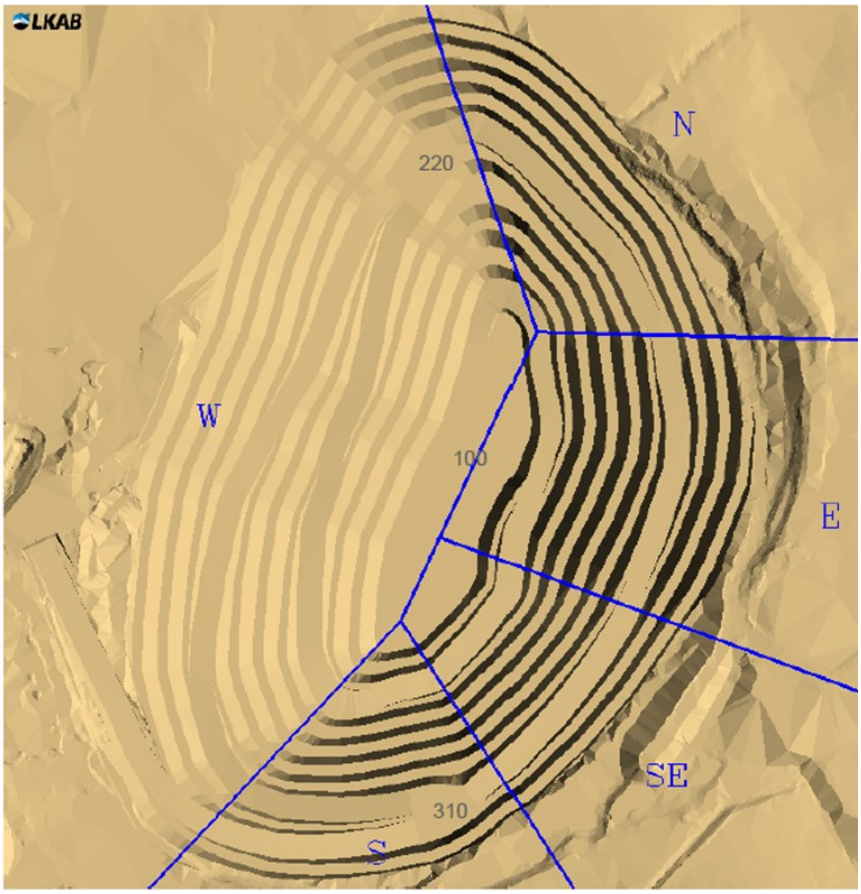

Figure 55 Rock mechanics domains at Leveäniemi open pit

Areas, where movement is not expected must be excluded from the measurements because of a noise production such as ramps, production areas, a bottom of the pit and areas which are not aimed for the radar monitoring system, such a part of -waste dumps or a top of the pit (Figure 56).

`

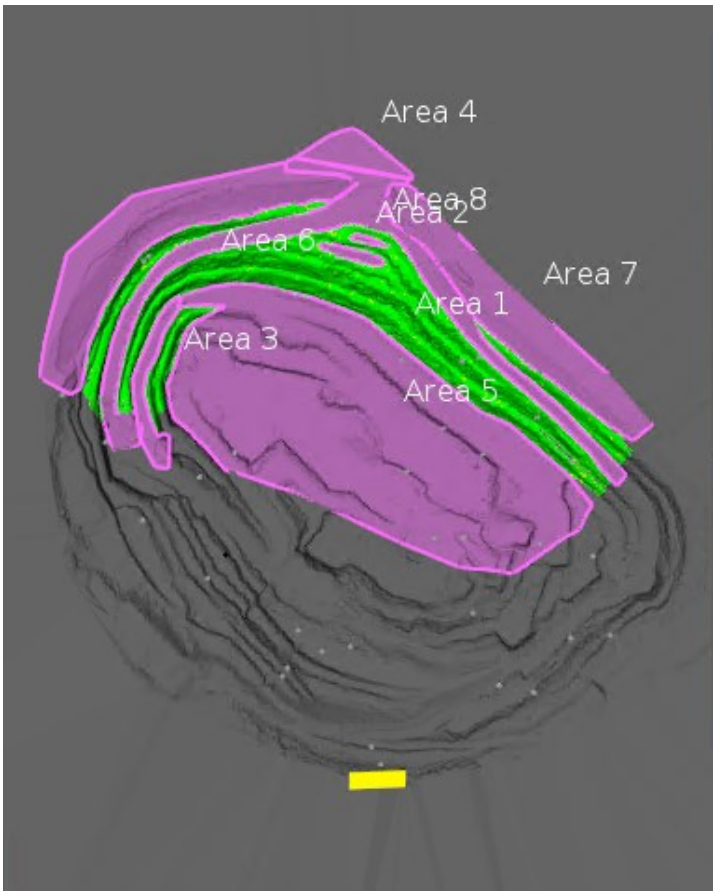

Figure 56 Areas excluded from slope stability monitoring. Pink-areas excluded, Green-areas included

For further analysis of deformation, it is crucial to define the type of failure that can occur in the pit. Due to Leveäniemi open pit geology planar and wedge are the likely failures that can take place.

By reviewing case studies, rock mass properties and experience of rock mechanics engineers Leveäniemi open pit threshold values range have been defined between 1-5mm/h. The radar calibration has started, by implementing alarms for the SSR monitoring system. Instability has to have at least 20 m^2 and exceed the threshold value for a minimum 3 hours. To avoid noises instability cannot be too small and need to last for a certain period of time. For a yellow alarm for the entire pit, an instability must exceed a rate of deformation 3 mm/h, where a red alarm has been established for the rate 5mm/h. The yellow alarm detects first signs of instabilities and informs that it is necessary to observe the unstable area. The red alarm warns against serious movement of the rock mass.

The calibration procedure will take for next months to find optimal threshold values. To define if the value is correct it is essential that the radar will run with set thresholds for a sufficient time period. This period has been set for one month. During this time all alarms have to collect and review. If the radar sends too many false alarms it necessary to increase threshold values. First increase time interval, then a deformation rate. If radar doesn't send any alarms or alarms seems to be too high it is crucial for safe operation to decrease threshold values.

`

4 Results

The radar has been installed on 18th July 2018. Basic settings were running for one month and after this period reviewed. It has been noticed that threshold values were too high and on 15th August 2018 new values have been implemented. New displacement rate 2,5 mm/h has been set for the yellow alarm. The red alarm has been set at the rate of 3,5mm/h.

At around 08:00 on 24th August 2018 the SSR system gave an alarm. The alarm was controlled in the Guardian software showing an area of the pit (Figure 57) which had repeated alarms of more than 2.5 mm/h of movement. These alarms had previously been disregarded as noise caused by truck traffic. The alarm on this day was different from previous alarms, this time the movement was registered near the crest of the bench rather than near the foot, as previous alarms.

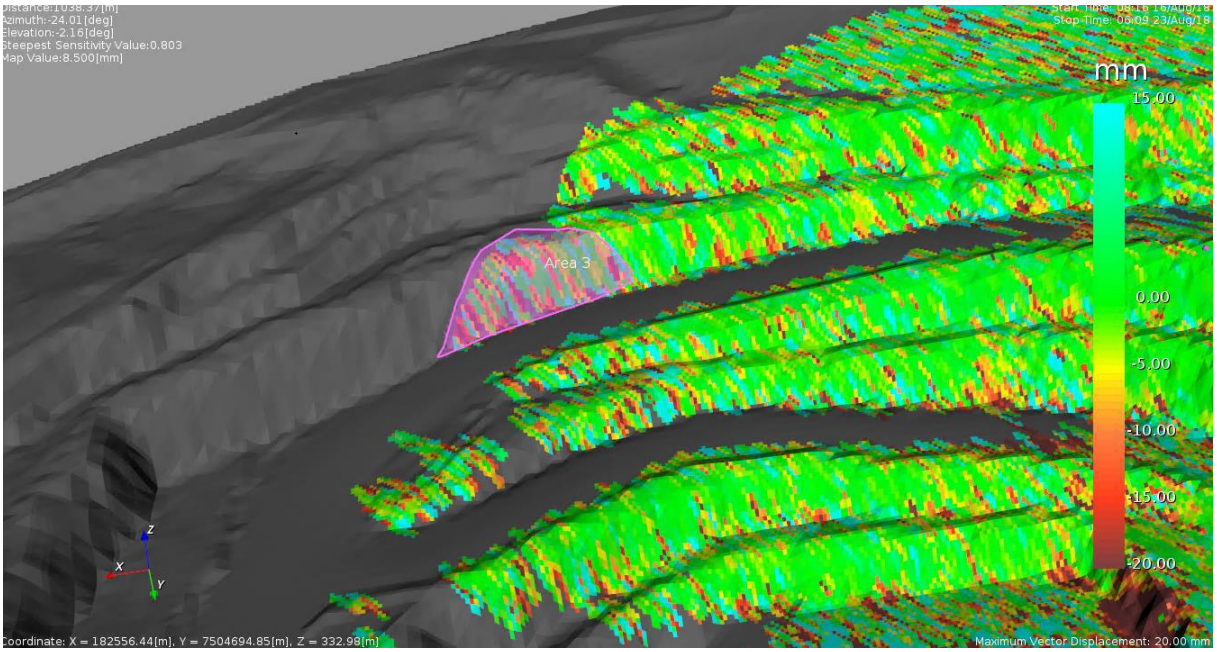

Figure 57 Displacement map of an instability area

The movement (Figure 58) was too high up to be caused by traffic, so further investigation was required. Upon an in-situ inspection of the bench, several dangerous structures were identified (see pictures below, Figures 59 and 60). Even though the radar system is new and still is in need of further calibration, the combination of repeated alarms in the same area and dangerous structures on the bench was taken seriously. These structures represented a possibility of the wedge and planar failure in the southern wall of the Leveäniemi open pit. Preventive measures were taken. One lane of the ramp was closed immediately, and scalers were brought over to start taking down the hazardous rock masses.

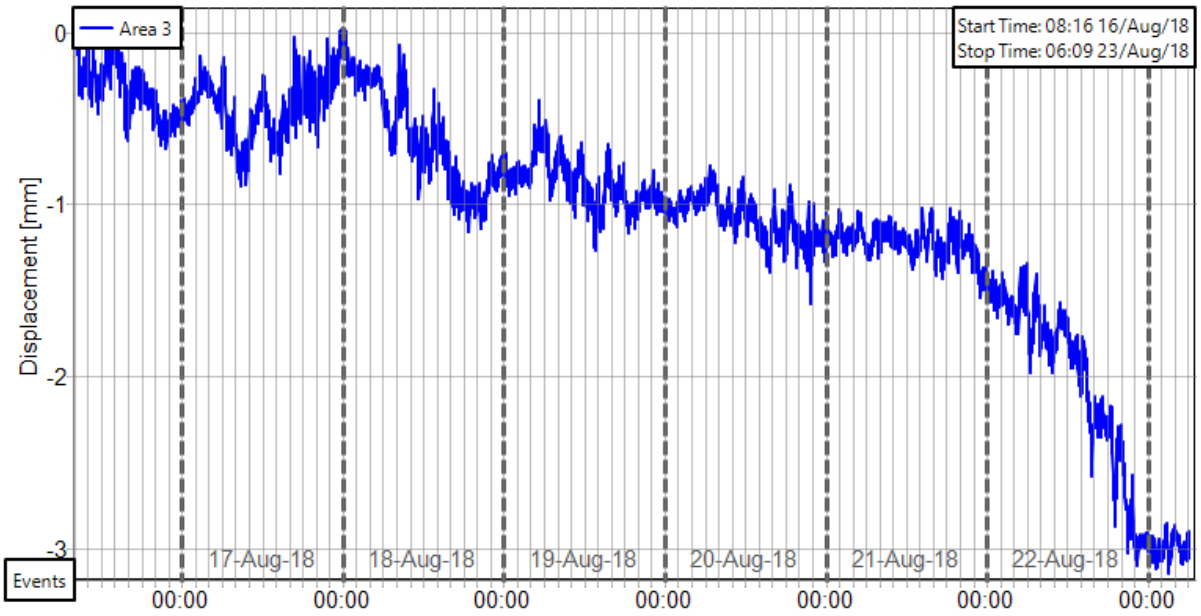

Figure 58 Displacement time series of area 3 under monitoring.

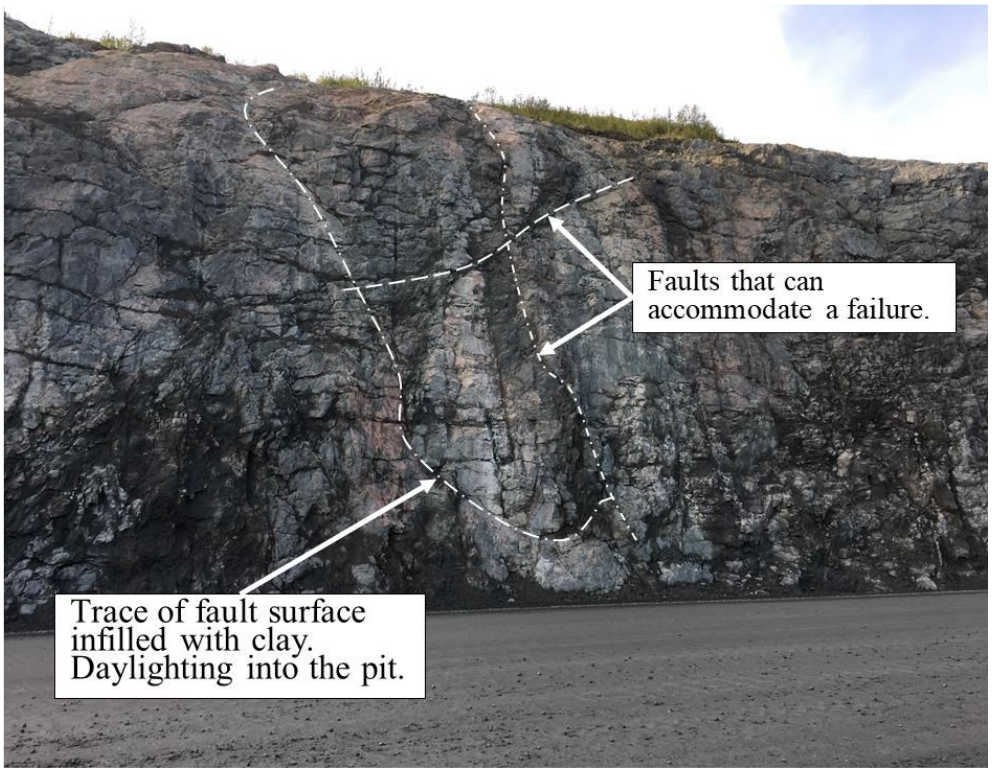

Figure 59 One of the dangerous structures identified on site. The main fault surface dips steeply, 65-70° perpendicular to the bench, towards the ramp, while the bench inclination is 80-85° (Offermo, 2018)

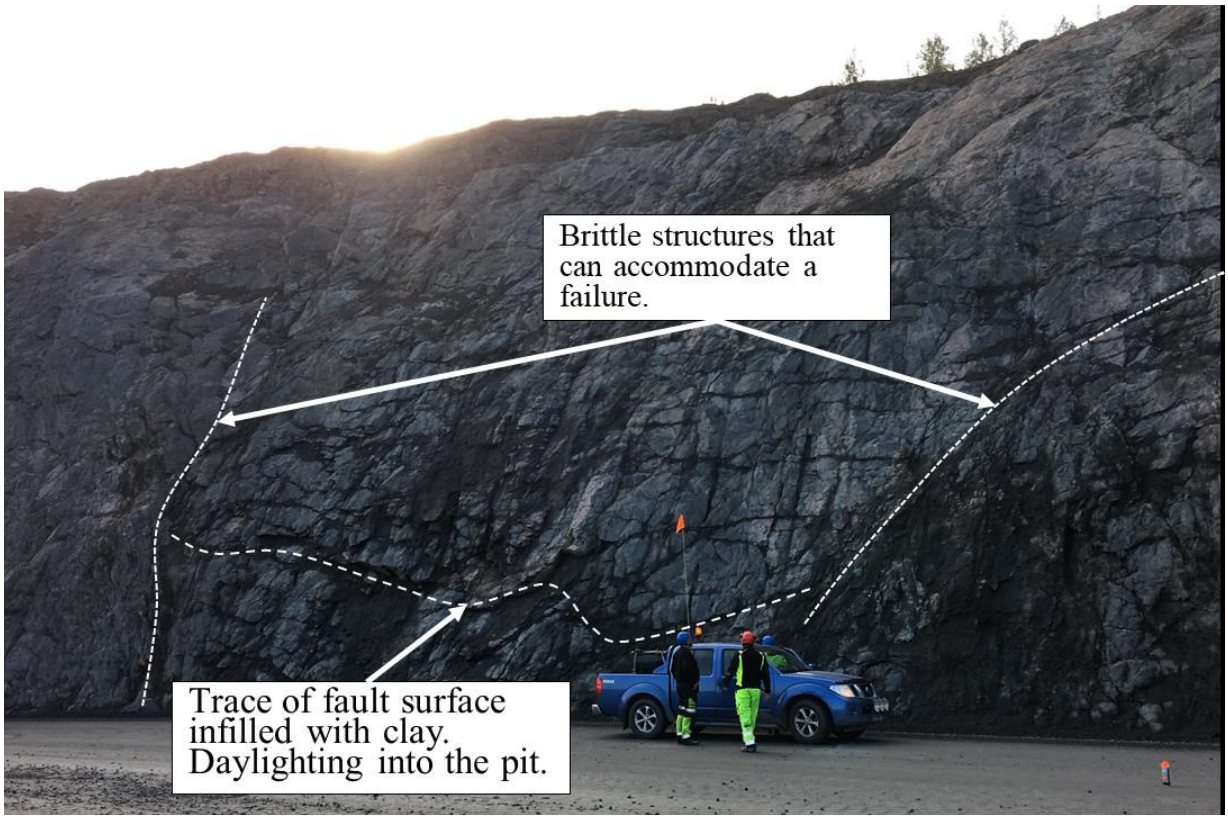

Figure 60 Another dangerous structures identified on site. The main fault surface dips steeply, 65-70° perpendicular to the bench, towards the ramp, while the bench inclination is 80-85° (Offermo, 2018)

After a scaling, no further alarms has been sent by the SSR system. The area has been visually investigated, the alarm was evaluated, the TARP has been removed and the monitoring system has resumed a normal monitoring.

On 12th September 2018, domains were implemented in the SSR system as presented in Figure 61. For both domains has been implemented threshold values. A back analysis of the instability event from 23rd August indicated that parameters: the size of instability area and the measurement interval are proper. Therefore, those parameters remain as it was implemented before. The displacement rate for the southern domain has been set at 1,5 mm/ h for the yellow alarm and 2,5 mm/h for the red alarm. For the western domain, the yellow alarm has been decided to implement 1 mm/h for the yellow alarm and 2,5 mm/h for the red alarm. The western domain contains more complex structures, therefore, the threshold should be lower than in the southern domain to allow for movement detection as early as possible.

`

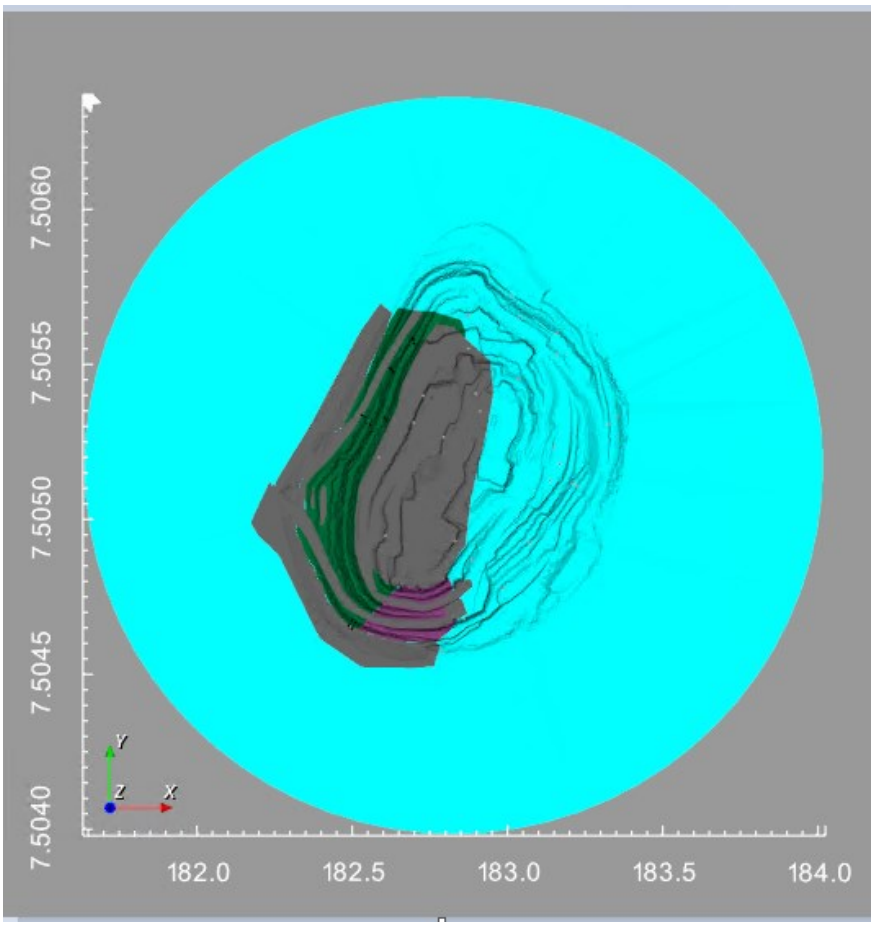

Figure 61 Rock mechanics domains implemented in the Guardian, green represents western domains, purple southern

`

5 Discussion

The calibration of the radar has to be continued and reviewed after each time when settings will be changed. At the moment threshold values for the displacement rate has been set at a low level comparing the first setting. It is because as the SSR system is a monitoring tool it is crucial to provide as soon as possible information about changes in the rock mass behavior. The required size of failure and the interval at which the SSR system will send an alarm to seem to be calibrated. Even when all threshold values will be calibrated, there must be reviewed as mine will develop. The rock mass properties can differ, deep down into the pit, stressed in slopes will increase, more ground-water will flow into the pit. All those factors can influence threshold values.

To deal with instabilities properly it is important that rock mechanics engineer has a deep knowledge, about the rock mass properties in the Leveäniemi open pit. One can use a procedure described by Dick and others (Dick, et al., 2014) in chapter 2.6 as a tool how to use a collected data by the SSR system. It describes step by step necessary actions that must be taken when the instability occurs.

Actually, on the side is placed only one radar. It detects movement in the almost whole western wall and half of the southern wall. Using the Planning Tool Software, the analysis has been made to define how many radars are necessary to cover with it range whole pit. 3 radars are necessary to monitor the whole pit with a very good sensitivity as it is presented in Figure 62.

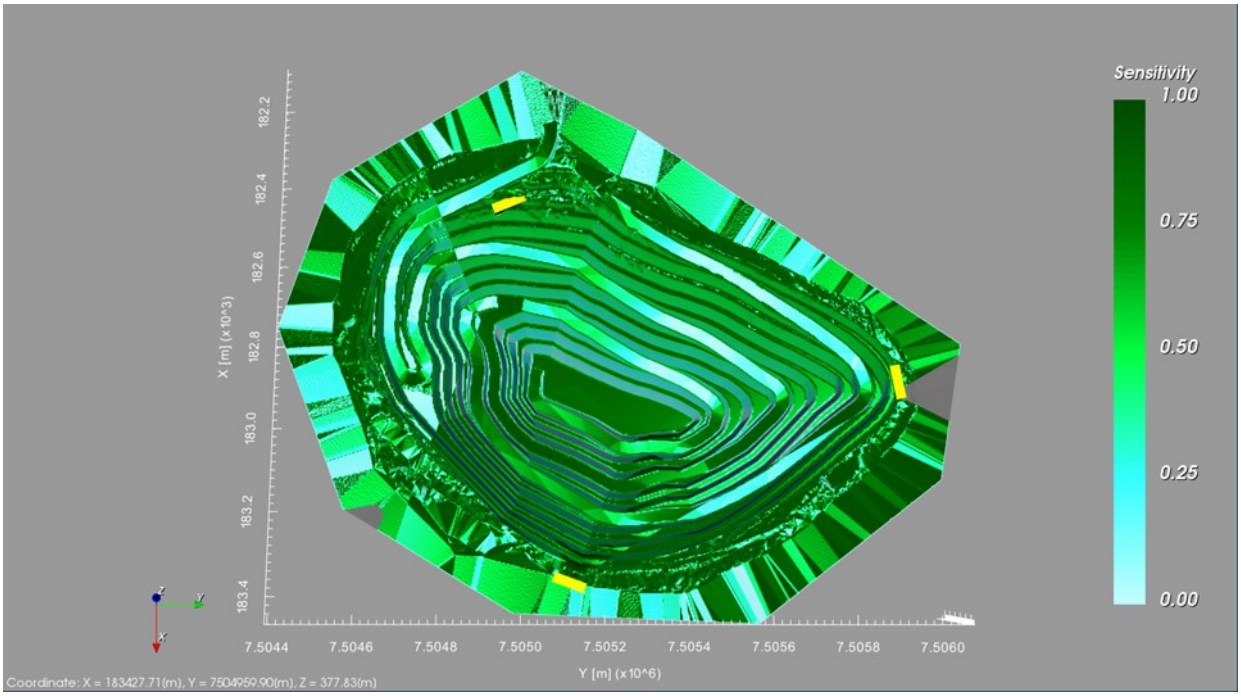

Figure 62 Monitoring of the pit by using 3 radars

Using 2 radars it is also possible to cover the whole of pit (Figure 63), but the sensitivity will be lower. This system will be more cost-effective than the system with 3 radars because the difference in the pit coverage will be disproportionate to incurred investment costs. Some areas can be assumed as stable and safe, therefore the movement is not expected there and areas can be excluded from the monitoring. Right now the SSR system in mounted on the

`

trailer, which makes it flexible. It is possible to move the radar and monitor different areas of interest. The most optimum solution will be to use two radars and mount them on the trailers that in any case it is possible to monitor whole all crucial points.

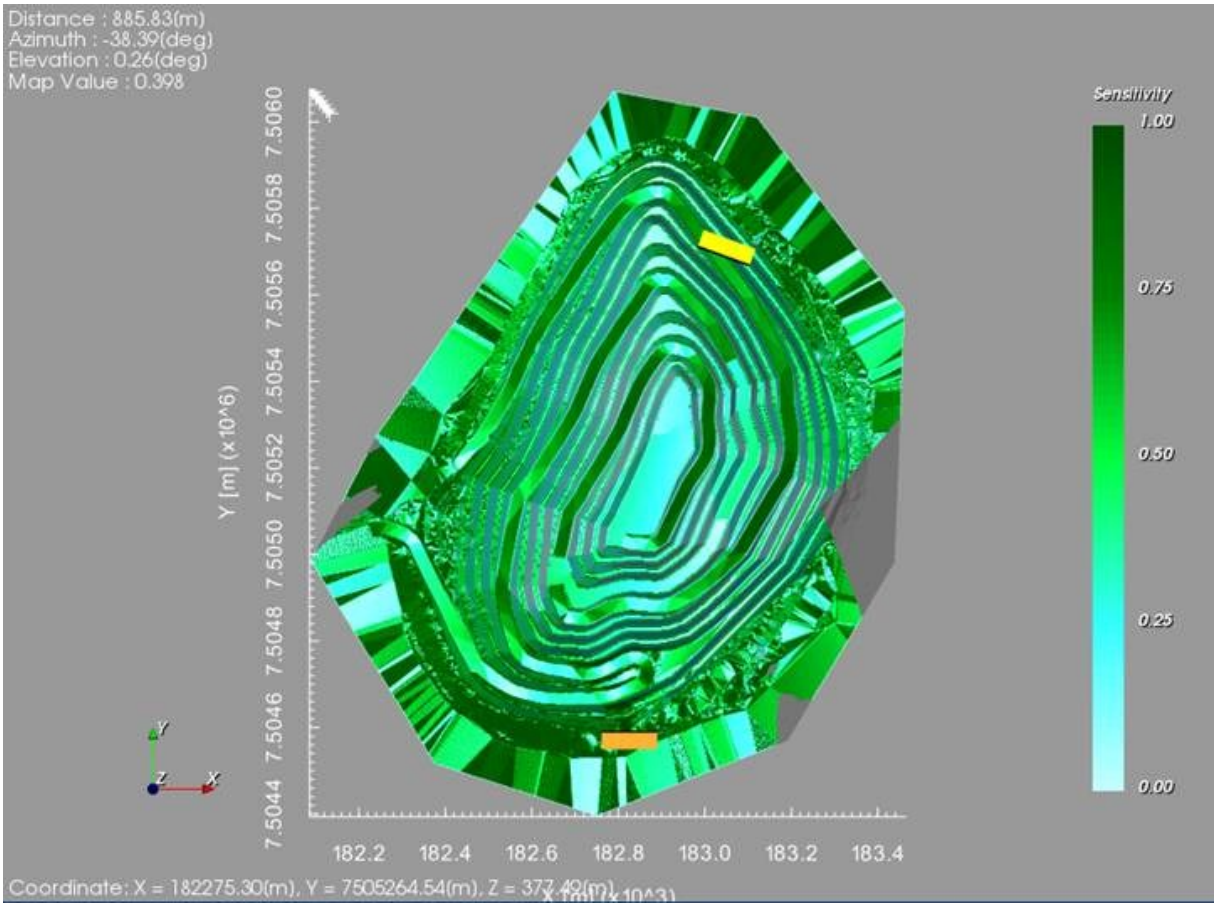

Figure 633 Monitoring of the pit by using 2 radars

`

6 Conclusions

Open pit mine walls movements and deformations occur constantly as a reaction to stress changes. Those movements depend on the local geology, slopes designs, the groundwater level, rock mass properties, and mining methods. In the worst scenario movement of the wall can result in a slope failure. There exist many methods, which can be used to monitor slope deformations. The SSR monitoring system is the state-of-art tool in slope monitoring technology and has many advantages over other methods. It is a useful device to predict slope failures and understand the rock mass behavior. Therefore mines can operate safely and cost-effective.

Leveäniemi open pit has a complicated local geology and weather conditions, together with a mine development slope failures could occur in the future. Therefore, mine managers decided to install the SSR monitoring system. The radar has been pointed in the direction of the southern wall, which is the most problematic wall in the mine. Basic settings have been applied and the radar calibration started.

The suggested threshold value range seems to be right. Through the calibration, values have been three times decreased. This process is a long-term mechanism, which requires an understanding of the data acquired by the radar. Time which is required to assume if the applied threshold values are good is limiting the research. Moreover, mine development can affect the threshold values.

During the calibration process, on 24th August 2018 movements, which exceeded threshold values occur at the southern wall and preventive measures have been taken, which had resulted in the alarm cancellation. After the event, the radar system continued the calibration process.

The event confirmed that the SSR monitoring system can provide a reliable data about deformations within mine slopes and can be used to help in the slope failure prediction. The most important is the data interpretation. The radar will not define the exact date of failure but helps to understand the rock mass behavior. The SSR system is just a tool, which collected the data. Rock mechanics engineer needs to interpret the data to define when the slope behavior changes to predict if failure will occur and to estimate the date of failure, that all preventive measures can be taken.

The SSR system still needs to be calibrating. As mention before, the threshold values which are implemented should be reviewed every month to find optimal ones. When a deformation will occur and exceed set thresholds values rock mechanics engineer should follow the procedure described by Dick and others (Dick, et al., 2014). Moreover, in Appendixes are described other procedures which should be implemented into the mine system.

`

References

Wyllie, D. C. & Mah, C. W., 2005. *Rock Slope Engineering, Civil and Mining, IV Edition.* New York: Taylor & Francis.

A Dictionary of Earth Sciences , 1999. *encyclopedia.com.* [Online]
Available at: https://www.encyclopedia.com/science/dictionaries-thesauruses-pictures-and-press-releases/angle-internal-friction
[Accessed 31 May 2018].

Ampatzi, G. et al., 2016. *Application of Terrstrial Laser Scanning (LIDAR) in Rock Slope Stability, an Example from Nothern Greece.* Thessalonik, s.n.

Anon., 2018. [Online]
Available at:
https://www.waterboards.ca.gov/lahontan/water_issues/programs/storm_water/docs/Chapter06.pdf

B. Reeves, D. N. G. S. D. L., 2001. Slope stability radar for monitoring mine walls. *SPIE Proceedings Vol. 4491.*

Broadbent, C. D. & Zavodni, Z. M., 1982. *Influence of rock structure on stability. Stability in Surface Mining.* Denver: Society of Mining Engineers.

Brox, D. & Newcomen, W., 2003. Utilizing strain criteria to predict highwall. *ISRM 2003–Technology roadmap for rock mechanics, South African Institute of Mining and Metallurgy,* pp. 157-161.

Carla, T. et al., 2017. On the monitoring and early-warning of brittle slope failures in hard rock masses: Examples from an open-pit mine. *Engineering Geology*, pp. 71-81.

Charles A. Kliche, 2011. *SME Mining Engineering Handbook, Chapter 8.3 Slope Stability.* s.l.:Society for Mining, Metallurgy, and Exploration, Inc..

Chaulya, S. K. & Prasad, G. M., 2016. *Sensing and Monitoring Technologies for Mines and Hazardous Areas,Monitoring and Prediction Technologies.* 1st ed. Amsterdam : Elsevier Inc..

content.inflibnet.ac.in, 2018. *www.content.inflibnet.ac.in.* [Online]
Available at: http://content.inflibnet.ac.in/data-server/eacharya-documents/53e0c6cbe413016f234436e8_INFIEP_3/2/ET/3-2-ET-V1-S1___causes_of_slope_failure.pdf
[Accessed 3 July 2018].

Cruden, , D. M. & Masoumzadeh, S., 1987. Accelerating Creep of the Slopes of a Coal Mine. *Journal of Rock Mechanics and Rock Engineering,* Volume 20, pp. 123-135.

Dalbehera , S. K., 2018. [Online]
Available at:
https://www.researchgate.net/publication/281745234_TACHEOMETRIC_SURVEYING

Dick, G. . J. et al., 2014. Development of an early-warning time-of-failure analysis methodology for open-pit mine slopes utilizing ground-basedslope stability radar monitoring data. *Canadian Geotechnical Journal,* pp. 515-529.

`

Fleurisson, J. A., 2012. *Slope Design and Implementation in Open Pit Mines: Geological and Geomechanical Approach.* Fontainbleau, Elsevier, pp. 27-38.

Flores , G. & Karzulovic, A., 2001. *The Role of the Geotechnical Group in an Open Pit: Chuquicamata Mine, Chile.* s.l., SME.

Floyd, J., 1998. The development and implementation of efficient wall control blast designs. *Journal of Explosives Engineering 15(3),* pp. 12-18.

Floyd, J., 2000 . *Explosives and Blasting Technique, Minimizing blast damage to rock slopes.* Rotterdam : Balkema .

Frederico, A. et al., 2012. Prediction of time to slope failure: a general framework. *Environmental Earth Science,* Volume 66, pp. 245-256.

Freeport-McMoRan, n.d. *The effects of snow on IBIS data,* s.l.: s.n.

Fukuzono, T., 1985. *A new method for predicting the failure time of a slope.* Tokyo, Japan Landslide Society.

gisresources, 2018. [Online]
Available at: http://www.gisresources.com/what-is-geodesy/

Harries, N., Noon, D., Pritchett, H. & Bates, D., 2009. *Slope Stability Radar for Managing Rock Fall Risks in Open Cut Mines.* Toronto, ROCKENG09.

Harries, N., Noon, D. & Rowley, K., 2007. Case studies of slope stabilityradar used in open cut mines. *International Symposium on Stability of Rock Slopes.*

Harris , N. & Holmstrom, M., 2007. The Use of Slope Stability Radar in Monitroing Slopes and Managing Slope Instability Hazards. *Queensland Roads Edition No 4,* pp. 39-44.

Hoek, E., 2006 . *Practical rock engineering.* Vancouver: s.n.

Hu, H., 2013. *Deformation monitoring and modeling based on LiDAR data for slope.* Aachen: RWTH Aachen.

IDS GeoRadar, 2017 . *IBIS-FM/FMT Training Course, Radar Basics and Working Principles,* s.l.: IDS GeoRadar.

Intrieri, E. et al., 2012. Design and implementation of a landslide early warning system. *Engineering Geology,* p. 124–136.

ISO, (. I. O. f. S., 2018. *www.iso.org.* [Online]
Available at: www.iso.org/obp/ui/#iso:std:44885:en

J. M. Girard, E. M., 2002. Detecting Problems with Mine Slope Stability. *31st Annual Institute on Mining Health, Safety, and Research.*

K. A. Niminye, K. J. B. a. G. N., 2016. *Optimizing Presplit Blasting for Environmental Control and Pit Wall Stability.* Tarkwa , s.n., pp. 12-18 .

Kane, W. F., Beck, T. J. & Hughes , J. J., 2001. *Applications of Time Domain Reflactometry to Landslide and Slope Monitoring.* Evanston, Northwestern University.

`

Kothari, U. C. & Momayez, M., 2018. New approaches to monitoring, analyzing and predicting slope instabilities. *Journal of Geology and Mining Research.*

Kumar , A. & Villuri, V., 2015. Role of Mining Radar in the Slope Stability Monitoring at Open Cast Mines. *Procedia Earth and Planetary Science, Volume 11,* pp. 76-83.

Kumar, A. & Rathee, R., 2017. Monitoring and evaluating of slope stability for setting out of critical limit at slope stability radar. *International Journal of Geo-Engineering.*

Kumar, V. & Parkash, V., 2015. A model study of slope stability in mines situated in south India. *Advances in Applied Science Research,* 6(8), pp. 82-90.

Larsson, M., Bergman, A., Malmgren, J. E. & Mwagalanyi, H., 2018. *Radar for slope monitoring.* s.l., Swedish Rock Engineering Association.

Little, M., 2005. *Slope monitoring strategy at Pprust open pit operation.* Johannesburg, The South African Institute of Mining and Metallurgy.

Martin, D. C., 1993. *Time dependent deformation of rock slopes,* London : University of London.

McHugh, E. L., Charles, S. & Long, D. G., 2018. *Applications of Ground-Based Radar to Mine Slope Monitoring.* s.l.:s.n.

Mercer, K. G., 2006. *Investigation into the time dependent deformation behaviour and failure mechanisms of unsupported rock slopes based onthe interpretation of observed deformation behaviour,* Johannesburg: University of the Witwatersrand.

Mine Design Technologies, 2018. *www.mdt.ca.* [Online]
Available at: https://mdt.ca/borehole-extensometer/

Mononen, S., Suikkanen, M., Coli, N. & Meloni, F., 2018. *Use of radar system for real-time safety-critical slope monitoring.* Sevilla, s.n.

Mufundirwa, A. & Fujii, Y., 2008. *New methods for prediction of geomechanical failure-time.* Gwangju, Korean Rock Mechanics Society.

Mufundirwa, A. & Fujii, Y., 2010. *Prediction of rock mass failure-time of geo-hazards.* Lausanne, Taylor & Francis.

N. Harries, D. N. H. P. D. B., 2009 . Slope Stability Radar for Managing Rock Fall Risks in Open Cut. *ROCKENG09: Proceedings of the 3rd CANUS Rock Mechanics Symposium.*

NPTEL, 2016 . *National Programme on Technology Enhanced Learning.* [Online]
Available at: www.nptel.ac.in/
[Accessed 17 August 2018].

onlinepubs.trb.org, 2018. *www.onlinepubs.trb.org.* [Online]
Available at: http://onlinepubs.trb.org/onlinepubs/circulars/ec129.pdf
[Accessed 8 August 2018].

Osasan, K. S., 2012. *Open-cast mine slope deformation and failure mechanism interpreted from slope radar monitoring, PhD Thesis.* Johannesburg: s.n.

`

people.eng.unimelb.edu.au, 2018. *people.eng.unimelb.edu.au.* [Online]
Available at: https://people.eng.unimelb.edu.au/stsy/geomechanics_text/Ch11_Slope.pdf
[Accessed 3 July 2018].

Prajapati, G., 2017. *www.slideshare.net.* [Online]
Available at: https://www.slideshare.net/GhanshyamPrajapati3/types-of-slope-failures
[Accessed 11 May 2018].

Prakash, A., Kumar, A. & Singh, K. B., 2015. *Highwall Mining: A critical appraisal.* Dhanbad, Minetech.

Priya, 2016. *www.civildigital.com.* [Online]
Available at: https://civildigital.com/failure-modes-in-rock-and-soil-slopes-slope-failure/#Wedge_Failure
[Accessed 11 May 2018].

Queen University Belfast , 2018. *www.qub.ac.uk.* [Online]
Available at: https://www.qub.ac.uk/geomaterials/weathering/causeway/rotationalslide.html
[Accessed 11 May 2018].

Raju, G. S., 2008. *Radar Engineering and Fundamentals of Navigational Aids.* New Delhi: I. K. International Publishing House Pvt. Ltd..

Ramamurthy, T., 2010. *Engineering in Rocks for Slopes, Foundations and Tunnels.* Second ed. New Delhi : PHI Learning Private Limited .

Rose, N. D. & Hungr, O., 2007. Forecasting potential rock slope failure in open pit mines using the inverse velocity method. *International Journal of Rock Mechanics and Mining Sciences,* Volume 44, p. 308–320.

Roux, R., Terbrugge, P. & Badenhorst, F., 2006. *Sloper managment at Nacachab gold mine, Nambia.* Johannesburg , The South African Institute of Mining and Metallurgy.

RST Instruments , 2018. *www.rstinstruments.com.* [Online]
Available at: https://www.rstinstruments.com/Borehole-Extensometers.html

Sarunic, W. & Lilly, P. A., 2006. *The use of CUSUMs as a tool to aid in the interpretation of slope monitoring data with specific examples from operating open pit mine.* Cape Town, The South African Institute of Mining and Metallurgy.

Saunders, P., Nicoll, S. & Christensen, C., 2016. *Slope stability radar alarm threshold validation at Telfer gold mine.* Perth, Australian Centre for Geomechanics.

Sjöberg, J., 1999. *Analysis of Large Scale Rock Slopes, Doctoral thesis,* Lulea: Lulea University of Technology .

SRK Consulting, 2014. *Structural pit mapping and core analysis,Levaniemi Fe Deposit, Sweden ,* Skellefteå: SRK Consulting.

Sullivan, T. D., 1993. *Understanding pit slope movements.* Rotterdam, Balkema.

Sullivan, T. D., 2006. *Pit slope design and risk- a view of the current state of the art.* Johannesburg, The South African Institute of Mining and Metallurgy.

`

Sullivan, T. D., 2007. *Hydromechanical Coupling and Pit Slope Movements.* Perth, Australian Centre for Geomechanics (ACG), The University of Western Australia.

T. Mametja, T. Z., 2017. Slope stability enhancement through slope. *Conference: 51st US Rock Mechanics / Geomechanics Symposium.*

The University of Alabama in Huntsville, 2018. *The University of Alabama in Huntsville.* [Online]
Available at: www.ece.uah.edu/courses/material/EE710-Merv/SARPart1_11.pdf
[Accessed 25 July 2018].

The University of Melbourne, 2018. *www.people.eng.unimelb.edu.au/.* [Online]
Available at: https://people.eng.unimelb.edu.au/stsy/geomechanics_text/Ch11_Slope.pdf
[Accessed 8 August 2018].

Toit, I. d., 2015. *Combining different technologies for better assessing slope stability on a mine.* Ekurhuleni, PositionIT.

Tose , S. S. J., 2006 . *A Review of the Design Criteria and Practical Aspects of Developing a Succesful Pre-split.* Johannesburg, The South African Institute of Mining and Metallurgy, pp. 525-546.

Verma , D., Thareja , R., Kainthola , A. & Singh, T., 2011. Evaluation of Open Pit Mine Slope Stability Analysis. *International Journal of Earth Sciences and Engineering,* Volume 04, pp. 590-600.

Washington State Uniwesity , 2018. *www.shorestewards.cw.wsu.edu.* [Online]
Available at: http://shorestewards.cw.wsu.edu/faq/using-plants-trees-for-stability/

Watkins, A. & Hughes, S., 2018. *Environmental Geology.* [Online]
Available at: http://geology.isu.edu/wapi/EnvGeo/EG4_mass_wasting/EG_module_4.htm
[Accessed 05 May 2018].

Wesseloo, J. & Sweby, G. J., 2008. *Microseismic Monitoring of Hard Rock Mine Slopes.* Perth , Australian Centre for Geomechanics, pp. 433-450.

Wessels , S. & Naismith , W., 2005. *Managment of a major slope failure at nchanga open pit, Chingola, Zambia.* Kitwe, The South African Institute of Mining and Metallurgy.

Wikipedia, 2018. *www.wikipedia.com.* [Online]
Available at: https://en.wikipedia.org/wiki/File:Freeport_Mine_Indonesia_Total_Station.JPG
[Accessed 8 August 2018].

Wolff, C., 2018. *www.radartutorial.eu.* [Online]
Available at:
http://www.radartutorial.eu/01.basics/Physical%20fundamentals%20of%20the%20radar%20principle.en.html#this
[Accessed 25 July 2018].

Work Package 6, 2008. *Slope Monitoring Methods A State of the Art Report,* Munich: The ClimChAlp partnership.

`

www.civildigital.com, 2018. *www.civildigital.com.* [Online]
Available at: https://civildigital.com/failure-modes-in-rock-and-soil-slopes-slope-failure/
[Accessed 11 July 2018].

www.idsgeoradar.com, 2018. *www.idsgeoradar.com.* [Online]
Available at: https://idsgeoradar.com/products/interferometric-radar/ibis-fm/
[Accessed 2 August 2018].

Wyllie, D. &. M. F., 1979. *The use of movement monitoring to minimize production losses due to pit slope failures.* Vancouver : Proceedings, 1st International Symposium on Stability in Coal Mining.

Yan, Y., Zhang, Y. & Huang, C., 2014. Impact of Blasting Vibration on Soil Slope Stability. *Information Technology Journal,* Volume 13, pp. 730-737.

Zavodni, Z., 2000. *Time-dependent movements of open-pit slopes.* Littleton: Slope Stability in Surface Mining .

Appendices

Table of movement values and thresholds used in the literature studies

Author	**Threshold value**	**Description**
Cruden and Masoumzadeh (1987)	1.2 mm/h	Initiation of second accelertion stage
	6 mm/h	Initiation of third acceleration stage
Martin (1993)	10 - 100 mm/day (or more) (0.4 - 4.1mm/hr)	Progressive stage
	0.2 to 2 mm/day (0.008 to 0.08 mm/hr)	Strain hardening
	0.1mm/day (0.004 mm/hr)	Initial response
Flores and Karzulovic (2001)	> 50mm/day (2.1mm/hr)	Mining is not allowed anymore
	30 - 50mm/day (1.25 - 2.1mm/hr)	There is potential for instability if the movement is continuing for longer than two weeks
	10 - 30mm/day (0.4 to 1.25mm/hr)	Cracks start to appear, it is necessary to provide more detailed monitoring
	<10mm/day (0.4mm/hr)	There is no signals of slope instaiblity
Zavodni (2001)	150mm/day (6.25 mm/hr)	Clear mining area (Regressive geometry)
	>100mm/day (4.2 mm/hr)	Clear mining area (Progressive geometry and progressive velocity)
	> 50mm/day (2.1 mm/hr)	Indicates progressive failure (total collapse expected within 48 days)
	< 15mm/day (0.63 mm/hr)	No failure expected within 48hrs
	<17mm/day (0.71 mm/hr)	No failure expected within 24hrs
	0.1mm/day (0.004 mm/hr)	Initial response
Naismith and Wessels (2005)	10 mm/day	Scram warning level
	5 mm/day	Alarm warning level
	3.5 mm/day	Alert warning level
	2 mm/day	Natural “relaxation” of the rock mass
Little(2005)	10mm/2h for area 80 m2	Red alarm
Roux and others (2006)	0.1 mm/day (0.004 mm/hr) for 3 days; downward vertical movement	Red alert
	0.2mm/day (0.008 mm/hr)	Evacuate
	0.5 mm/day (0.02 mm/hr) for 10 days; horizontal movement	Orange alert
	1.0 mm/day (0.04mm/hr) for 3 days; horizontal movement	Red alert
	2.0 mm/day (0.08mm/hr) horizontal movement	Evacuate

Sullivan (2007)	0.1 - 0.25 mm/day (0.004 - 0.01 mm/hr)	Definite movement of slope related to shear of displacement on structures	
	0.25 - 0.5 mm/day (0.01 - 0.02 mm/hr)	Likely to fail sometime in future	
	1 mm/day (0.04 mm/hr)	High chance of failure	
	More than 1.0 mm/day (>0.04 mm/hr)	Pre-failure collapse movements	
Osasan (2012)	1.4 mm/h	The rate of Displacement at Onset of Failure	Unknown (copper mine)
	5 mm/h	The rate of Displacement at Failure	
	1.4 mm/h	The rate of Displacement at Onset of Failure	New Vaal Coal Mine (Ramp 0)
	4 mm/h	The rate of Displacement at Failure	
	1 mm/h	The rate of Displacement at Onset of Failure	Landau Coal Mine (Ramp 5)
	3 mm/h	The rate of Displacement at Failure	
	0.5 mm/h	The rate of Displacement at Onset of Failure	New Vaal Coal Mine (Ramp 11)
	2 mm/h	The rate of Displacement at Failure	
	0.5 mm/h	The rate of Displacement at Onset of Failure	New Vaal Coal Mine (Ramp 12)
	2 mm/h	The rate of Displacement at Failure	
	1.2 mm/h	The rate of Displacement at Onset of Failure	Unknown
	2 mm/h	The rate of Displacement at Failure	
Saunders (2016)	2 mm/hr	Insufficient notification period	
	1.5 mm/hr	The most appropriate notification period prior to failure	
	4 mm/ 4hr	Appropriate notification period prior to collapse	
	1 mm/hr	Limited success due to frequent unwanted alarms caused by noise in the data	

Carla and others (2017)	1-2 mm/h	Threshold level 1 - the initial stage of emergency management
	>1-2 mm/h	Threshold level 2- established when the movement exceeds threshold level 1, may be increased after evaluation of radar mechanism
	30 mm/h and 20mm/h2	Threshold level 3-combines both velocity and acceleration is a separation between failures and non-failures. After this point movement has to be continuously monitored
Mononen and others (2018)	1,8 mm/h	Red hazard (critical condition) for entire radar map
	0,9 mm/h	Yellow hazard (alert condition) for entire radar map
	2-3 mm/h	Aggressive velocity threshold for ANGELA radar
	4-5 mm/h	Conservative velocity fo MIA radar
	1-2 mm/h	Alternative velocity threshold for ANGELA radar
	10mm/h	Alternative velocity threshold for MIA radar
Larsson and others (2018)	1 mm/h	Alarm level 1, sent to designated (a) competent person
	1.5-1.9 mm/h	Alarm level 2, Alarm sent to the mining center and selected supervisors. Competent person calculates "inverse velocity". Also sent to the mining center and selected supervisors. Competent person calculates "inverse velocity".
	2.8 mm/h	Alarm level 3, evacuation of the area under alarm area

The procedure changing the radar position

1. Prepare a new place for the radar. It is necessary that radar is placed on the stable ground. There must be a clear view in front of the trailer if there are trees in the line of sight them must be cut. Contact three teams electricians, network (internet) and surveying team. Electricians will provide electricity cable for the trailer. Network team will ensure an Internet connection for the trailer. The surveying team needs to provide information on the radar and the camera coordinates.
2. Turn off the radar session in the IBIS Controller and close down the IBIS Controller
3. Turn off the PC
4. Tied up the PC to the Power Supply Unit
5. Turn off the sensor, the scanner, the PC and the Camera on the control module in Power Supply Unit
6. Switch off Isolation point on the power module in the Power Supply Unit
7. Plug out the Radar Sensor connectors: power and USB.
8. Screw out the Radar Sensor of the Linear Scanner and placed at the safe location. The radar sensor is a really sensitive and expensive device, especially antennas require special attention !!! Screw out antennas from the Radar Sensor and placed the Radar in the black case
9. Screw out the Eagle Vision Camera from the tripod and placed it at the safe location. The camera is a sensitive device !!!
10. Unplug the electrical cable and the Internet cable from the trailer, roll cables into a bun
11. Screw out and lift the legs of the Camera platform.
12. Slide the Platform to the Trailer
13. Place the car with the hook under to the trailer hook
14. Lift the first the front legs of the trailer, if you will lift also back legs trailer could tilt back.
15. Lower the trailer using the black crank
16. Lock the trailer hook into the car hook, you should hear “click” and the pin should be hidden. It is important that the hooks are properly attached to each other.
17. Connect breaks cable and electrical cable to the car
18. Now you can move the radar to a new place. Ride slowly and carefully, radar is sensitive and expensive equipment.
19. Ensure that the place is properly secure. The trailer is located on the side of the edge of the pit.
20. Place the trailer in the right position according to have the best line of sight.
21. Lower the back legs of the trailer. It ensures that the trailer will not tilt back
22. Lower the black crank
23. Plug out cables (break and lights)
24. Lower the front legs of the trailer
25. Slide back the platform with the camera tripod and lower the legs of the platform
26. Connect the electricity and internet to the trailer
27. Mount the camera on the tripod and level it using screws and connect cables
28. Place a level on the trail, at which the Radar Sensor is moving and level the Linear Scanner using the golden spherical thrust bearings Ensure that the sphere is in the right position. Check figure 1

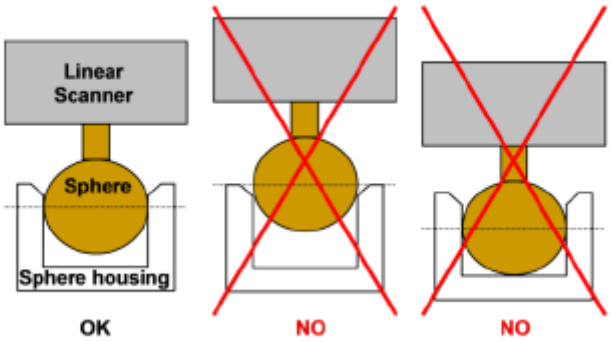

Figure 1 The correct position of contact between the spherical housing and the sphere

29. Screw in the antennas to the Radar Sensor
30. Mount the Radar Sensor on the Linear Scanner
31. Plug the Radar Sensor connectors (power and USB)
32. Switch on Isolation point on the power module in the Power Supply Unit
33. Turn off the sensor, the scanner, the PC and the Camera on the control module in Power Supply Unit
34. Turn on the PC
35. Open the IBIS controller and start a new session

Generalized time and event dependent rock mass deformation model

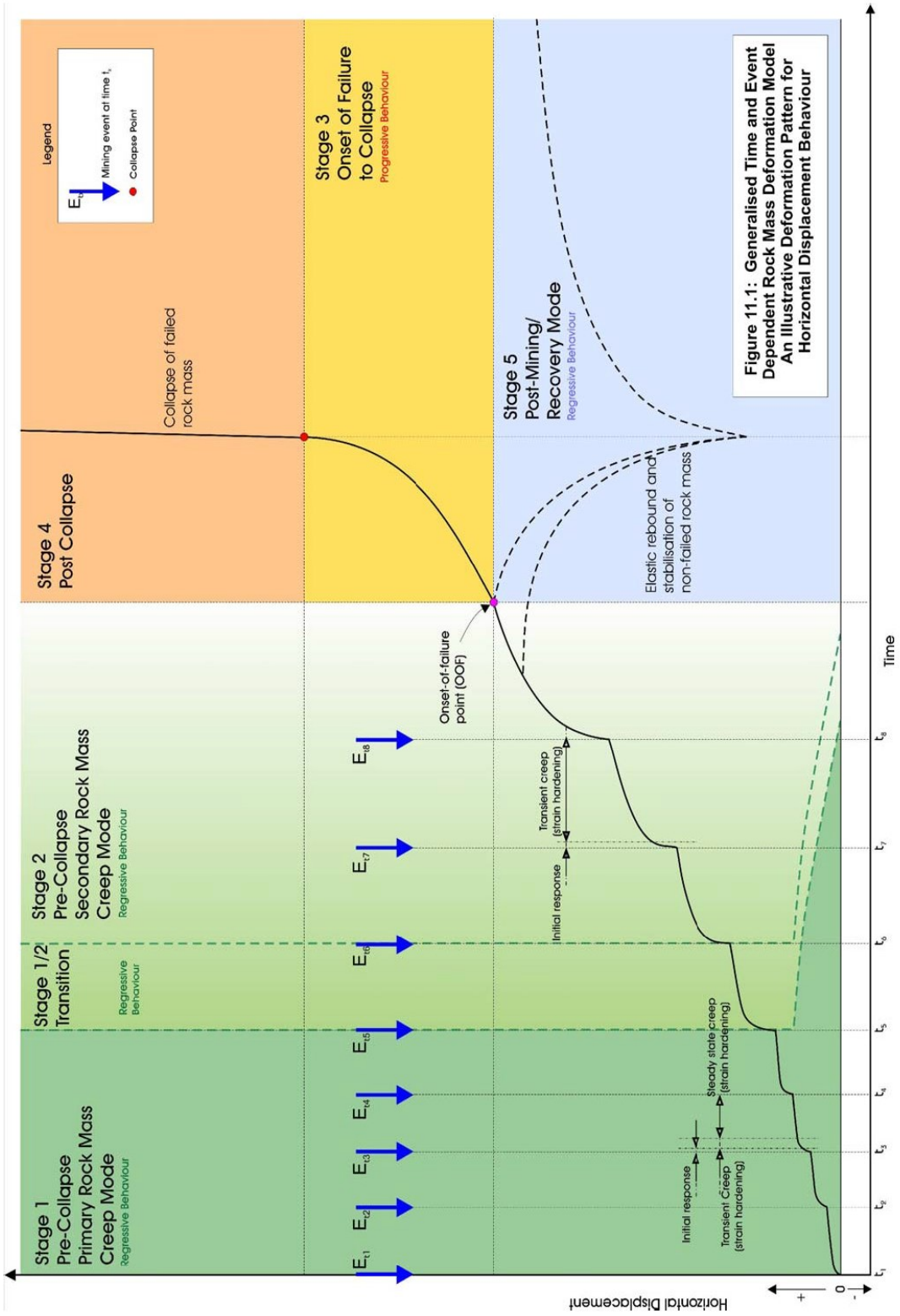

F

Generalized time and event dependent rock mass deformation model. An illustrative deformation pattern for horizontal displacement behavior

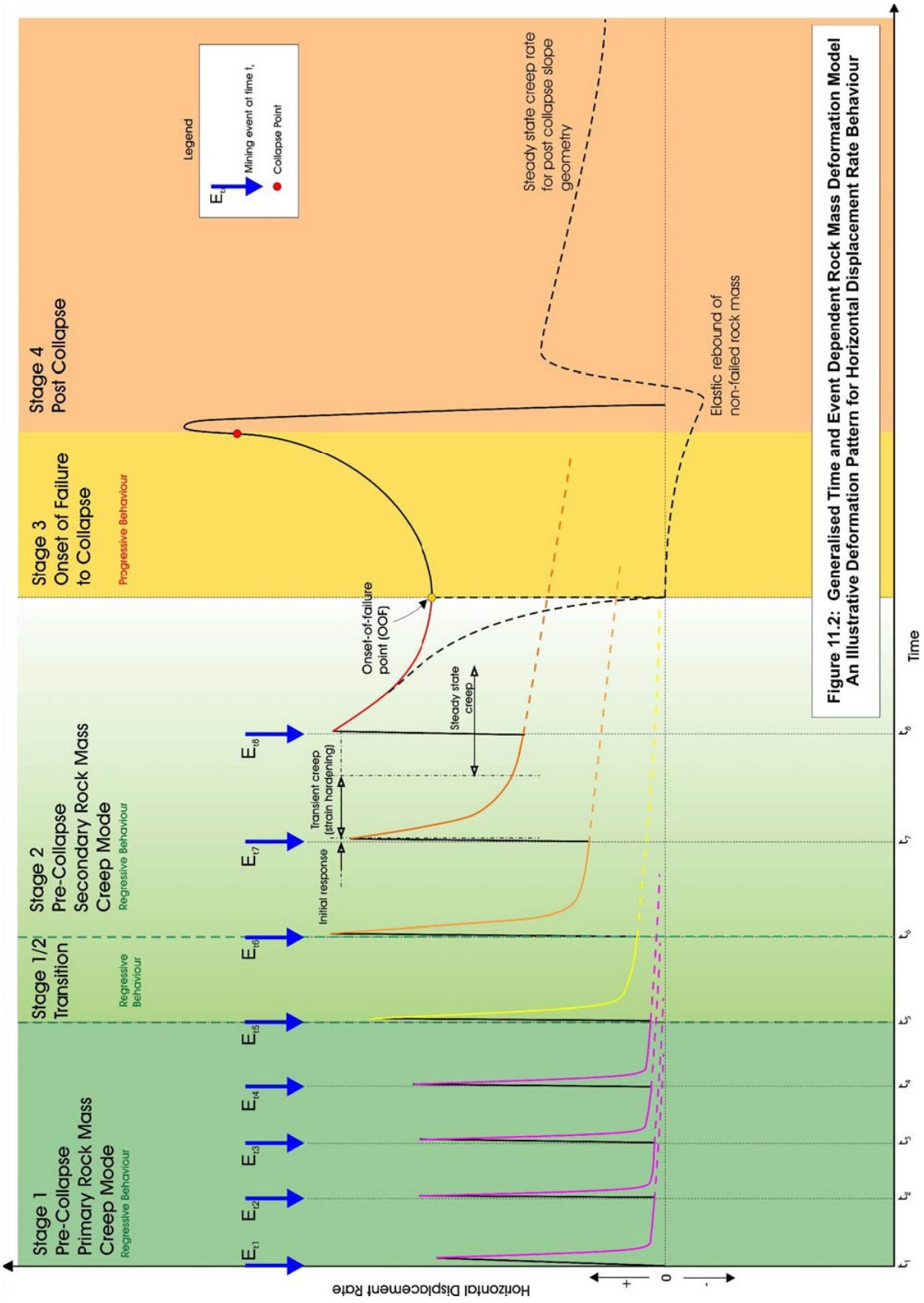

Generalized time and event dependent rock mass deformation model. An illustrative deformation pattern for horizontal rate behavior

Removal of atmospheric contribution

In IBIS manual is described the removal of atmospheric contribution in phase calculations. A measurement of a phase difference must take into account an atmospheric contribution. A signal phase is based on a frequency (f) and a flight time of wave (t_w).

$$\phi = -2\pi f t_w \tag{1}$$

A wave time flight depends on a wave velocity (v_w).

$$t = \frac{2r}{v_w} \tag{2}$$

Electromagnetic waves a moving with the speed of light (c). Depending on an atmospheric medium, c has to be divided by the specific refractive index (n) to obtain an exact value of a wave speed.

$$v = \frac{c}{n} \tag{3}$$

Therefore, a wave flight time can be written like this :

$$t = n\frac{2r}{c} \tag{4}$$

A phase difference is the sum of the phase related with object displacement and the phase related with an atmosphere. A noise is negligible and can be not taken into account.

$$\Delta\phi = \Delta\phi_{def} + \Delta\phi_{atm} \tag{5}$$

Equation (34) can be rewrite as follow:

$$\Delta\phi = -\frac{4\pi}{\lambda}\Delta d - \frac{4\pi}{\lambda}\Delta n \cdot d \tag{6}$$

To achieve a real displacement an atmospheric contribution has to be removed. To do that special assumptions must be taken:

- Certain areas of the measurement are not moving

$$\Delta\phi_{\mathrm{def}(CA)} = 0 \tag{7}$$

- A difference in phase in those areas is recorded by a radar as atmospheric changes

$$\Delta\phi_{(CA)} = \Delta\phi_{atm} \tag{8}$$

- Atmospheric changes are the same in a whole measured area

Therefore, it is possible to calculate a real displacement (Figure 46).

$$\Delta\phi_{def} = \Delta\phi - \Delta\phi_{atm} \tag{9}$$

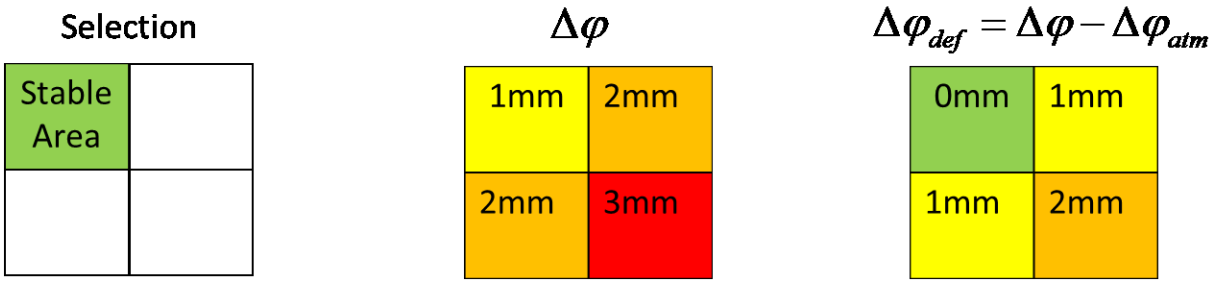

Removal of the atmospheric contribution

This method has few limitations: an atmospheric compensation is based only on small areas pretended to be stable, which needs constant checks if they are still stable; atmospheric changes can vary in a pit, therefore stable areas can be far from movements; the method can be applied only for a range and the technique works only for restricted distances.

To remove an atmospheric contribution the Guardian follows three steps :

1. Pixel Classification-the software applies a pile of interferometric images to classify pixels, where changes in $\Delta\phi$ are measured for a real movement and for the atmosphere. A real movement is correlated in time- does n't much fluctuate and it is localized -has a high-frequency correlation, whereas atmosphere is uncorrelated, vary frequently and it is extensive -has a low-frequency correlation. For a better stable pixels classification, the program uses a multi-scale classification. It uses a different time classification to categorize points with a low velocity as unstable points. A multi-scale classification (Figure 47) uses three different intervals: the real-time thread, the first subscale, which uses one image every 12 images and the second subscale, which uses one image every 144 images.

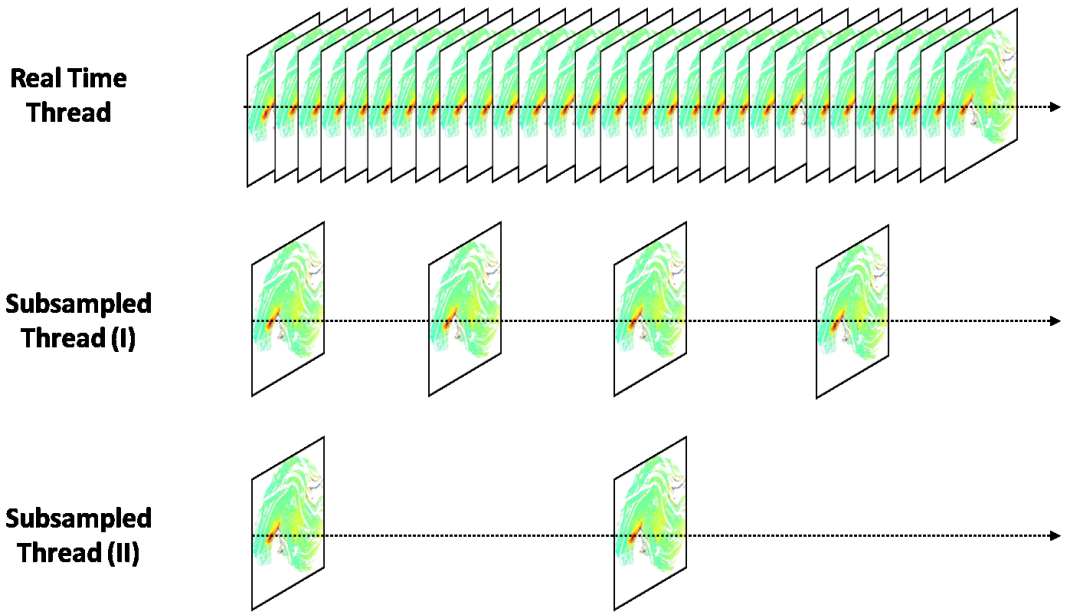

Multi-Scale classification

2. Atmospheric fitting- an estimation of an atmospheric model, which uses all not moving points as a reference. It is calculated and updated after every new acquisition.
3. Atmospheric removal- an atmospheric model is taken away from raw data.